

Optical Probes of Membrane Physiology

Chemistry: Joe Wuskell and Ping Yan

Optics: Andrew Millard and Corey Acker

Collaborators: Srdjan Antic and Larry Cohen

Supported by NIBIB and NIH Roadmap



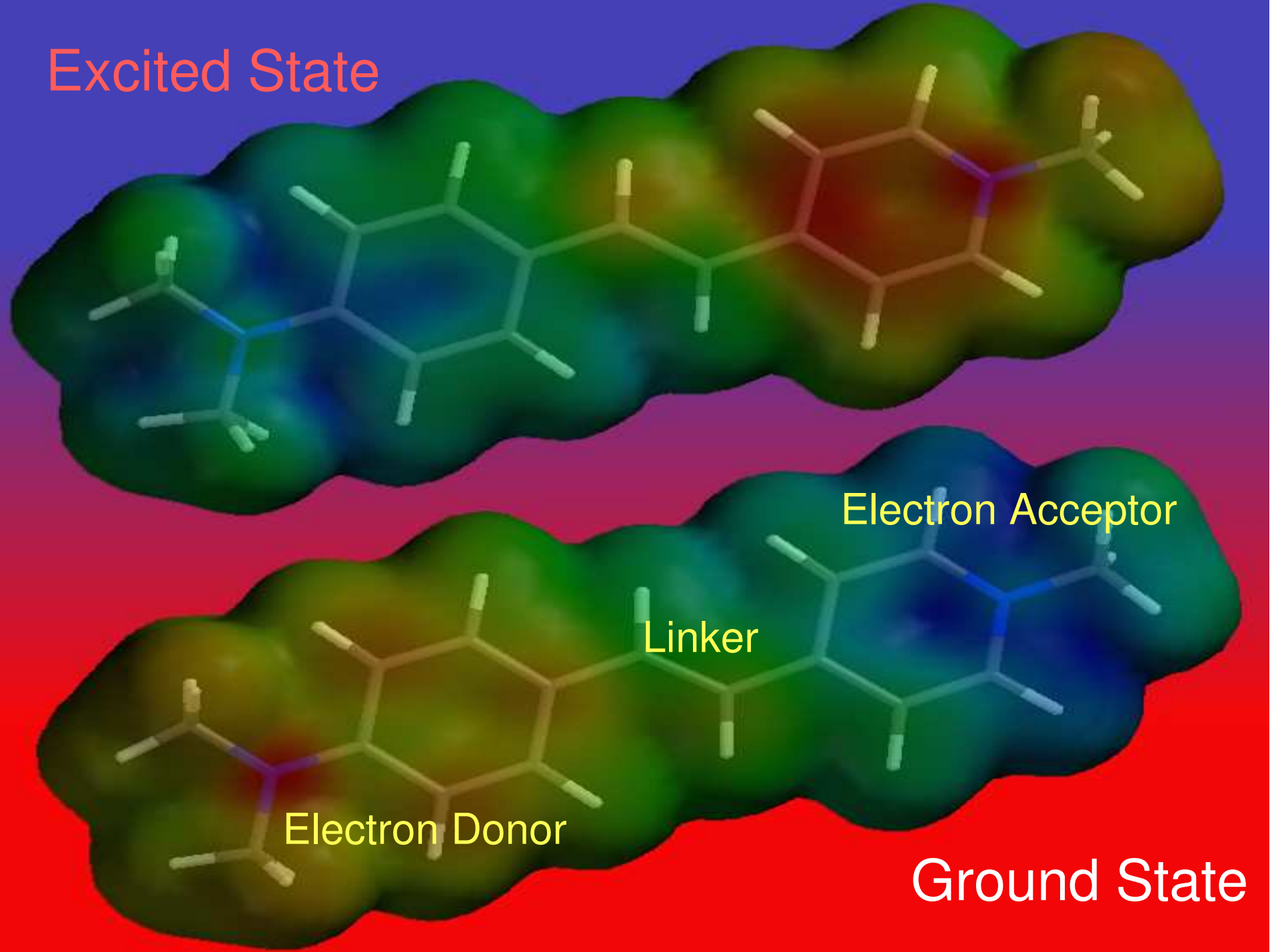
Richard D. Berlin
Center for Cell Analysis and Modeling

National Technology Center for Networks and Pathways

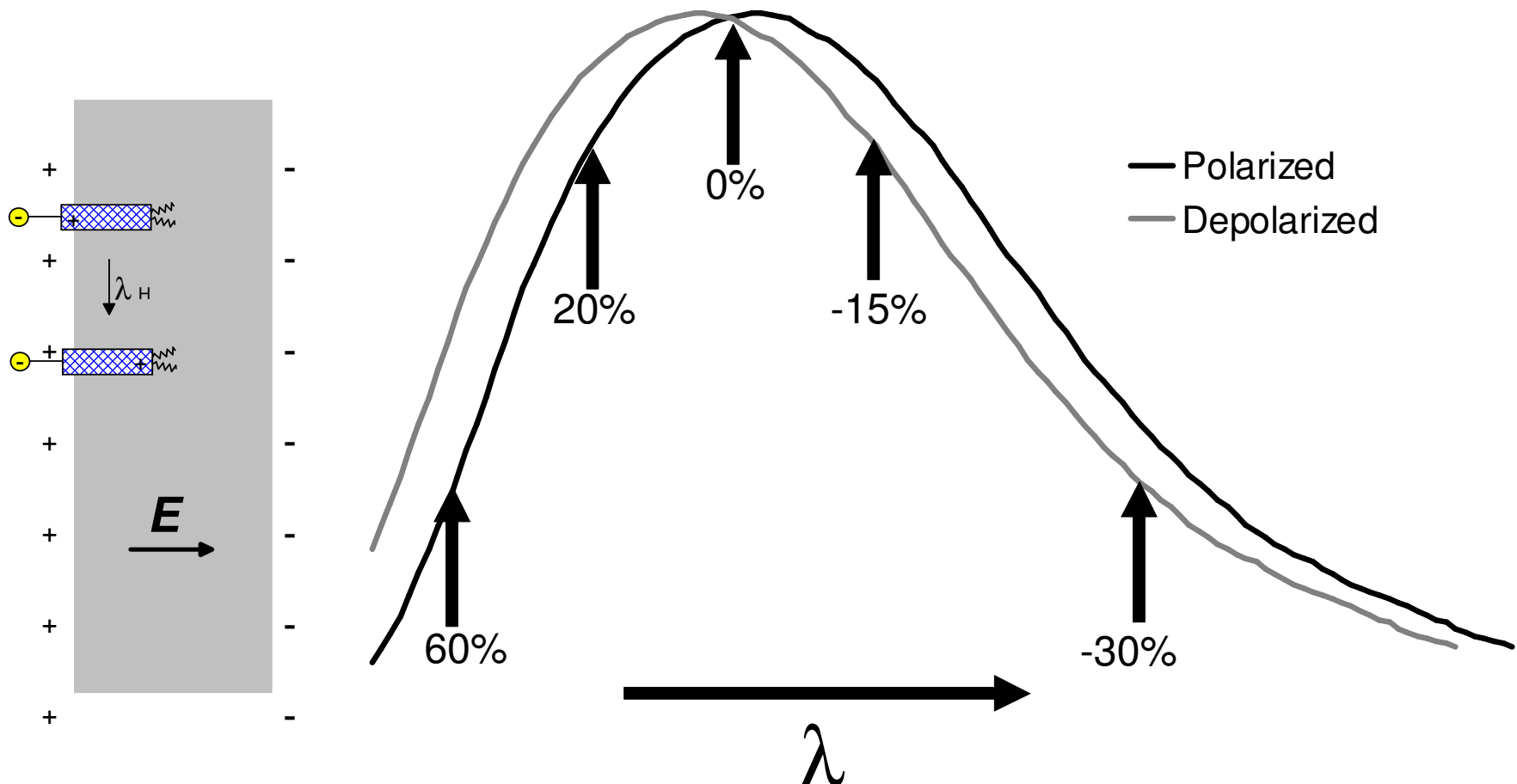
Optical Probes of Membrane Physiology

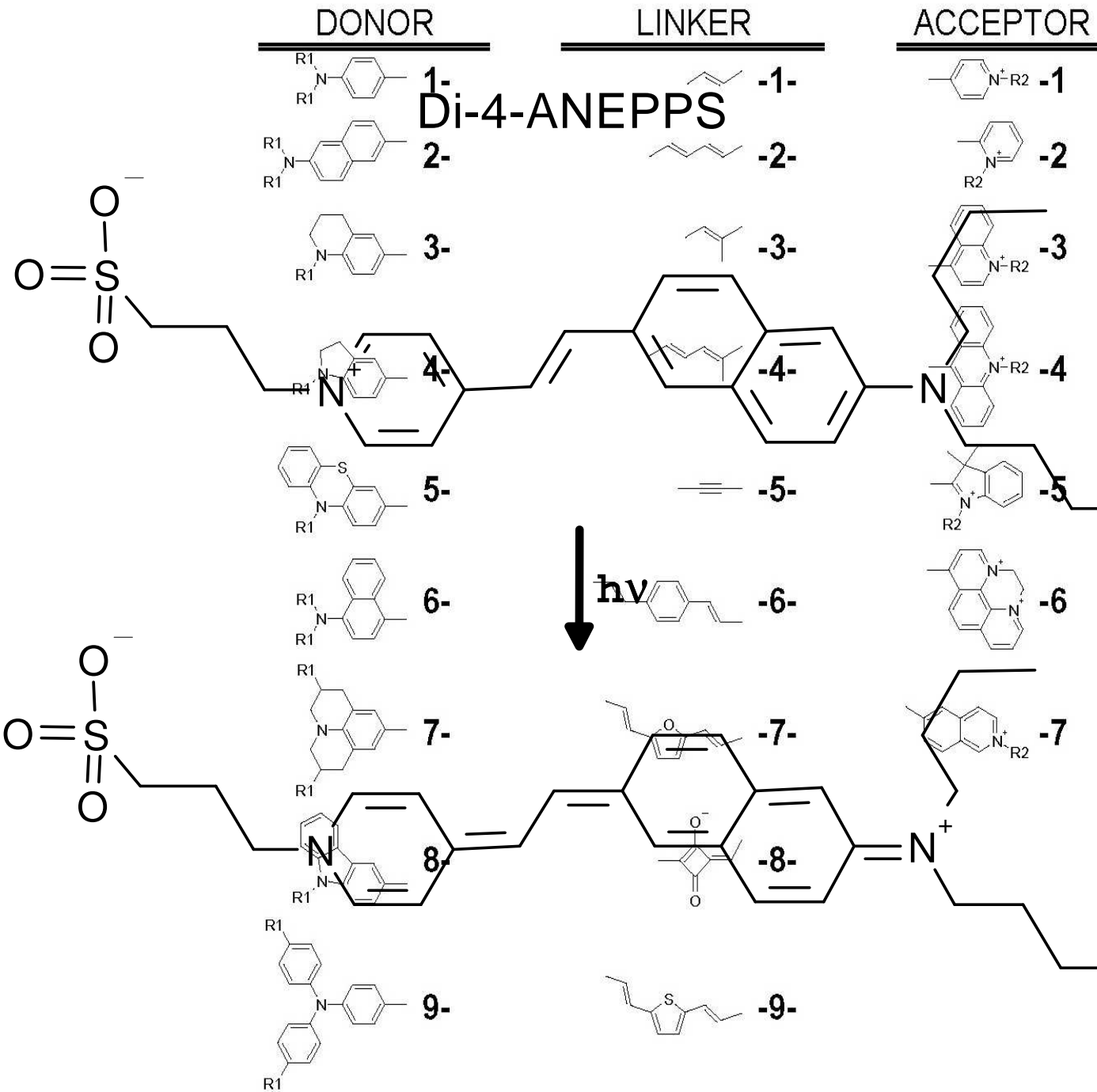
- Primer on the physical chemistry of VSDs
- Sampling of applications
- Non-linear optical measurements of membrane voltage change
 - the latest and greatest
- Brief look at Virtual Cell

Excited State

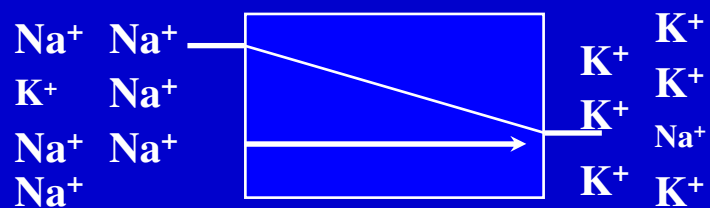


Voltage-dependent Spectral Shift: Choose the Right Wavelengths

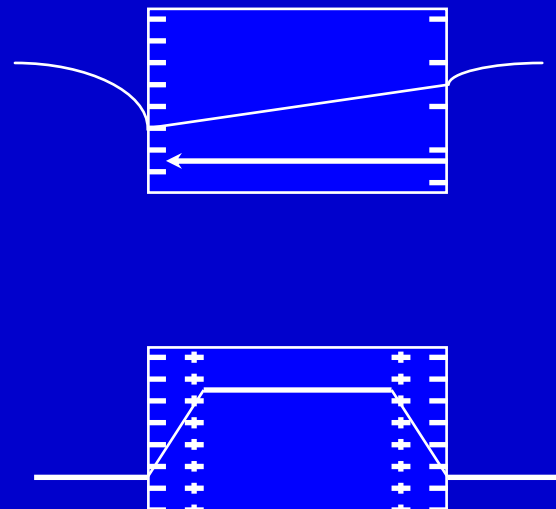




Intramembrane Electric Fields

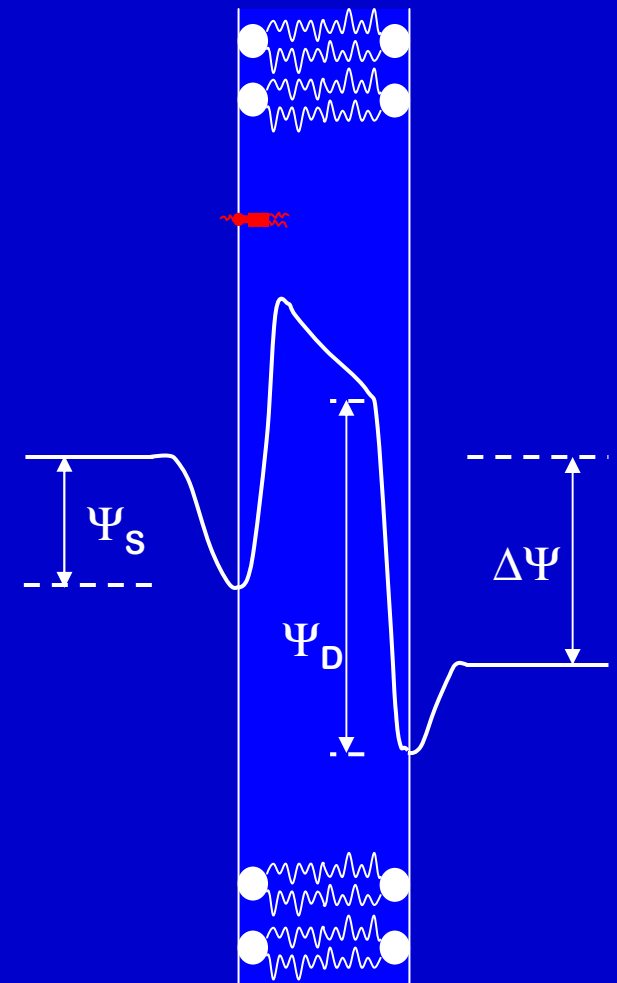


Transmembrane
Potential

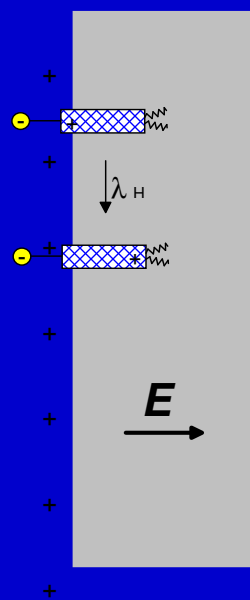
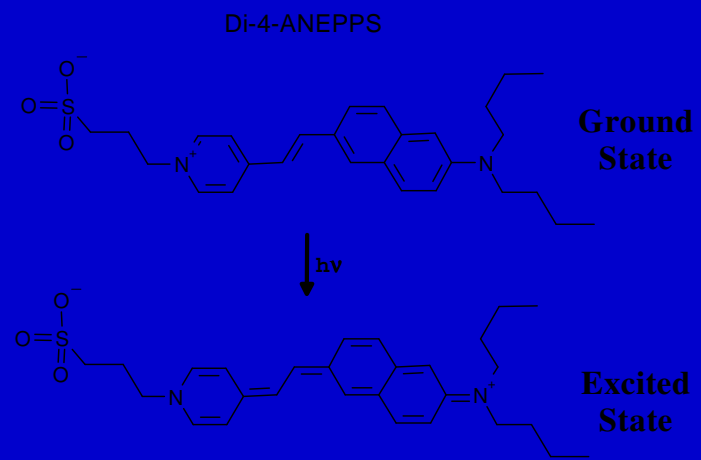
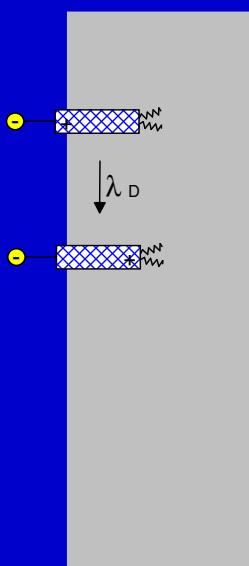
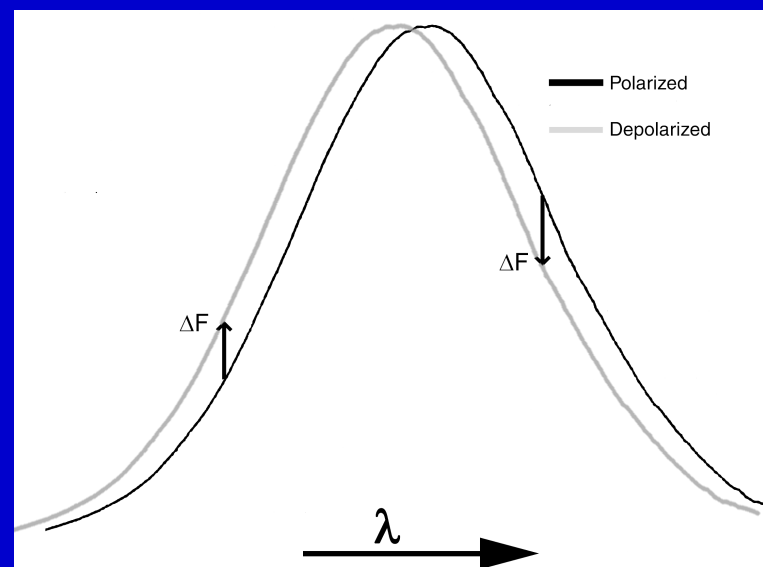


Surface Potential

Dipole Potential



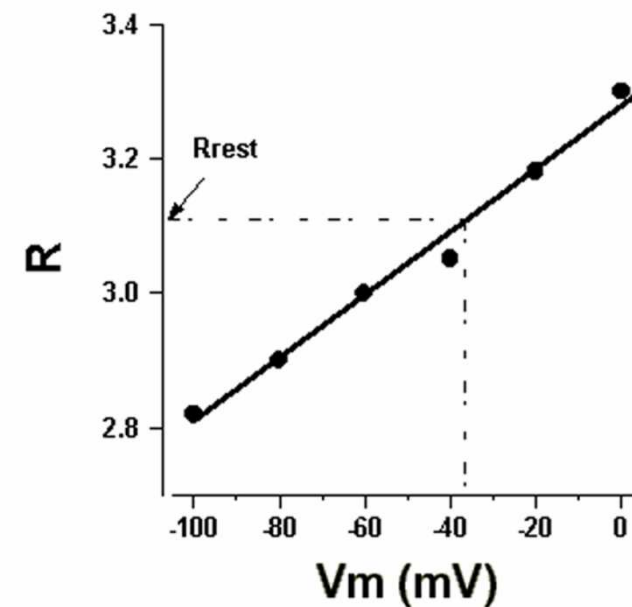
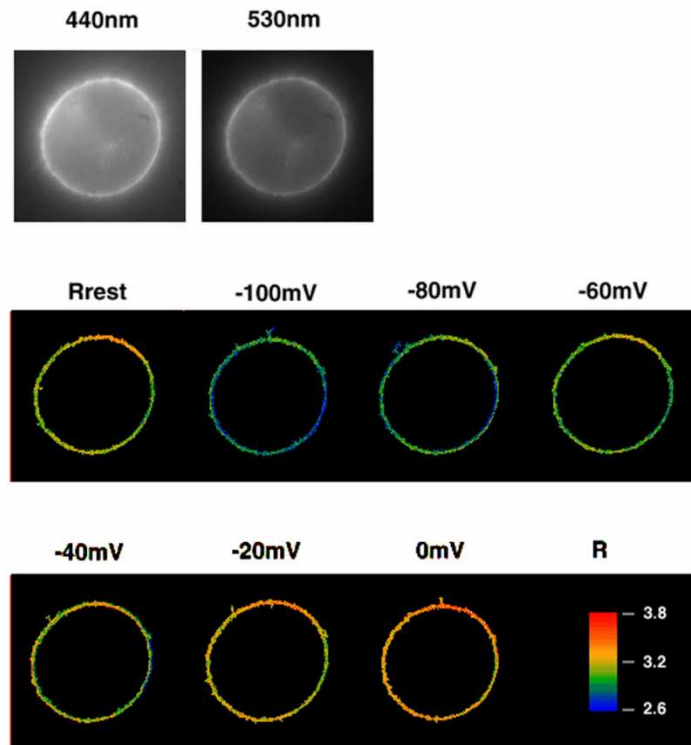
Putative Mechanism of Voltage-dependent Spectral Shifts in Styryl Dyes - 'Electrochromism'



$$\lambda_H - \lambda_D \approx E$$

Dual Wavelength Ratios of Di-8-ANEPPS are Linear with Membrane Potential

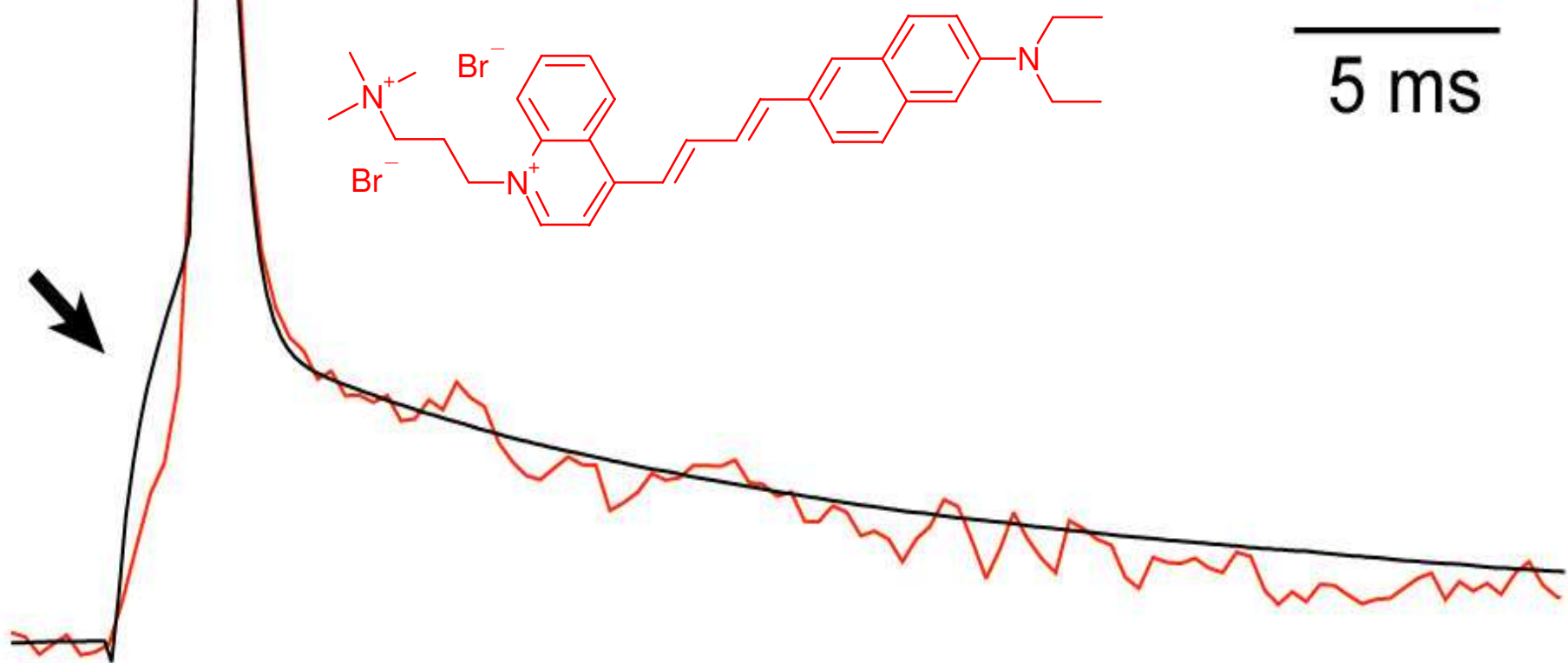
(Montana et al., 1989; Zhang et al., 1998)



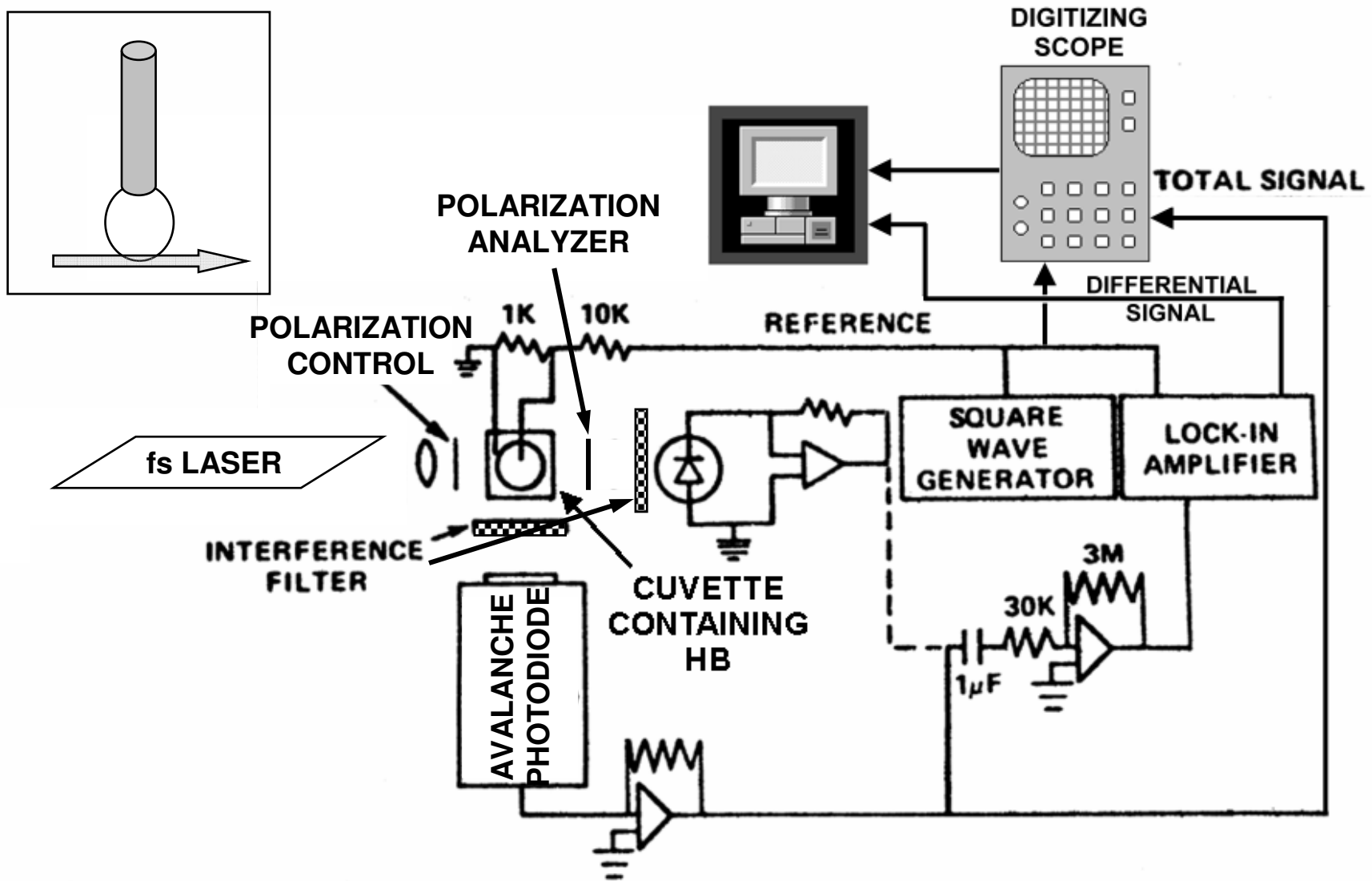
Zhou, W.-L., Y. Ping, J.P. Wuskell, L.M. Loew
and S.D. Antic. J. Neurosc. Meth. 2007

whole-cell
JPW-4090

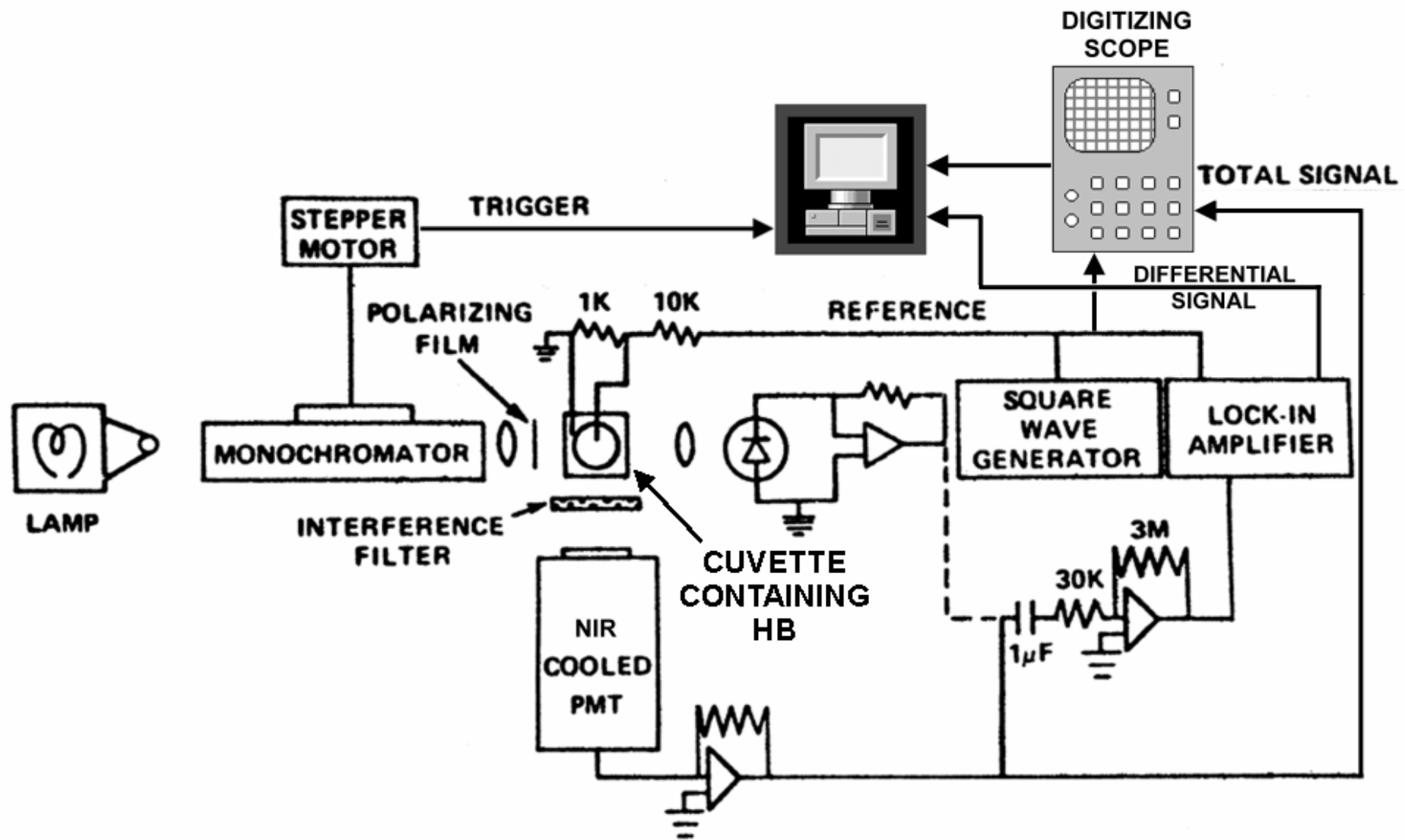
10 mV |
1 % |
— 5 ms

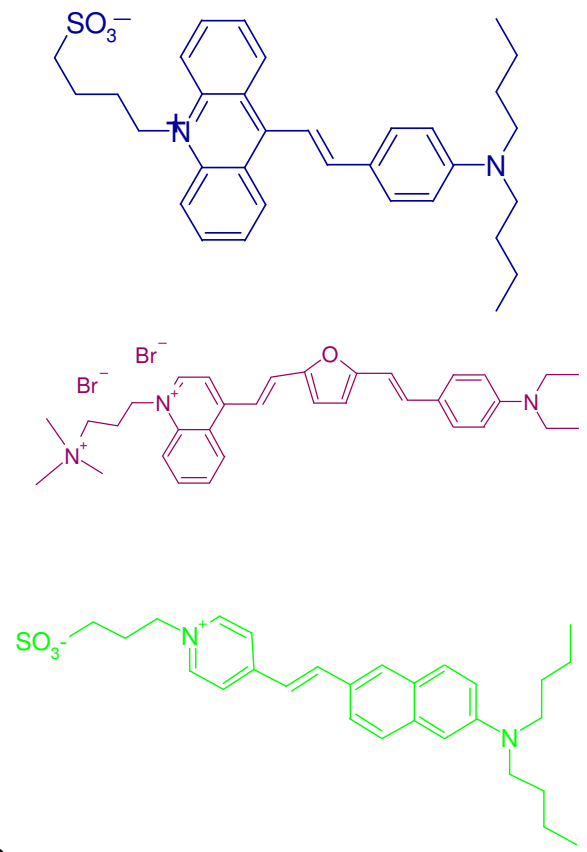
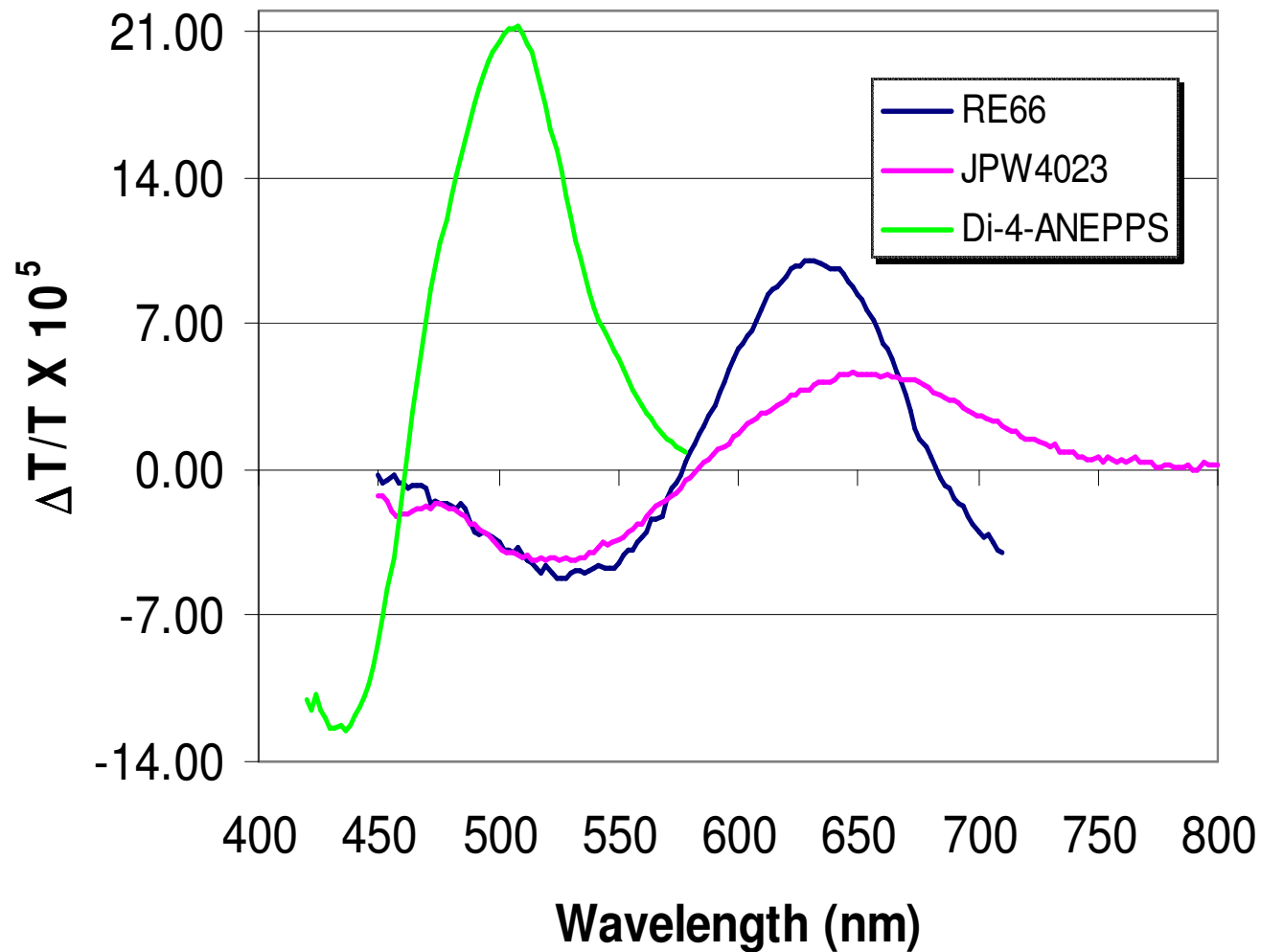


Hemispherical Bilayer Apparatus

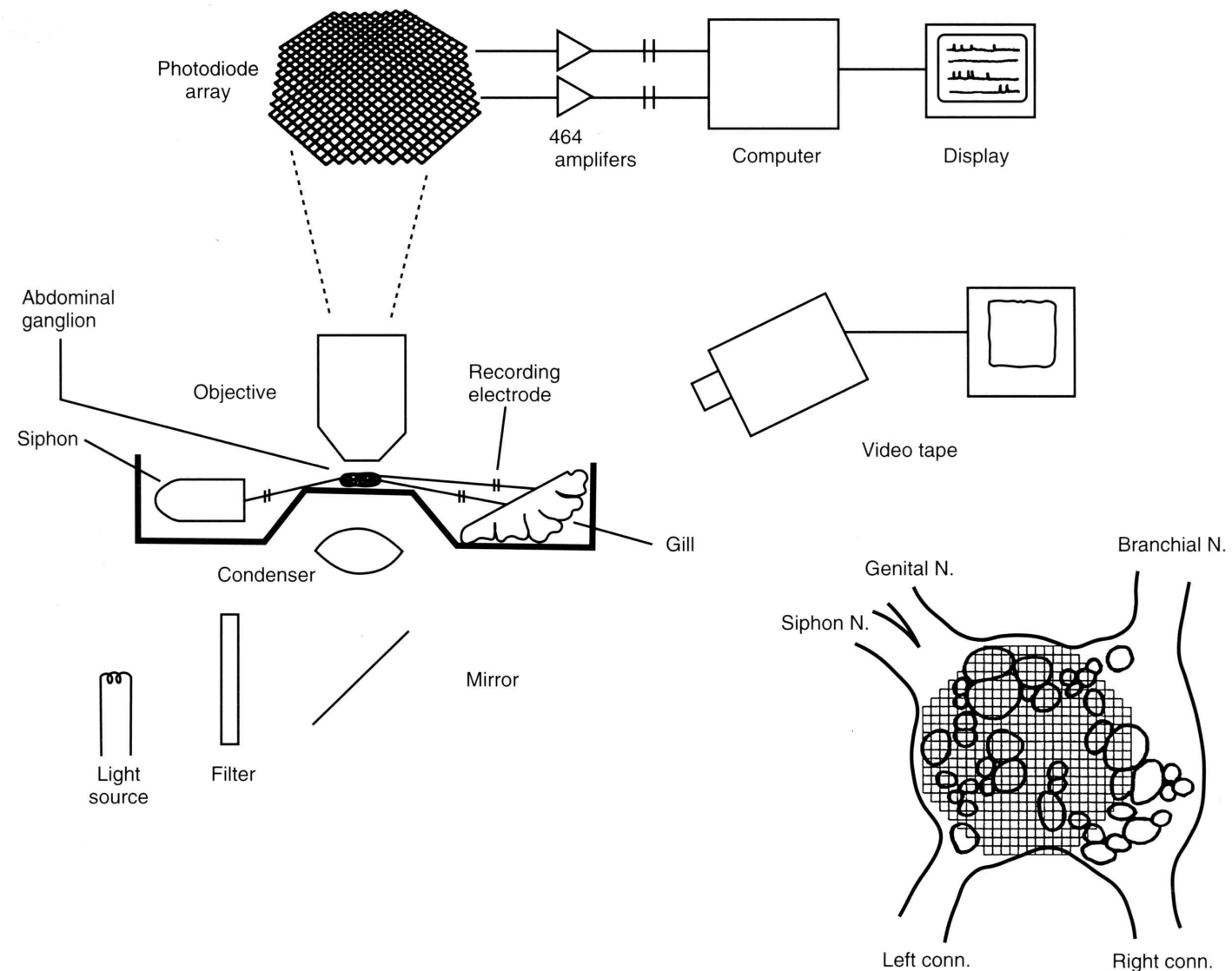


Transmittance Response Spectra from a Voltage-Clamped Hemispherical Bilayer

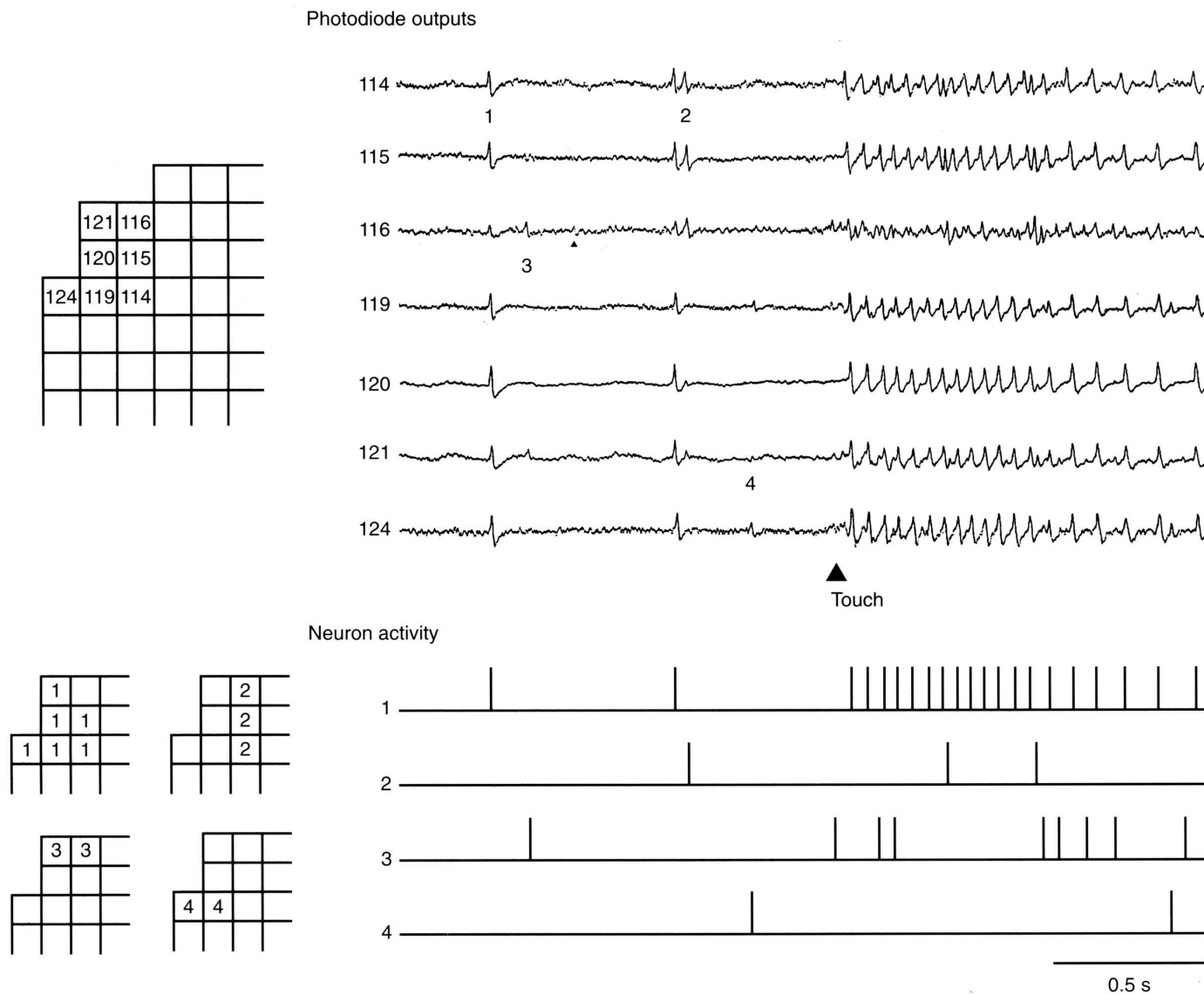




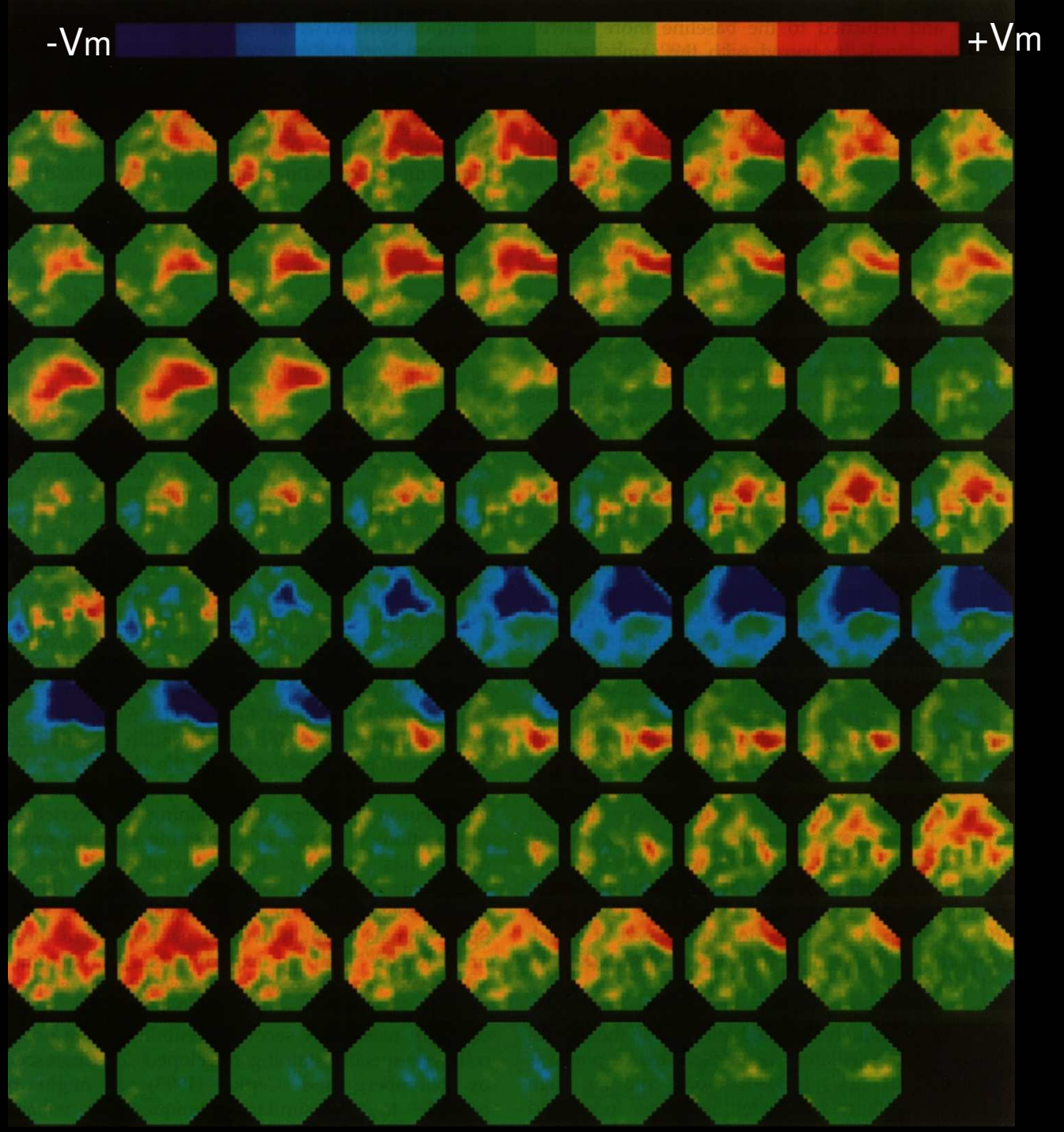
Larry Cohen's Apparatus for Recording from the Aplysia



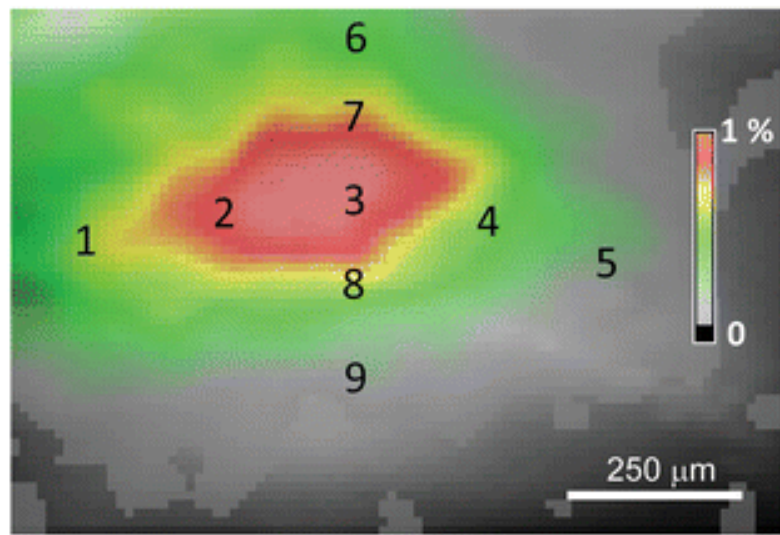
Example Multisite Records and Their Analysis



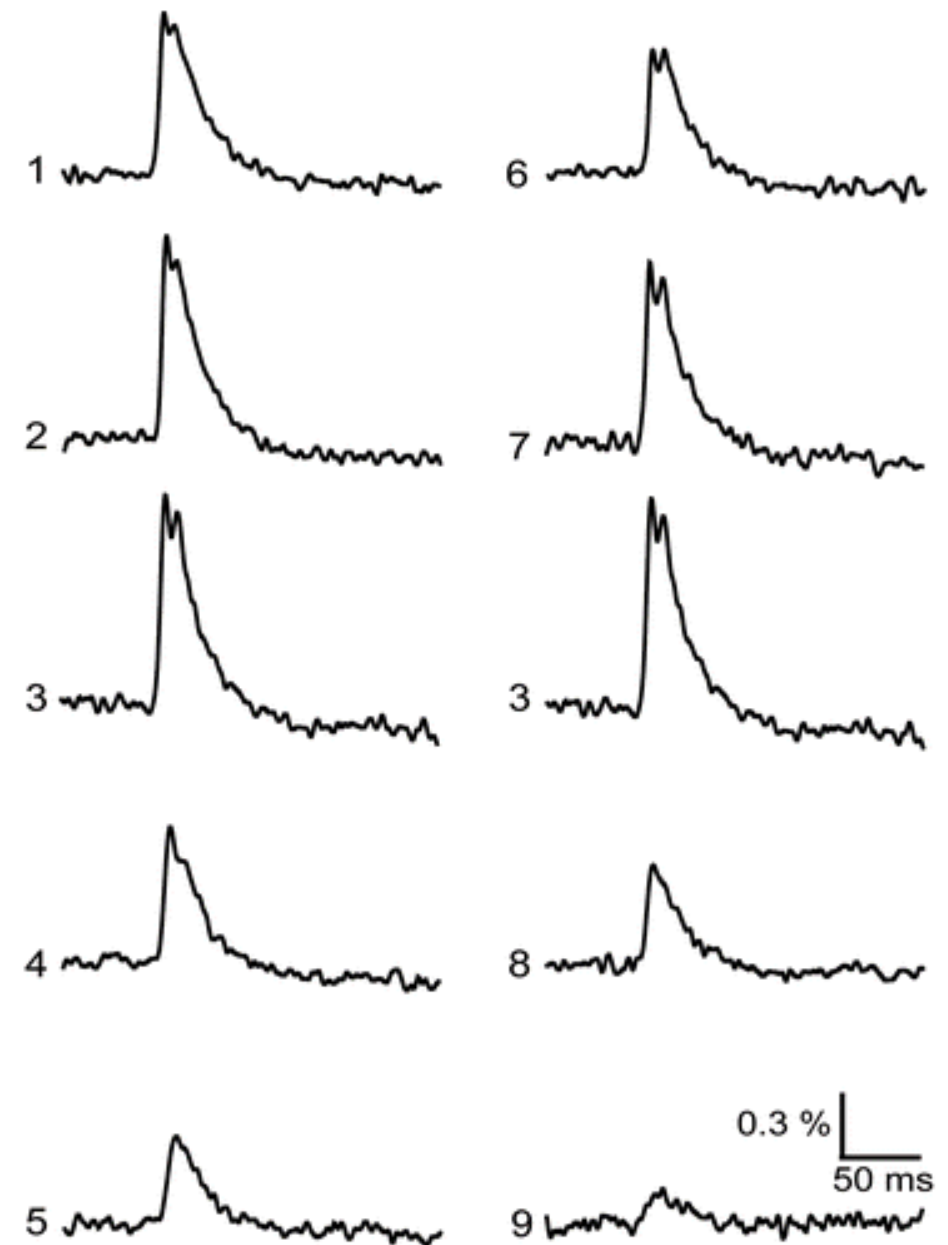
Response to a Looming
Stimulus in Turtle
Visual Cortex



4ms/frame

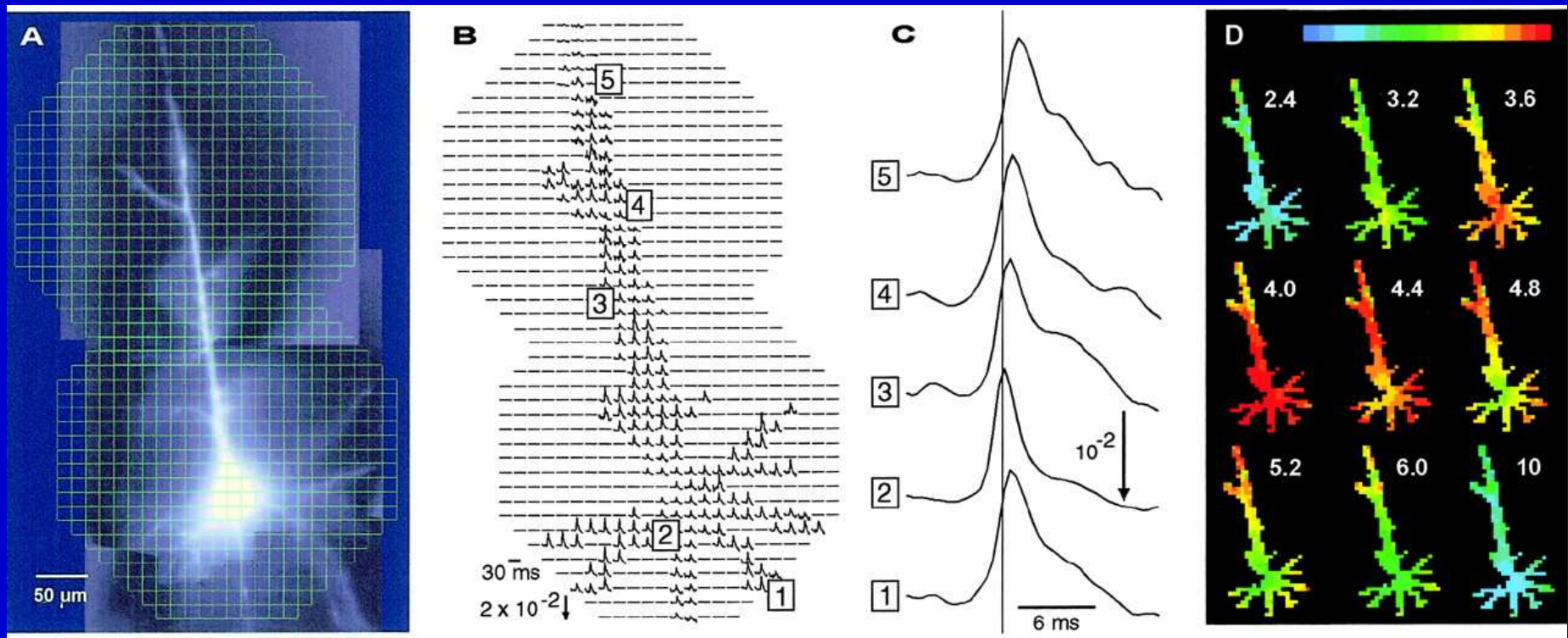


Spatio-temporal
features of responses
reported by di-2-
ANBDQPO following
stimulation of a mouse
hippocampal brain slice



Recording from Single Pyramidal Neurons in a Slice

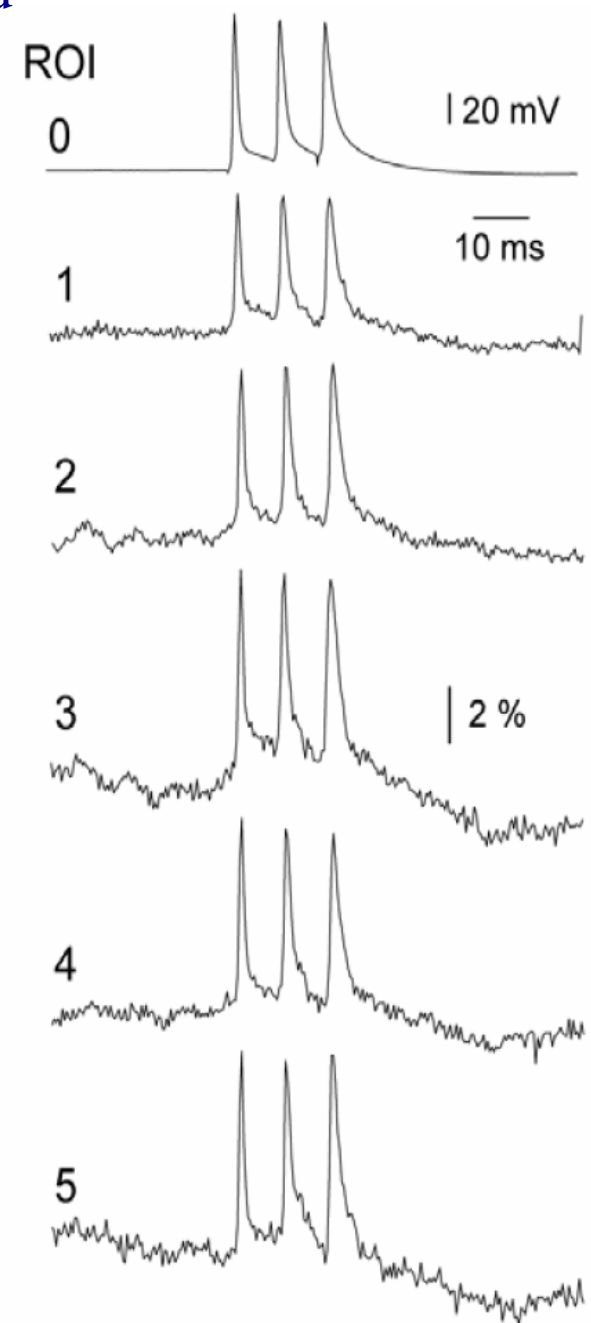
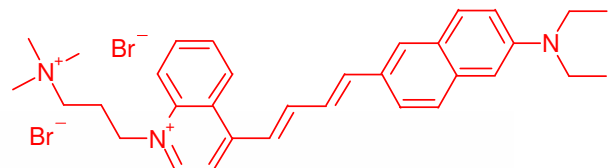
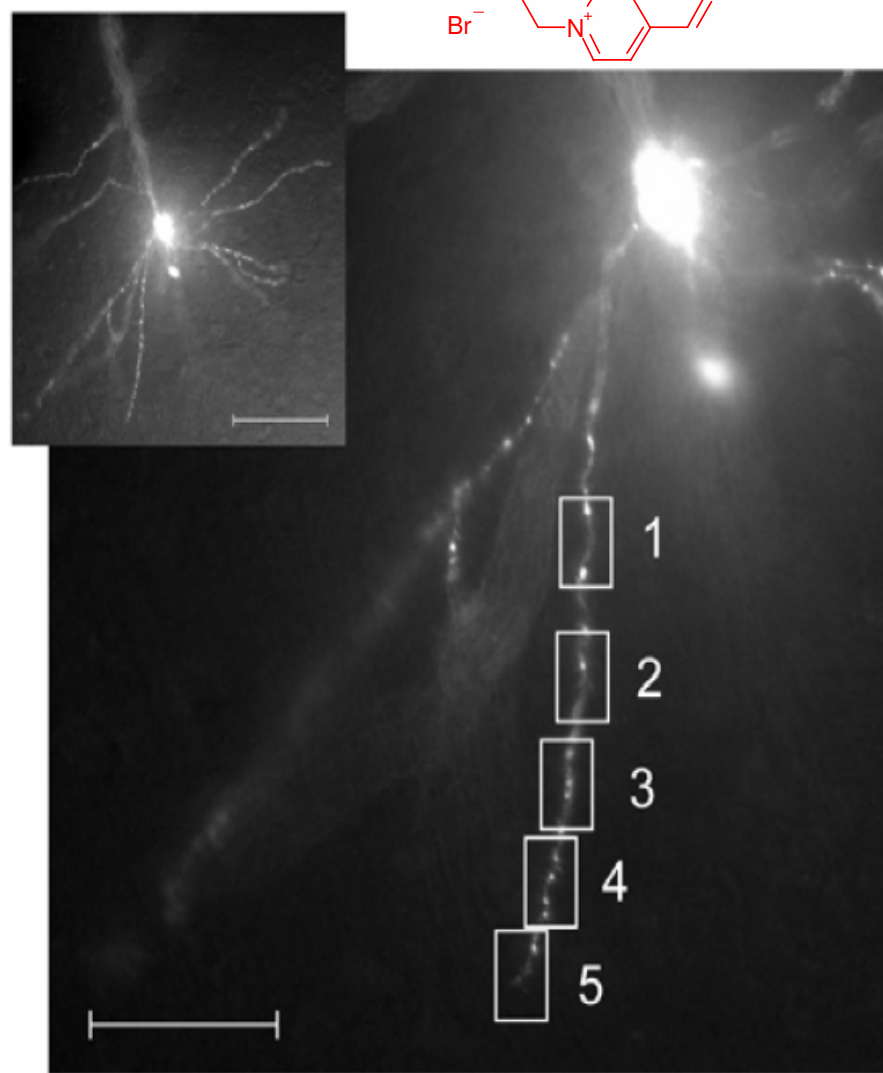
Antic, et al., J. Neurophys. 1999



Patch with internal solution
containing ~2mM JPW3028

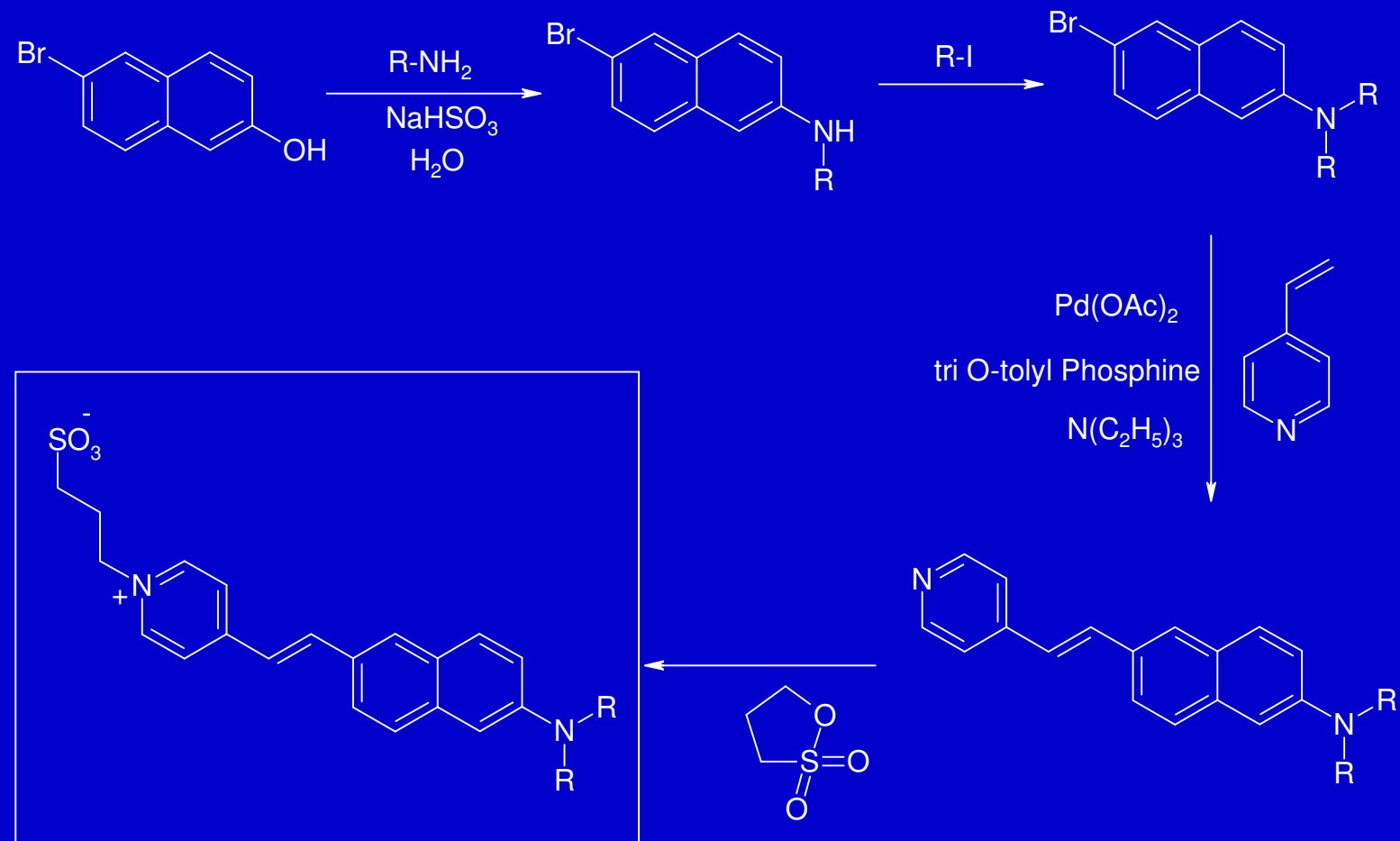


Zhou, W.-L., Y. Ping, J.P. Wuskell, L.M. Loew and
S.D. Antic., Eur J Neurosci. 27:923-936, 2008

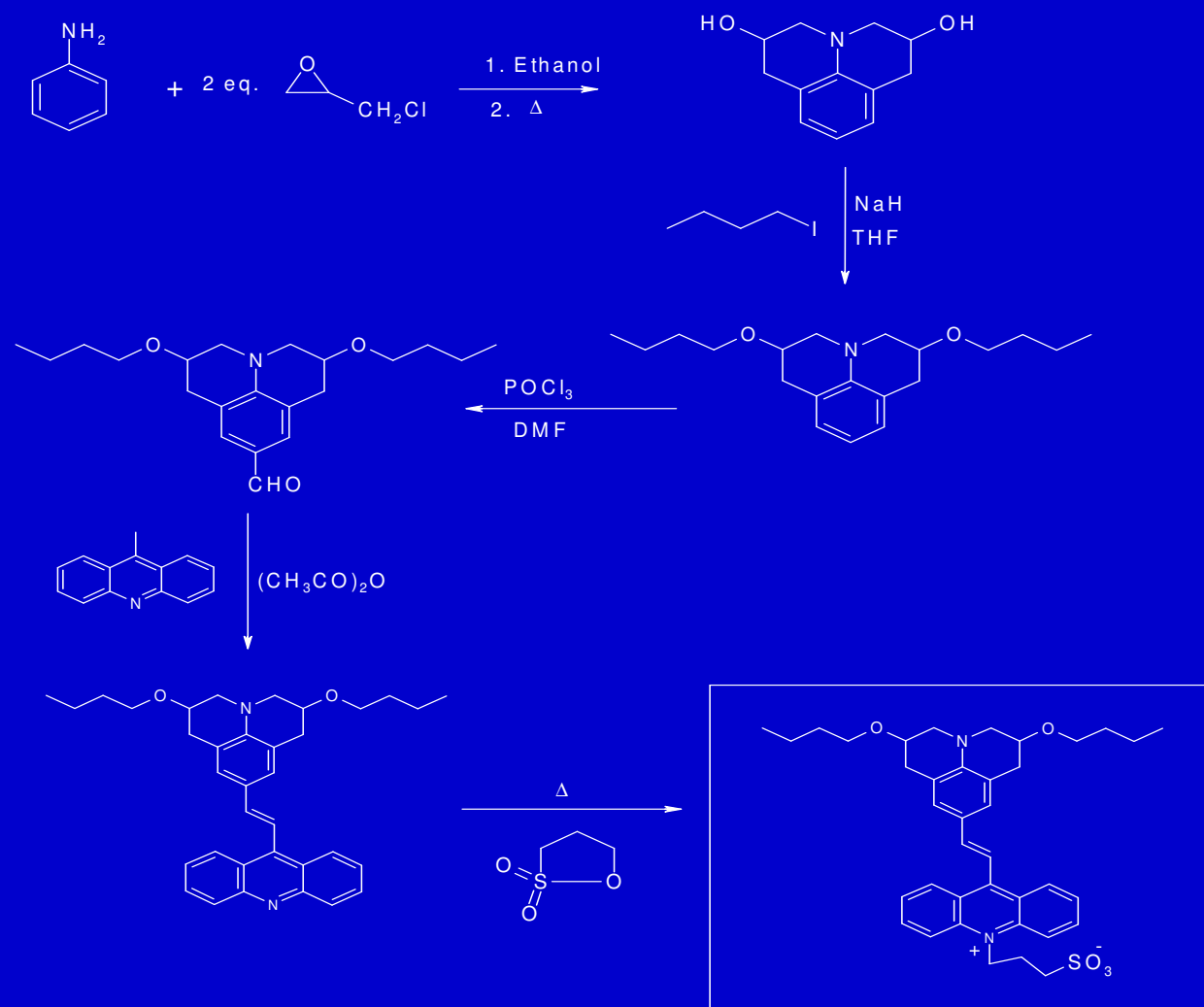


Synthesis of Naphthylstyryl Dyes via the Heck Reaction

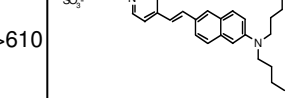
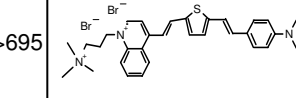
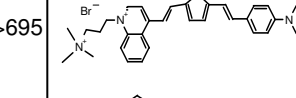
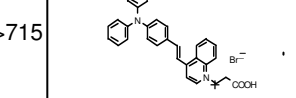
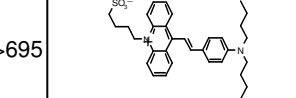
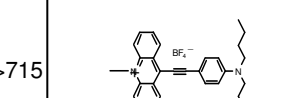
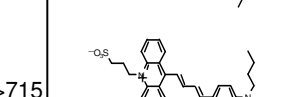
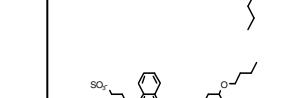
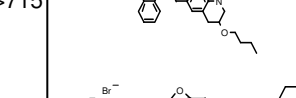
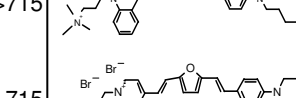
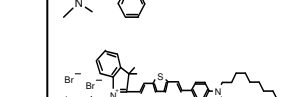
Hassner, A.; Birnbaum, D.; Loew, L. M., *J. Org. Chem.* 1984, 49, 2546-2551.



Synthesis of Styryl Dyes via Aldol Condensation



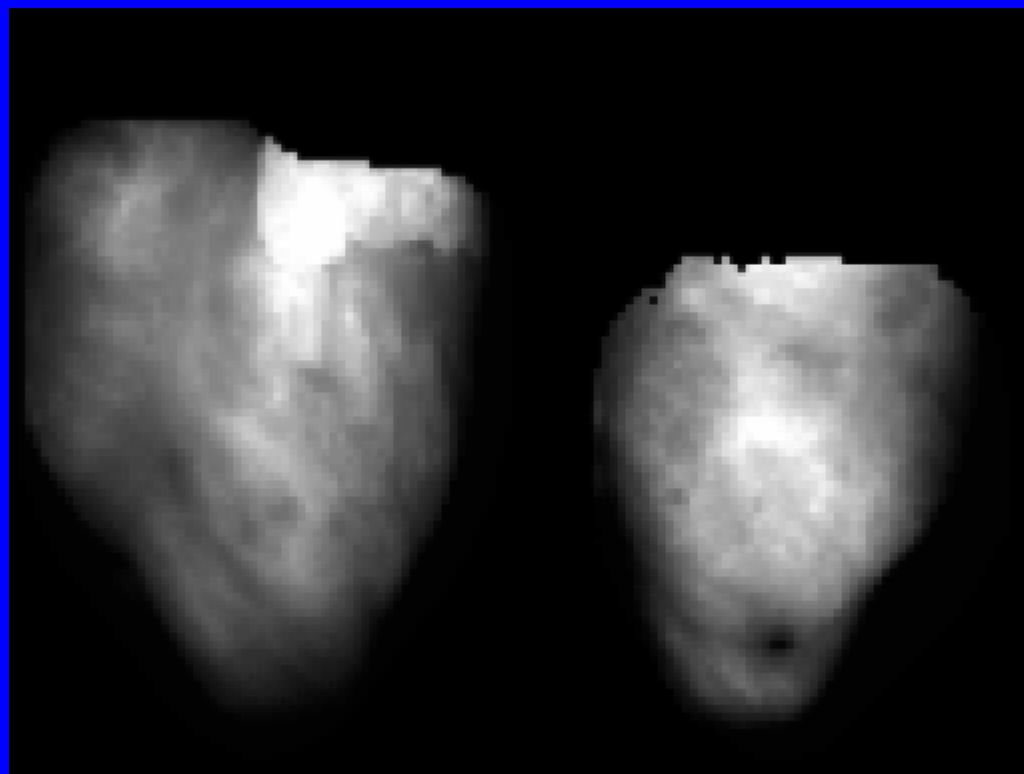
*Linear
Optical
Potential
Sensitivities
of a Selection
of Styryl
Dyes*

Name	ABS (nm)	EM (nm)	$\Delta T/T$ HB	Best $T\lambda$	$\Delta F/F$ HB	Best Ex/EM λ	F S/N Nerve	Nerve Ex/Em λ	Structure
Di-4-ANEPPS	502	723	3.0E-004	515	0.1000	520/ >600	10.0	520/>610	
JPW3066	602	924	8.0E-005	620	0.0140	630/ >695	3.0	620/>695	
JPW3080	630	896	6.0E-005	640	0.0080	645/ >715	26.0	630/>695	
RE 18	524	730	1.0E-004	535	0.0200	530/ >570	8.0	570/>715	
RE 66	663	744	1.0E-004	630	0.0140	630/ >695	7.0	630/>695	
RE 79	638	750	5.5E-006	590	0.0000		0.0	660/>715	
RE 136	696	820	8.0E-005	660	0.0120	670/ >780	2.0	660/>715	
RK57	713	760	8.0E-005	670	0.0090	680/ >780	0.0	660/>715	
JPW4012	620	824	1.2E-004	660	0.0110	670/ >715	5.0	660/>715	
JPW4023	660	964	4.5E-005	640	0.0100	650/ >715	36.0	660/>715	
JPW-5026	706	873	2.1E-004	680	0.0250	680/>780			

Termination of spiral waves during cardiac fibrillation via shock-induced phase resetting

Richard A. Gray and Nipon Chattipakorn

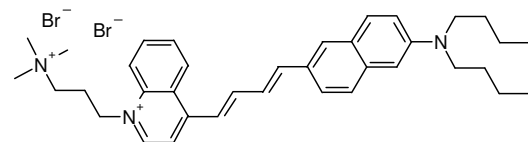
PNAS 2005



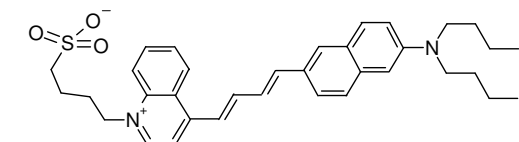
Anterior and Posterior surfaces of pig heart stained with di-4-ANEPPS

Arvydas Matiukas et al. 2007
Activity in blood perfused heart
Ex 650nm, Em >720nm

JPW-6003



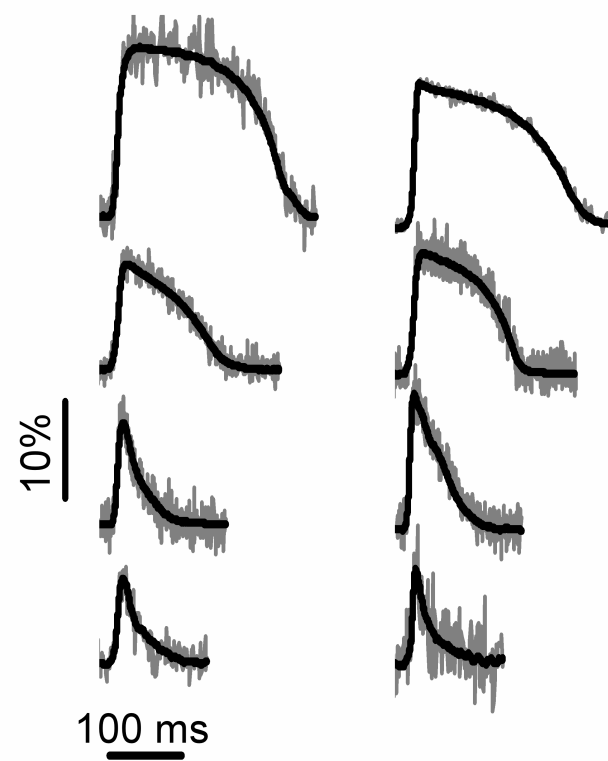
JPW-6033



A

JPW-6003 JPW-6033

Pig



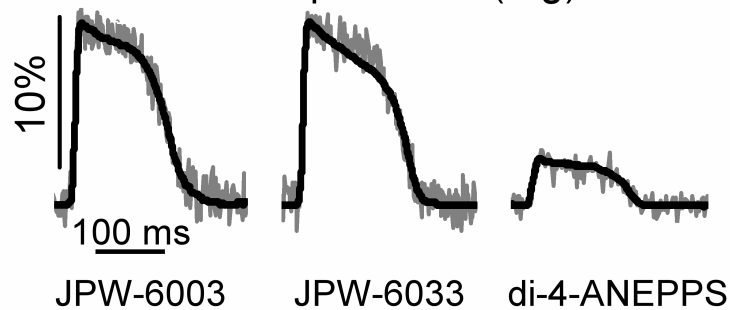
Guinea Pig

Rat

Mouse

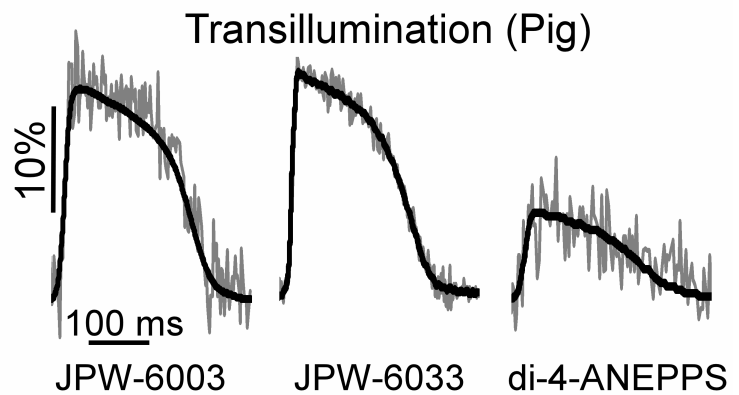
B

Blood-perfusion (Pig)



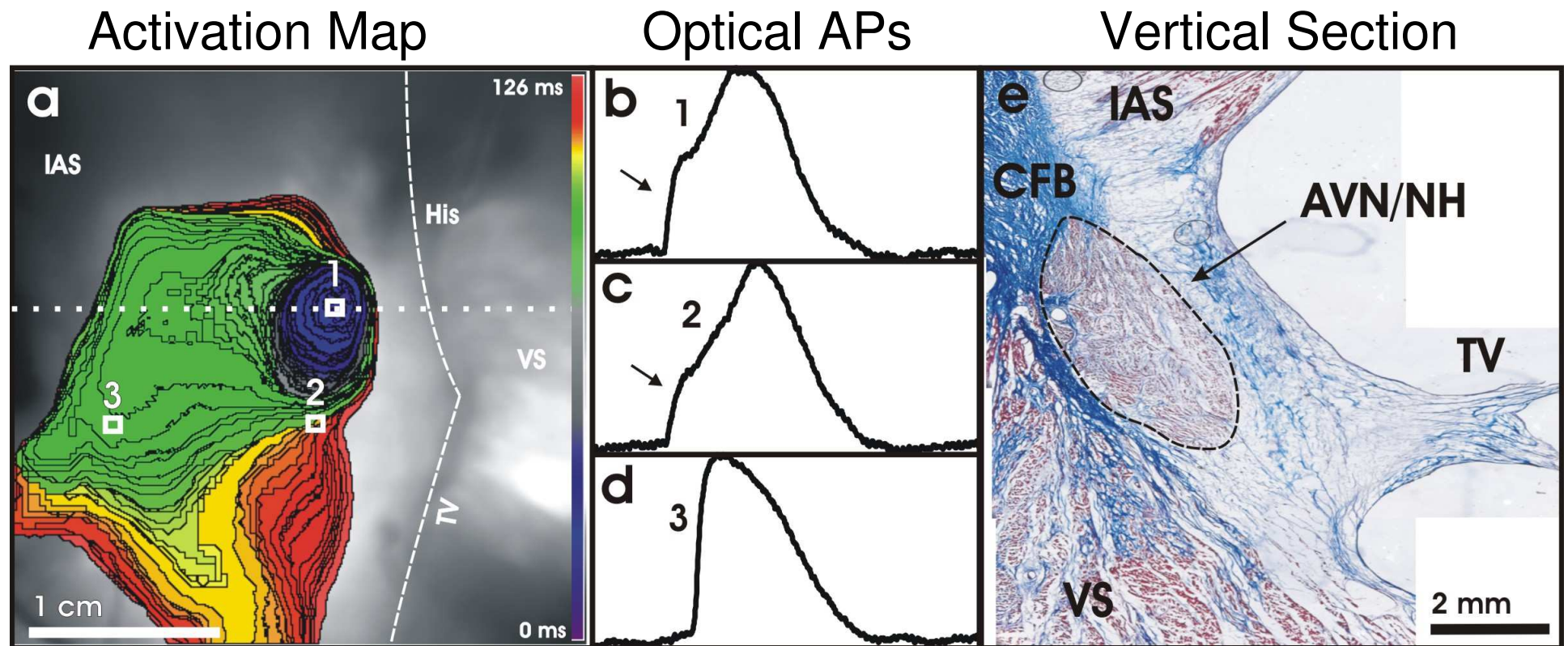
C

Transillumination (Pig)



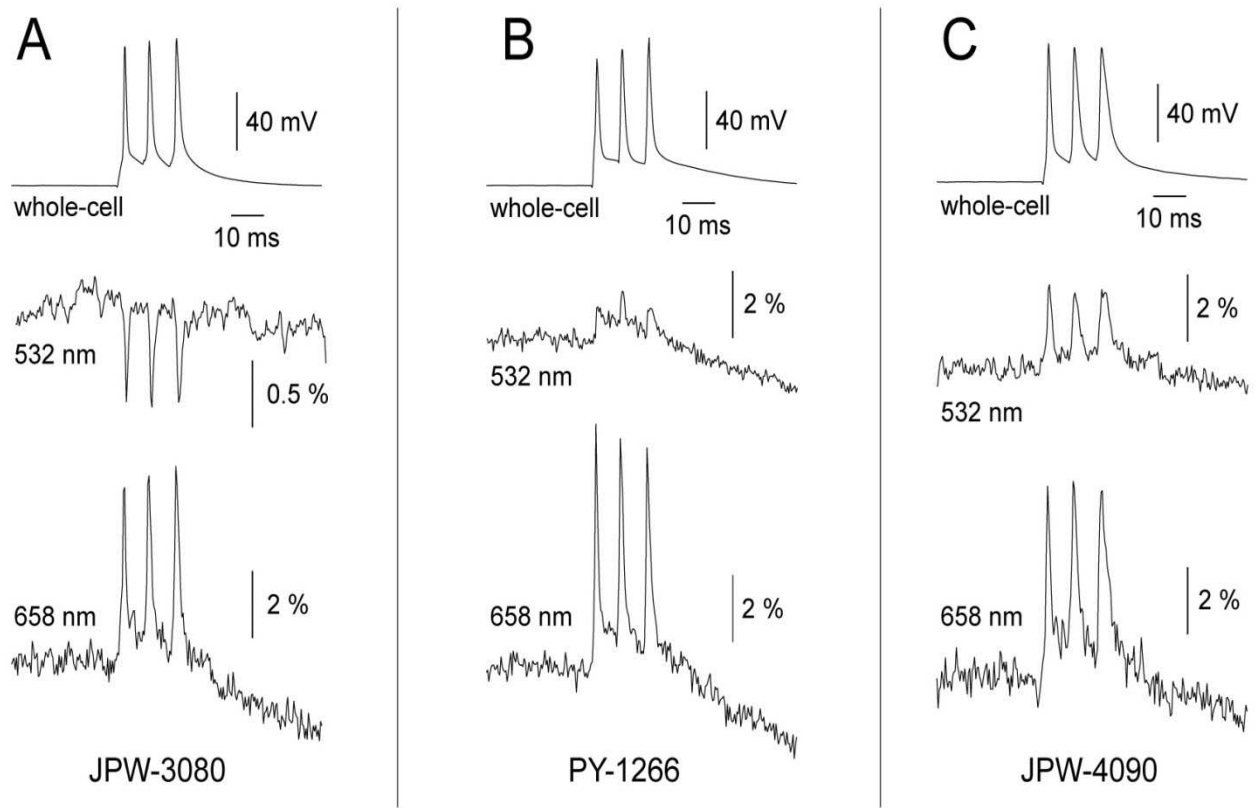
Optical Mapping of the *Human Atrioventricular Junction* using di-4-ANBDQBS

Igor Efimov, Washington U.

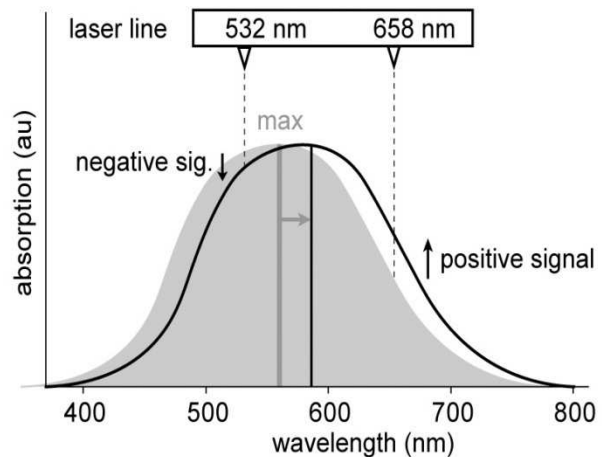


The early APs originate from the 1mm deep AVN
These could not be imaged with older VSDs

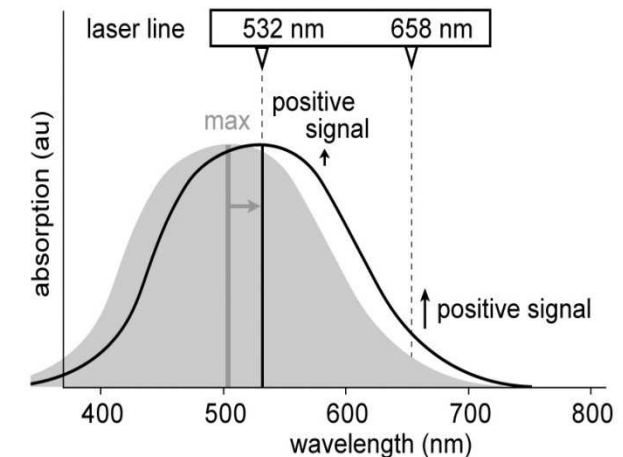
Zhou, W.-L., Y.
Ping, J.P. Wuskell,
L.M. Loew, and
S.D. Antic. 2007.

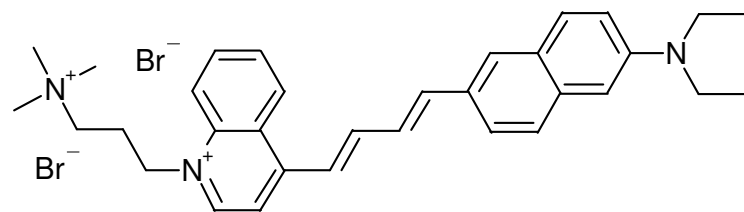


D Spectral shift for JPW-3080

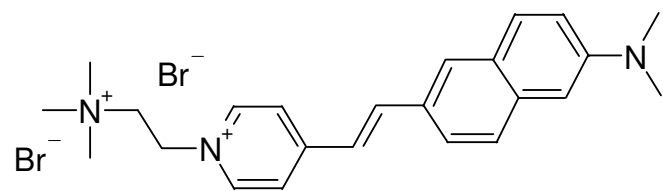


E Spectral shift for JPW-4090

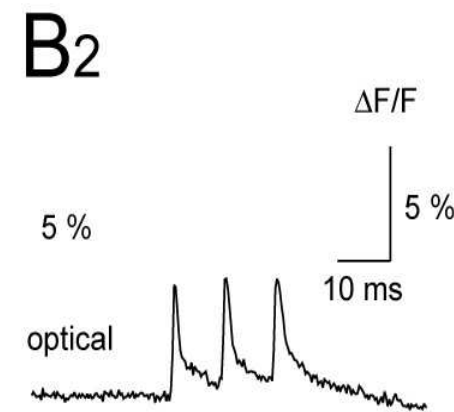
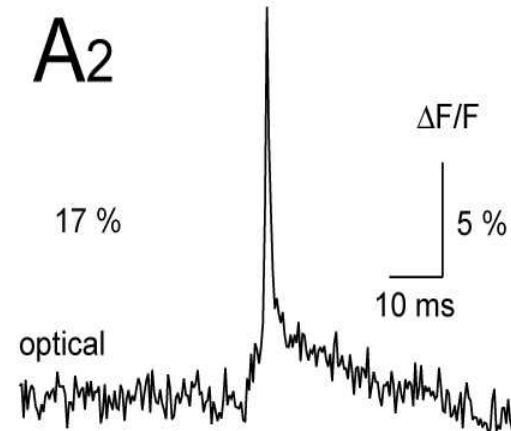




JPW-4090
Ex 658nm

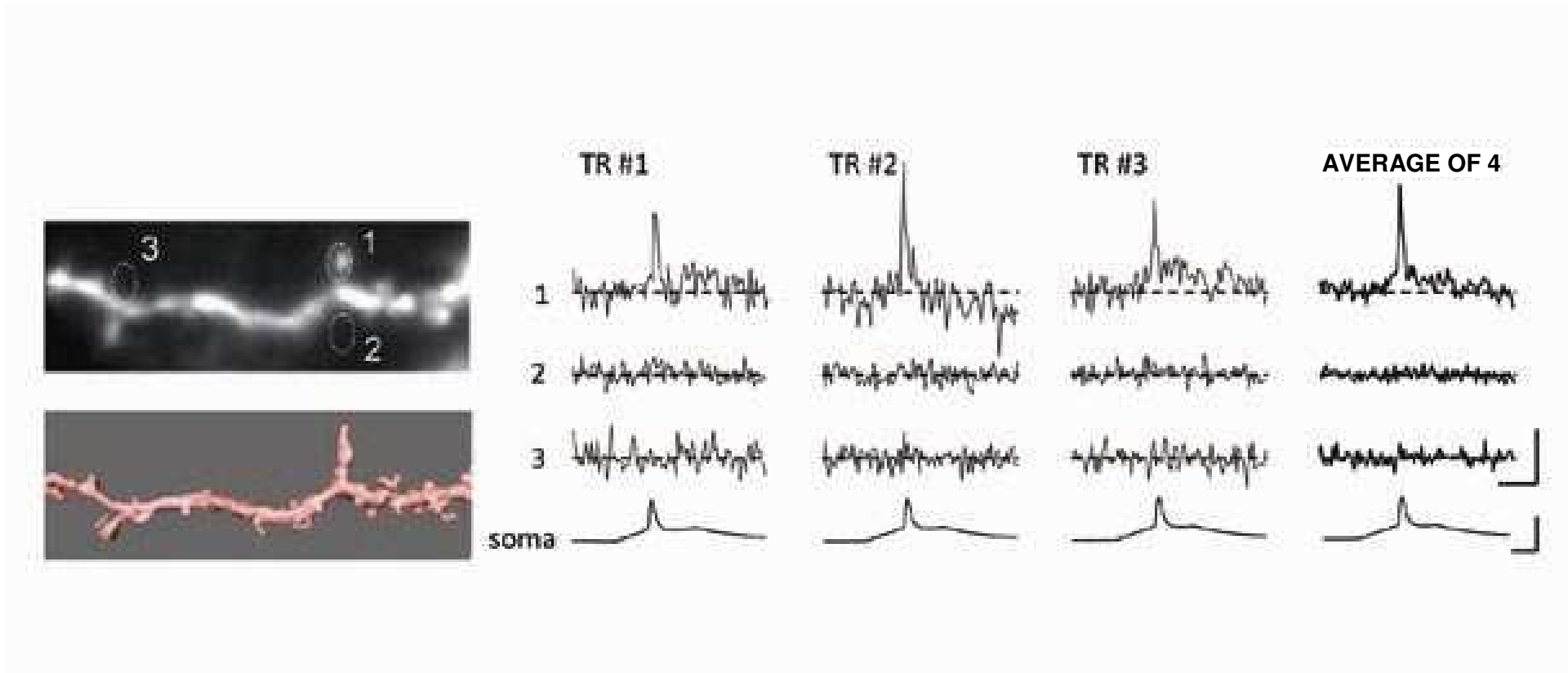


JPW-3028
Ex 532nm



Back Propagating APs in Single Dendritic Spines in a Brain Slice

Dejan Zecevic



In vitro OCT and optical mapping of the human AVJ using novel near infrared voltage sensitive dye Di-4-ANBDQBS

Igor Efimov, Washington U.

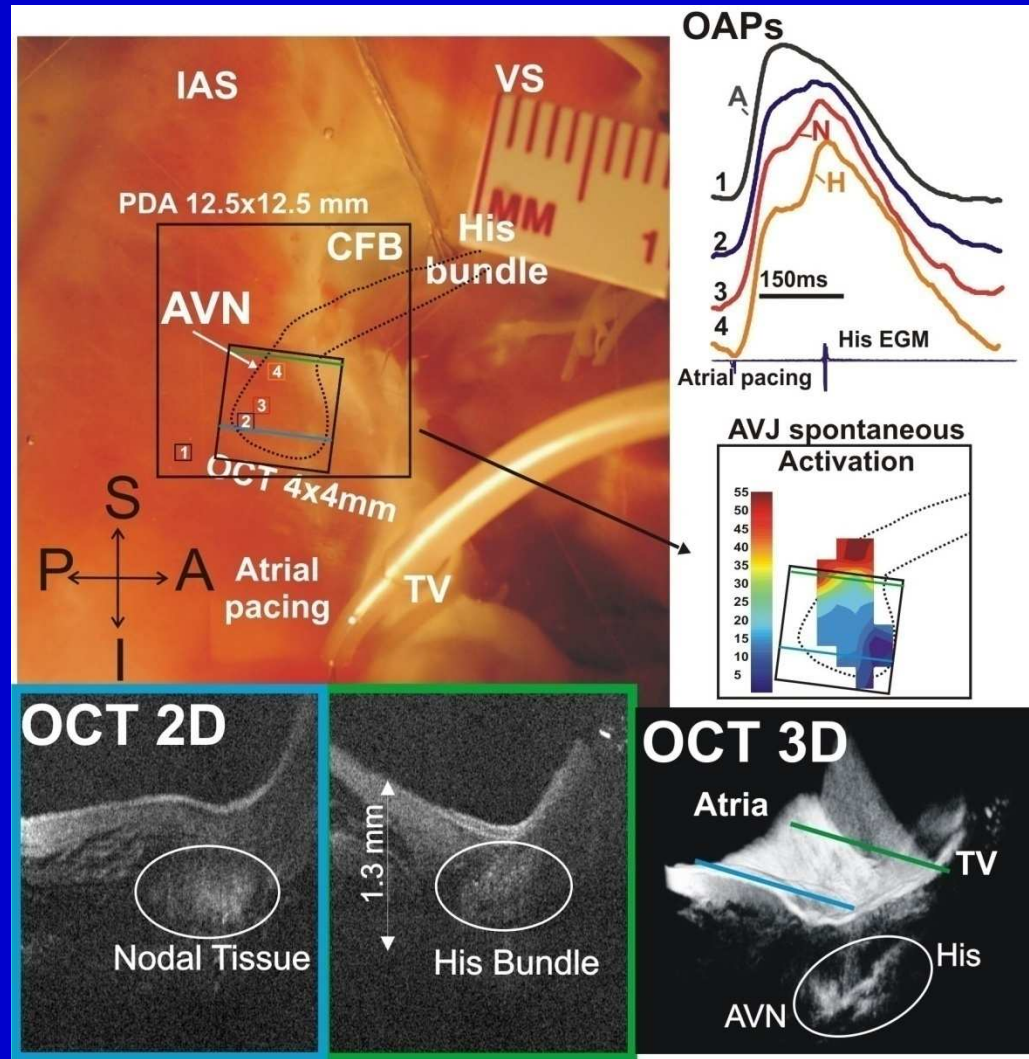


Table 3. Half-lifes of total and voltage-sensitive fluorescence of JPW-6003 and JPW-6033(Tyrode's-perfusion, epifluorescence).

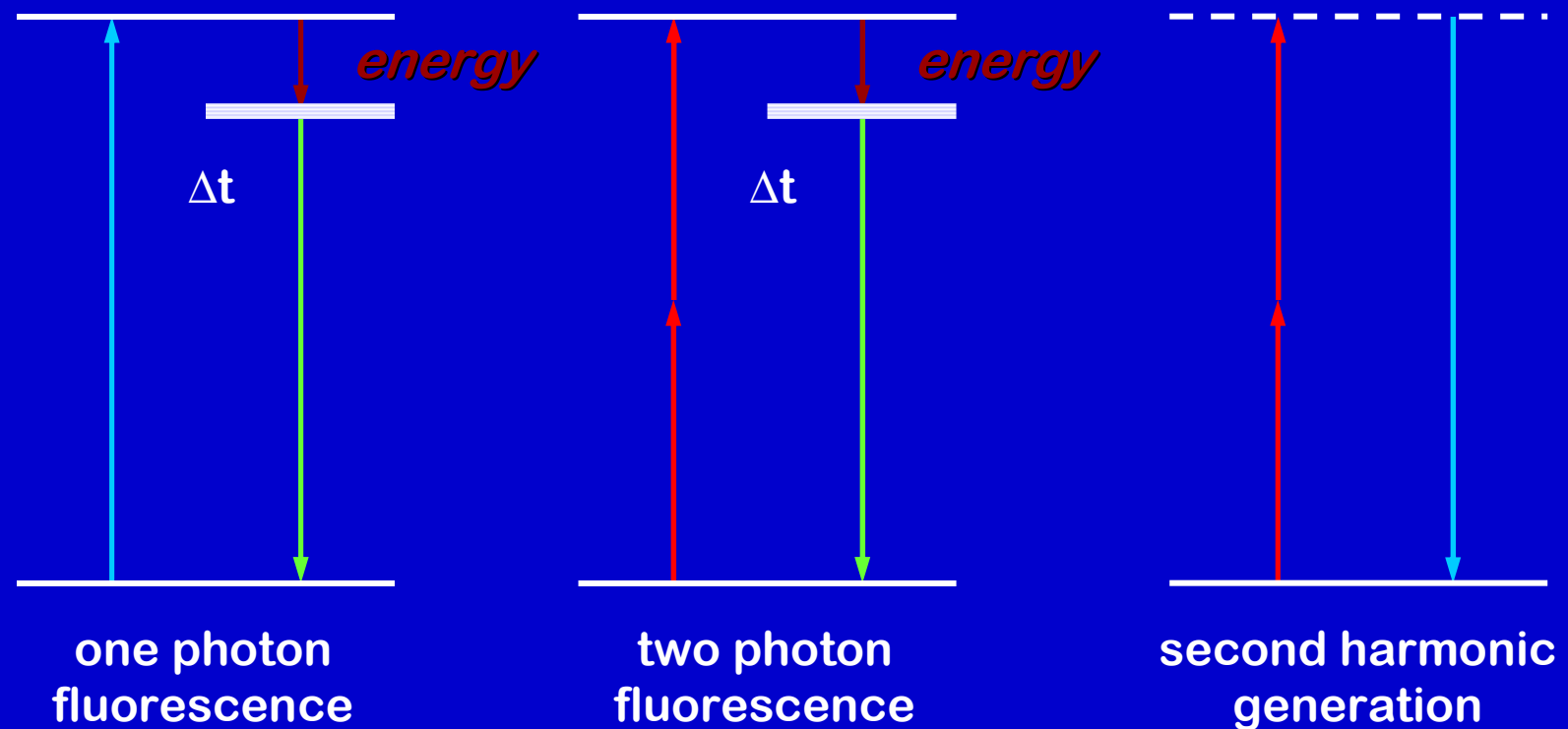
Animal	Dye/Parameter					
	JPW-6003		JPW-6033		di-4-ANEPPS	
	$\tau_{1/2}(F)$	$\tau_{1/2}(\Delta F/F)$	$\tau_{1/2}(F)$	$\tau_{1/2}(\Delta F/F)$	$\tau_{1/2}(F)$	$\tau_{1/2}(\Delta F/F)$
Pig	>160**	210**	>160**	165**	17±3	67±3
Rat	>170	161±11	>160	119±15	15±2	32±2
Guinea pig	>180	149±16	>160	131±15	23±2	22±2
Mouse	>120	105±15	>90	80±9	-	-

Values are means ± SD (in minutes). $\tau_{1/2}(F)$ - half-life (washout time) for normalized total fluorescence. $\tau_{1/2}(\Delta F/F)$ – half-life of relative voltage-sensitive fluorescence. Last column shows data for di-4-ANEPPS.

** extrapolated.

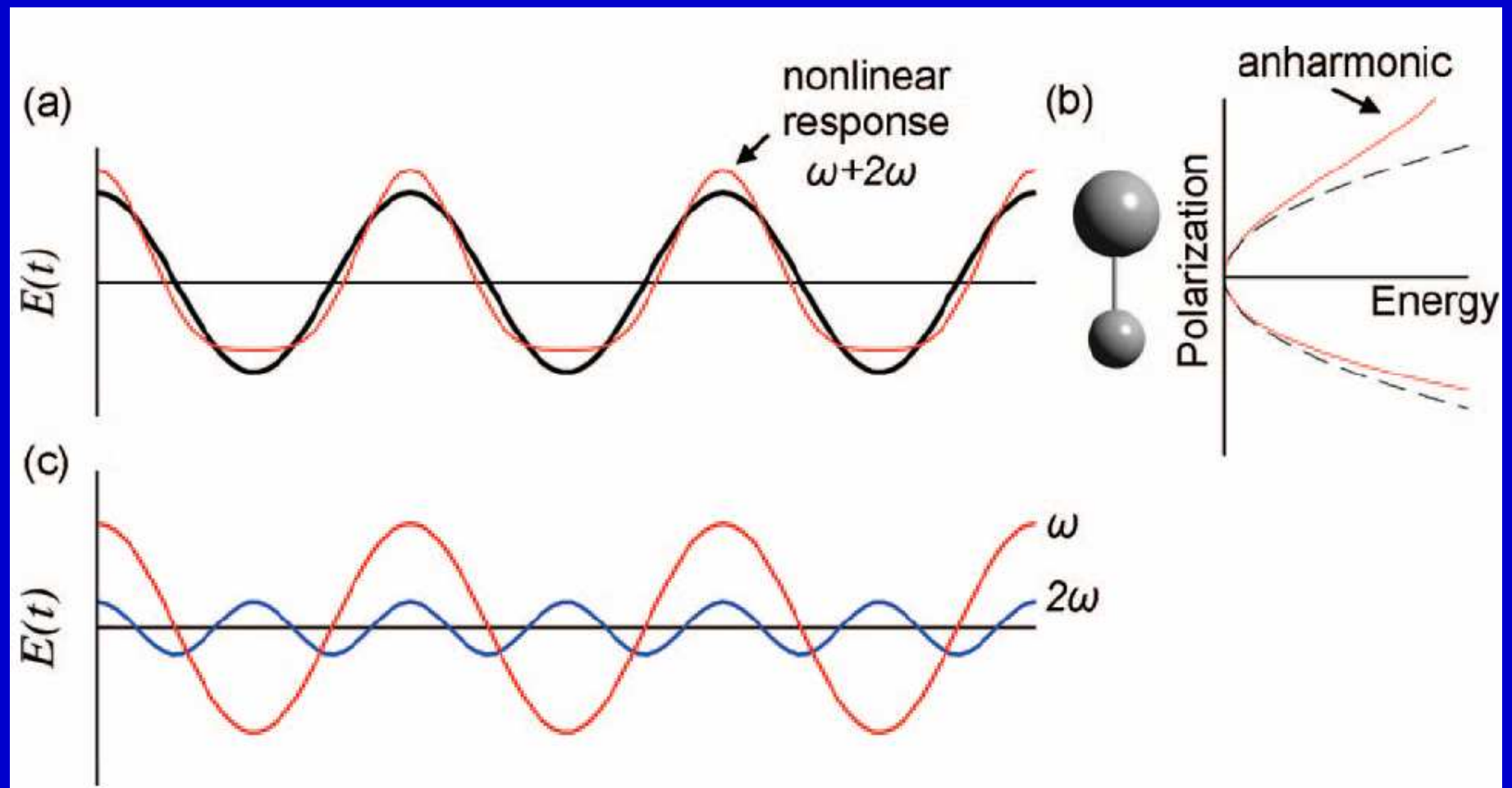
Second Harmonic Generation

A Coherent Near-Instantaneous Process



Second Harmonic Generation

A Coherent Near-Instantaneous Process



Non-Linear Polarisability

$$P = \chi^{(1)} \square E + \chi^{(2)} \square E \square E + \chi^{(3)} \square E \square E \square E +$$

...

- | **multi-photon absorption**
- | **harmonic generation**
- | **voltage sensitivity**

Simple Relationships Govern SHG

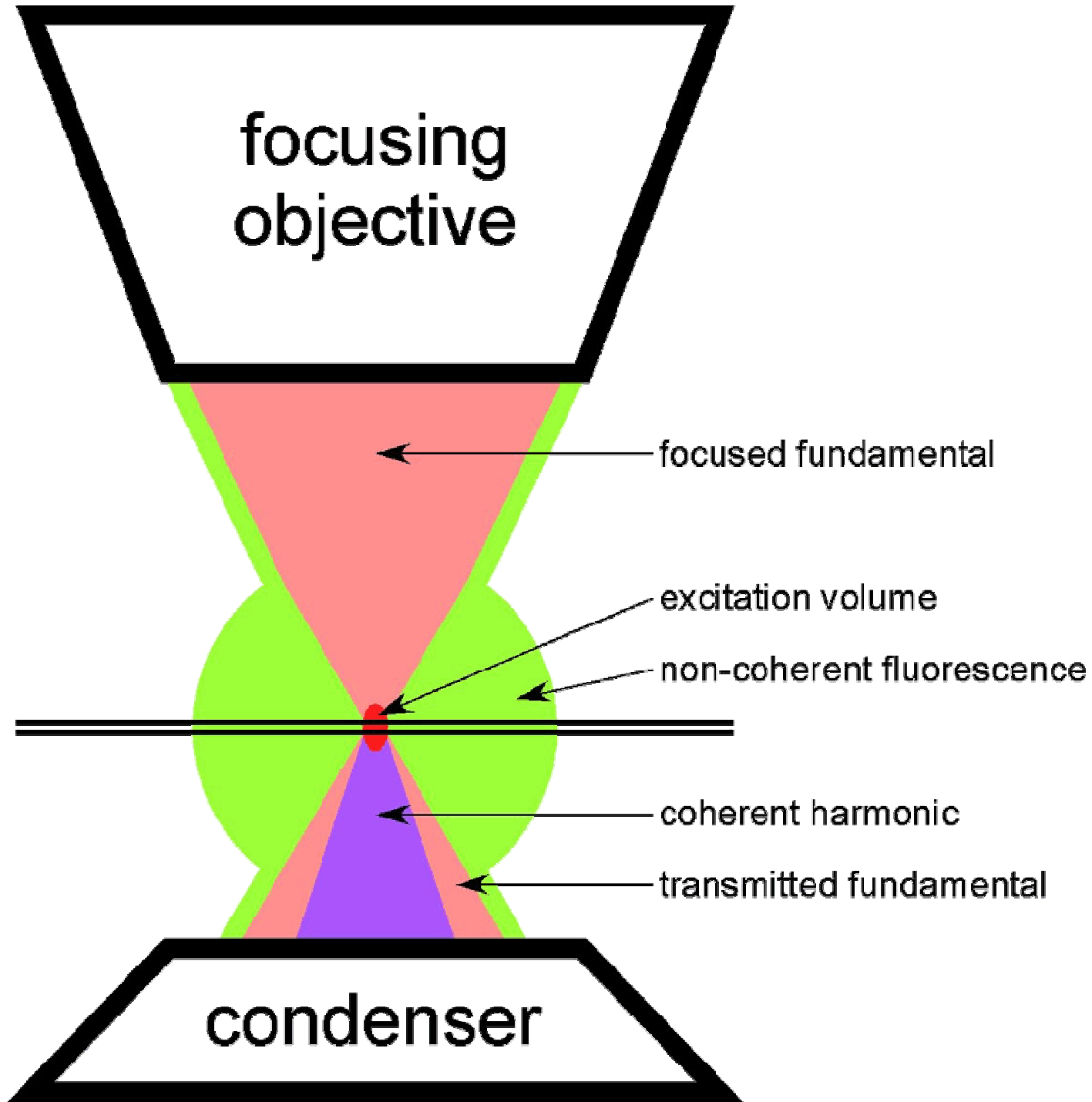
$$I(2\nu) \propto [\chi^{(2)} I(\nu)]^2$$

$\chi^{(2)}$ is the second-order nonlinear susceptibility (a bulk property)

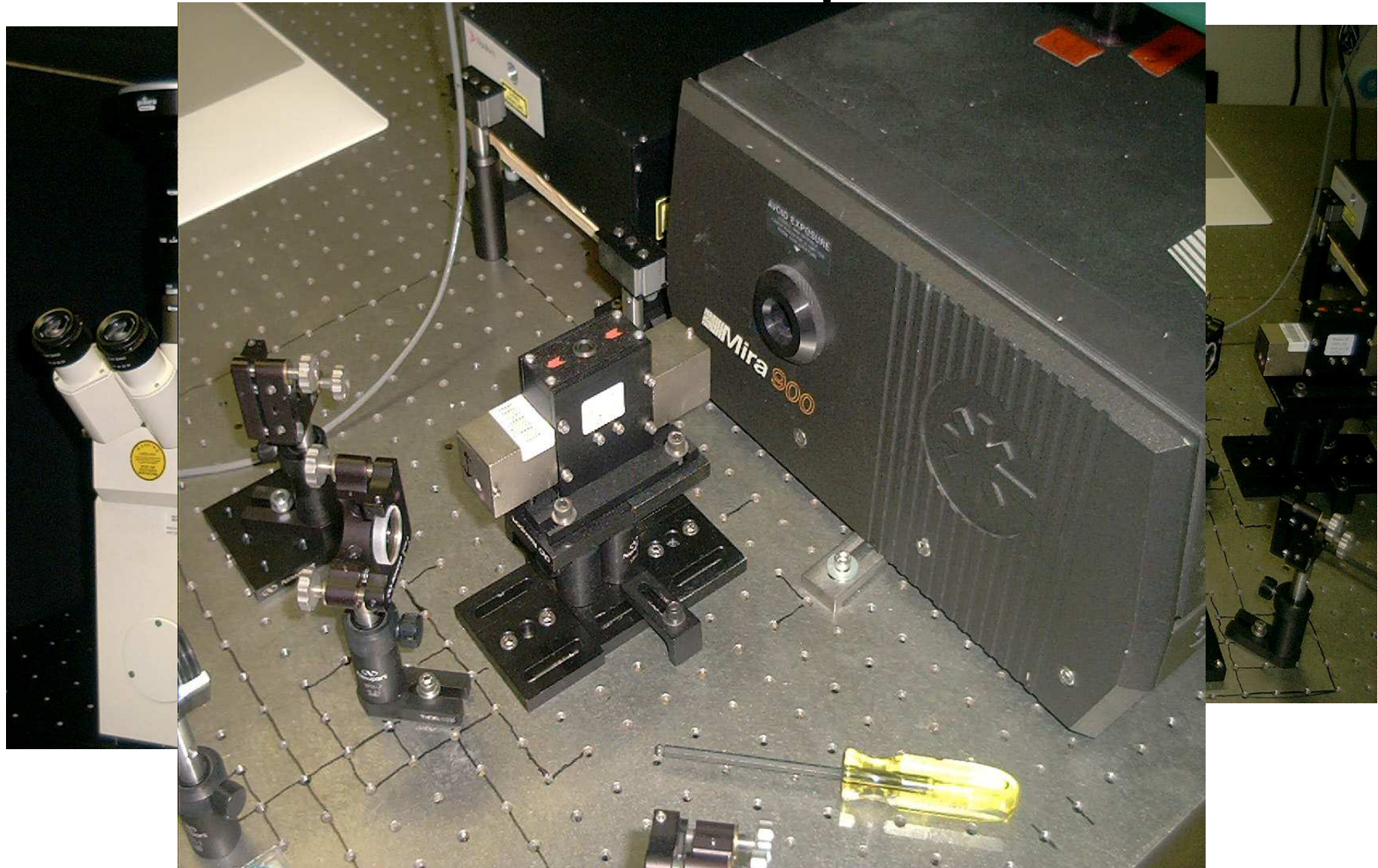
$$\chi^{(2)} = N_s \langle \beta \rangle_{OR}$$

β is the molecular hyperpolarizability of the SHG active molecules and N_s is the surface density of these molecules

- » SHG is proportional to the square of the light intensity
- » SHG vanishes for a centrosymmetric distribution of active molecules
- » SHG is proportional to the square of the density of active molecules



The Second Harmonic Microscope



SHG versus Multi-Photon Fluorescence

SHG

- Excitation depends on square of power.
- Intensity depends on the square of staining level.
- Few photons are emitted.
- Emits coherently in forward direction — need short- and band-pass filtering.
- Emitted light is polarised.
- Emission band is narrow.

MPF

- Excitation depends on square or cube of power.
- Intensity depends linearly on staining level (until quenching).
- Many photons are emitted.
- Emits incoherently in all directions — need short-pass filtering.
- Emitted light is unpolarised.
- Emission band is broad.

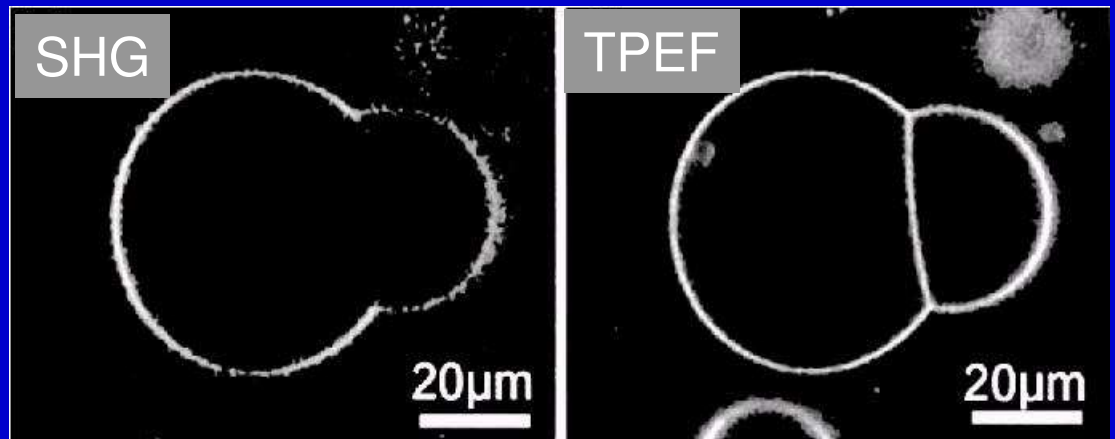
Perturbation Theory Model for Resonance Enhanced β of CT Dyes

$$\beta = \frac{4\mu_{eg}^2(\mu_e - \mu_g)}{3h^2(\nu_{eg}^2 - \nu^2)(\nu_{eg}^2 - 4\nu^2)}$$

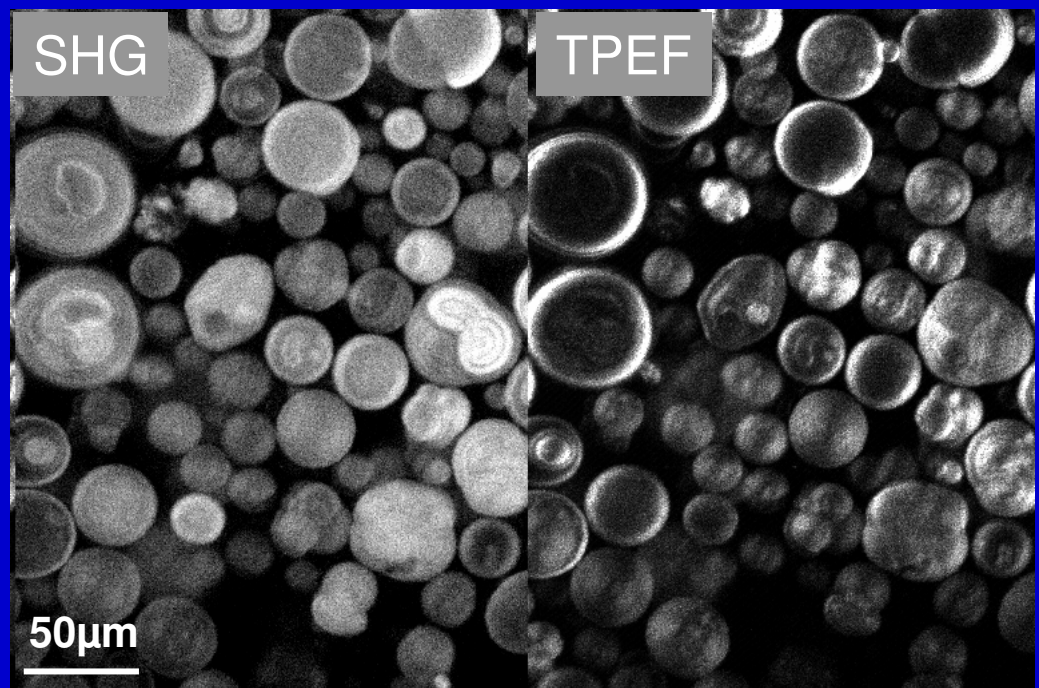
- » SHG can be resonance enhanced - i.e. when $\nu_{eg} \approx 2\nu$
- » SHG-active molecules should have large transition moments
- » SHG-active molecules should have large dipole moment changes upon excitation

SHIM of Liposomes Illustrate Differences in Image Contrast Compared to TPEF

SHG is extinguished in apposed regions of membranes of adherent liposomes
(Moreaux, Sandre, Blanchard-desce, Mertz, *Opt. Lett.*, 2000)

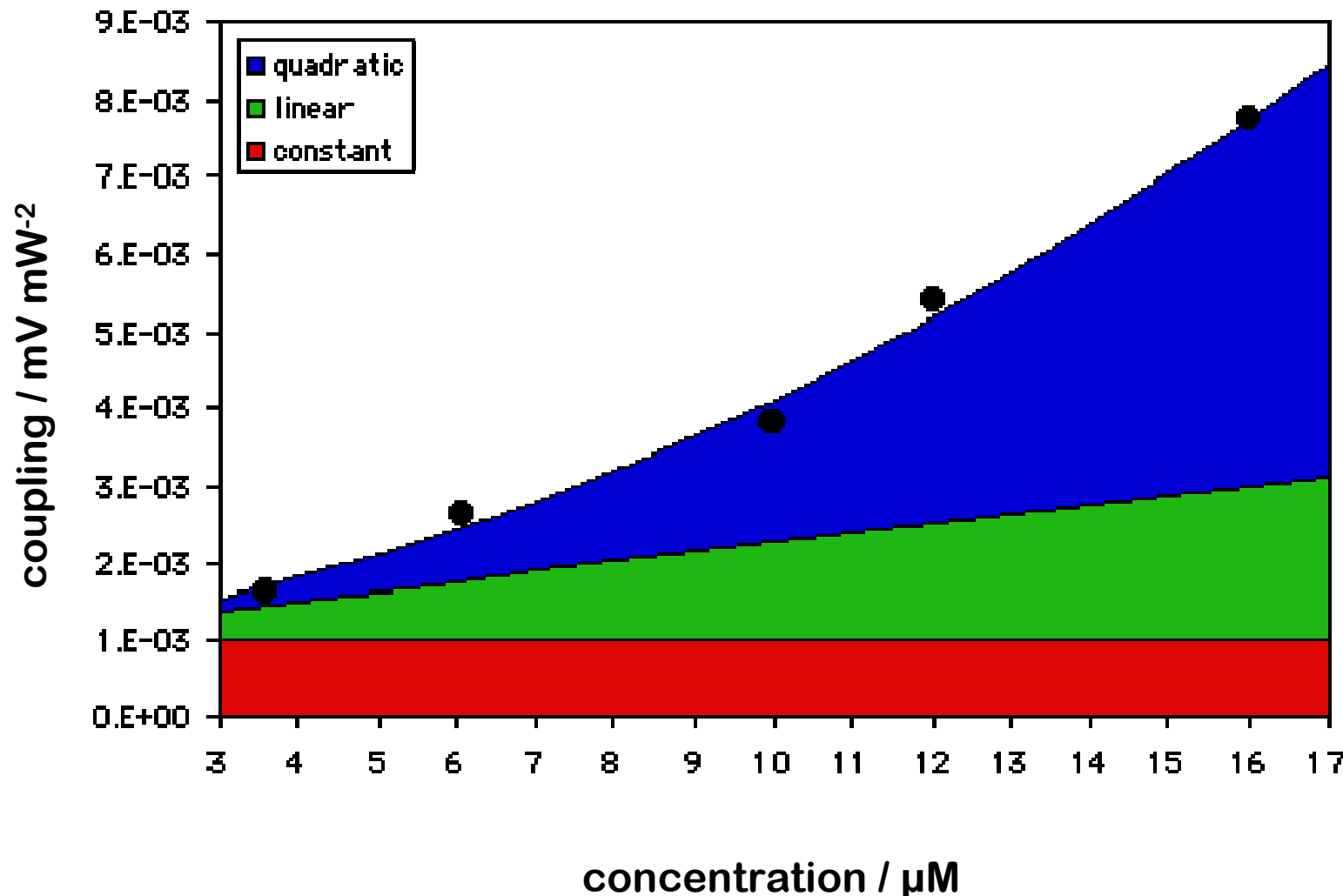


At high concentrations of a chiral dye, SHIM and TPEF show very different patterns



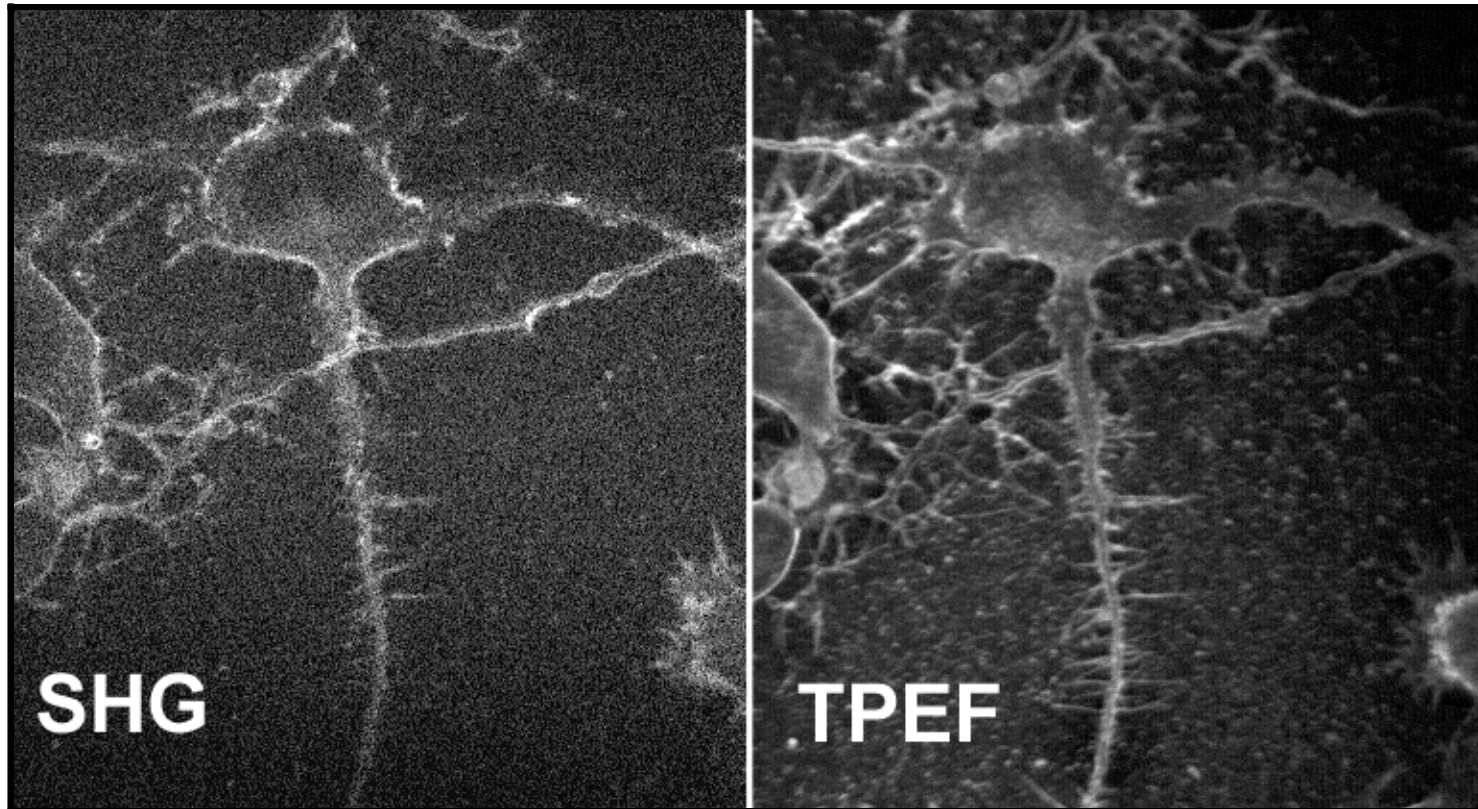
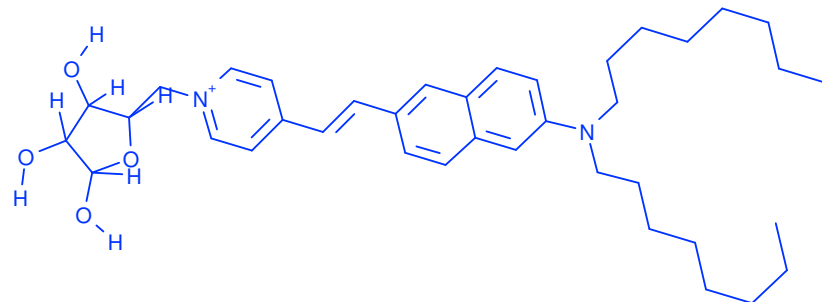
SHG Dependence on Staining

unilamellar vesicles stained with di-8-ANEPMRF



Two Photon and SHIM of Neurons Stained with a Chiral Dye

Campagnola et al., 1999

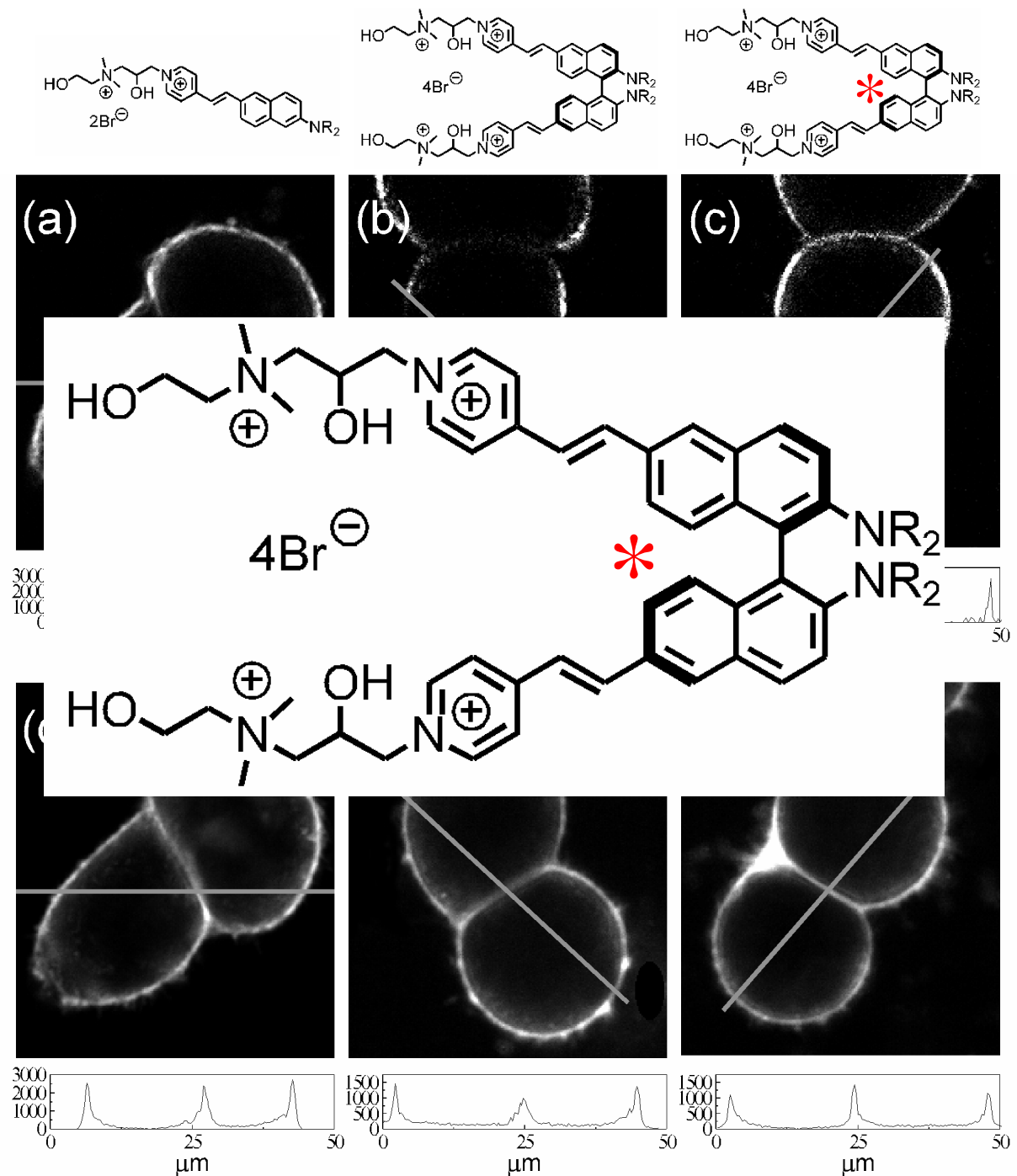


For membrane staining styryls,
SHG is ca. 2X higher for chiral vs. achiral dye structures

Ping Yan, et al.

Unique Contrast Patterns
from Resonance-Enhanced
Chiral SHG of Cell
Membranes.

J. Am. Chem. Soc. 2006.

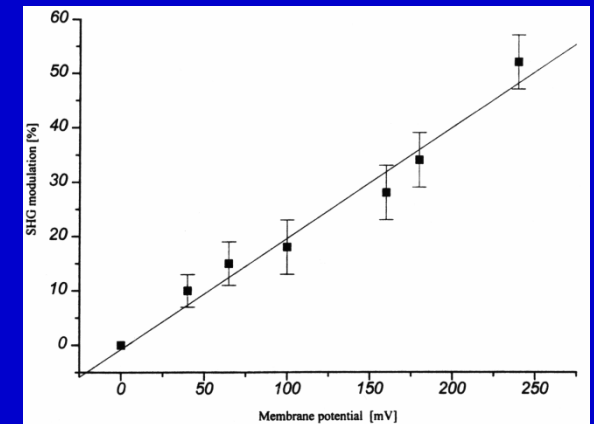


SHG is Highly Sensitive to Membrane Potential

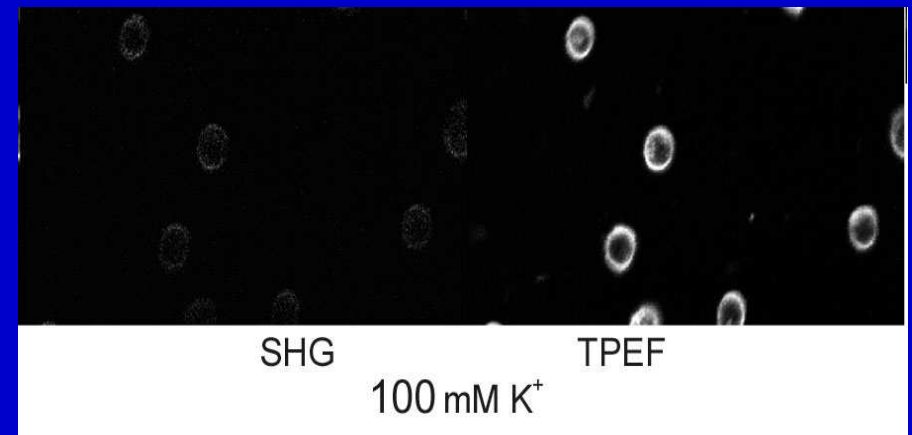
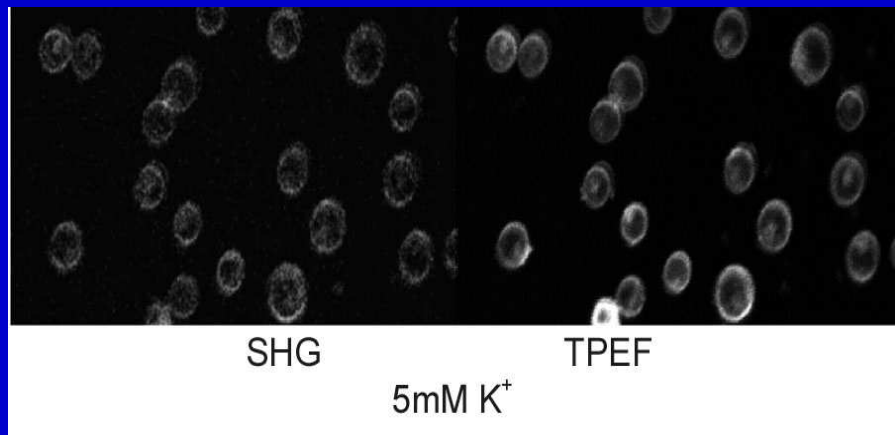
$\Delta F/F$ for di-4-ANEPPS = 10%/100mV

$\Delta \text{SHG}/\text{SHG}$ on lipid bilayer =
20%/100mV (Bouevitch, 1993)

$\Delta \text{SHG}/\text{SHG}$ on photoreceptors =
40%/100mV (Peleg, 1996)



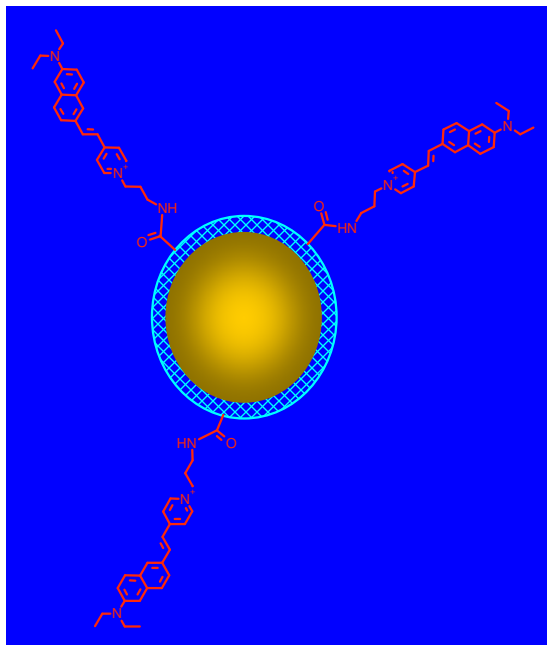
SHIM of L1210 Lymphocytes (Campagnola et al., 1999)



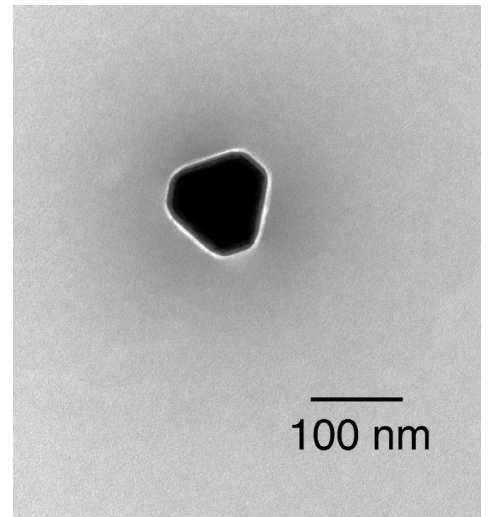
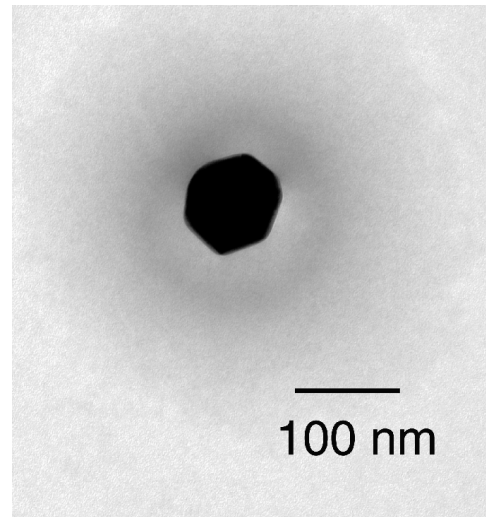
$$\frac{(\text{SHG}/\text{TPEF})_{\text{pol}}}{(\text{SHG}/\text{TPEF})_{\text{depol}}} = 2 \quad (\approx 100\%/\text{100mV})$$

Can SHG be enhanced near gold nanoparticles?

- Roughened metal surfaces can enhance non-linear optical signals by 10^4
- Gold particles and gold-antibody conjugates onto dye stained cells increases SHG by ca. one order of magnitude (Peleg et al., 1996; 1999)



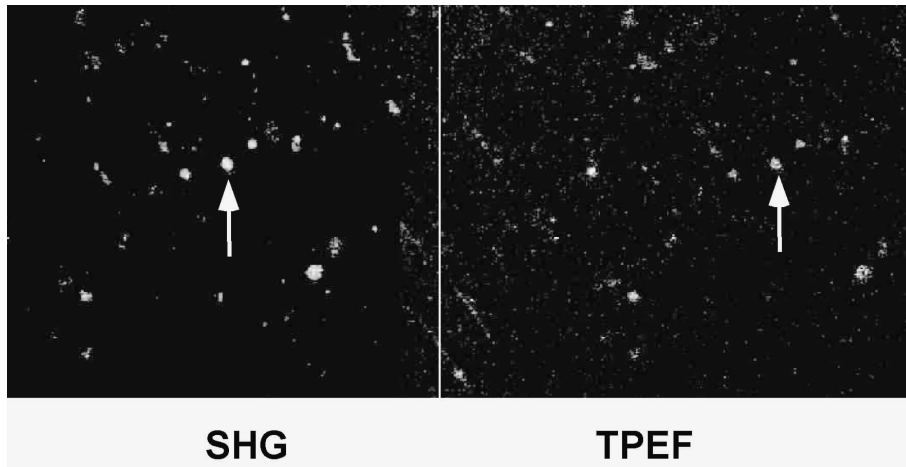
Cartoon of polymer encapsulated Au nanoparticles conjugated to aminonaphthylstyryl pyridinium dyes.



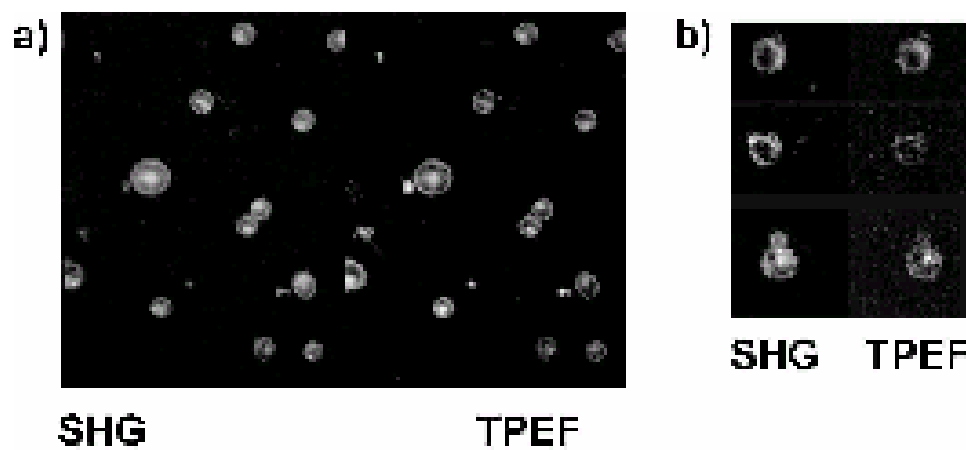
Negative stain TEM of bare Au (left) and polyacrylamide encapsulated Au nanoparticles

Clark et al., JACS 2000

SHG from styryl dye conjugated polymer encapsulated gold nanoparticles



Nonlinear optical images of dye conjugated Au nanoparticles. The signal is at least 100 fold higher than the same dye conjugated to 100nm latex beads.



Nonlinear optical images of L1210 cells. Left - cells stained with JPW4041; right - cells stained with polymer encapsulated dye-Au conjugate.

$$SHG_{enhancement} = \frac{[SHG/TPEF]_{gold}}{[SHG/TPEF]_{nogold}} = 21 \pm 9$$

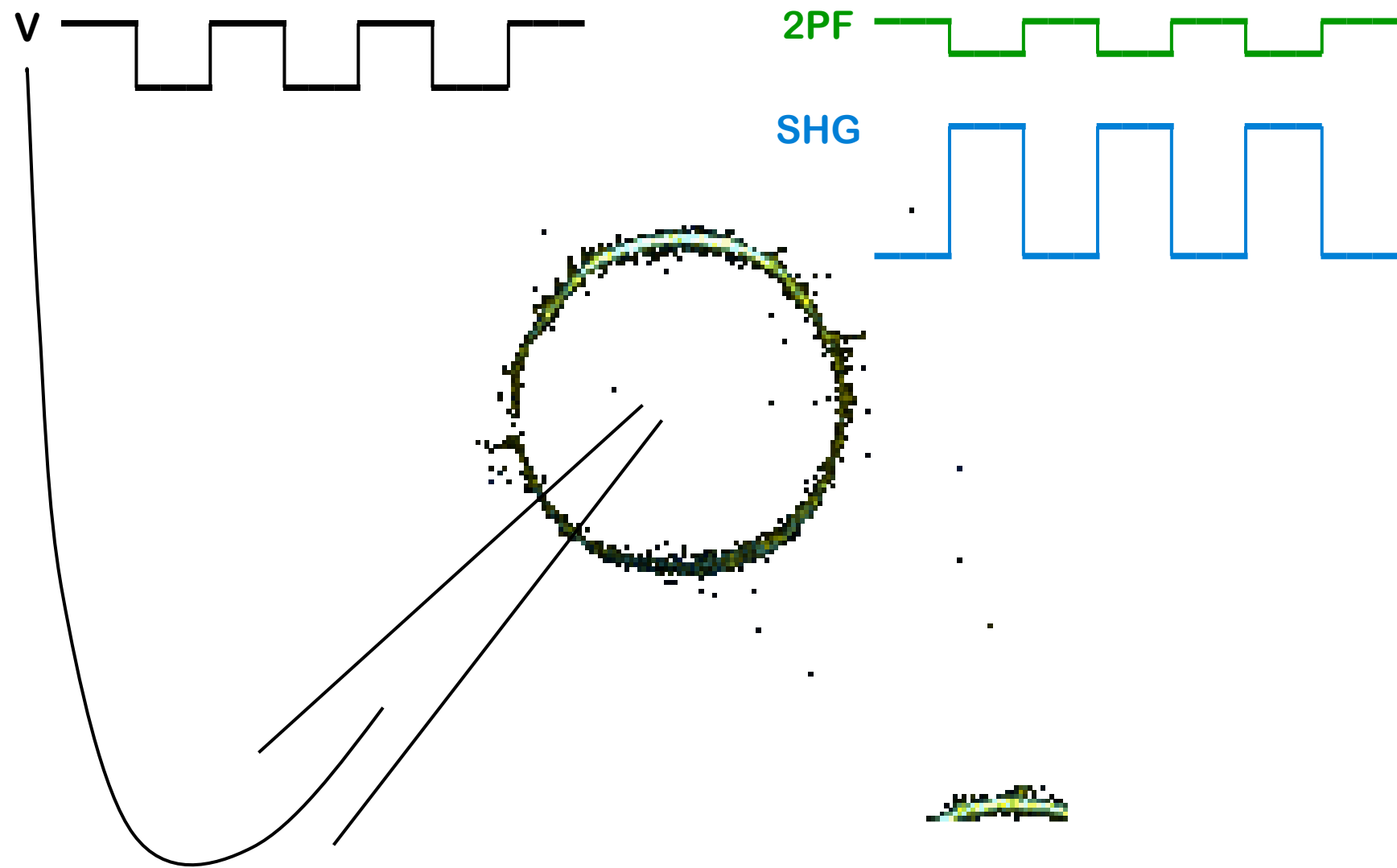
Potentiometric SHIM

A constant electric field may modulate the SHG via $\chi^{(3)}$, so that SHG from a cellular membrane may depend on trans-membrane potential.

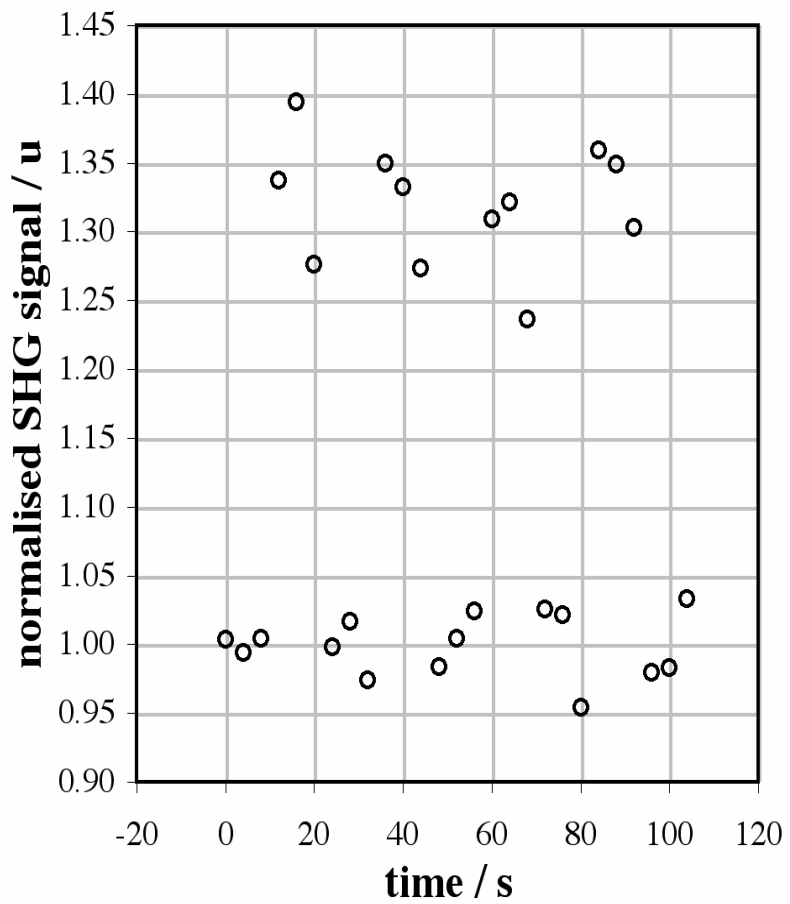
$$P = \chi^{(2)} \square E(\omega) \square E(\omega) + \chi^{(3)} \square E \square E(\omega) \square E(\omega)$$

$$= \chi_{\text{eff}}^{(2)}(E) \square E(\omega) \square E(\omega)$$

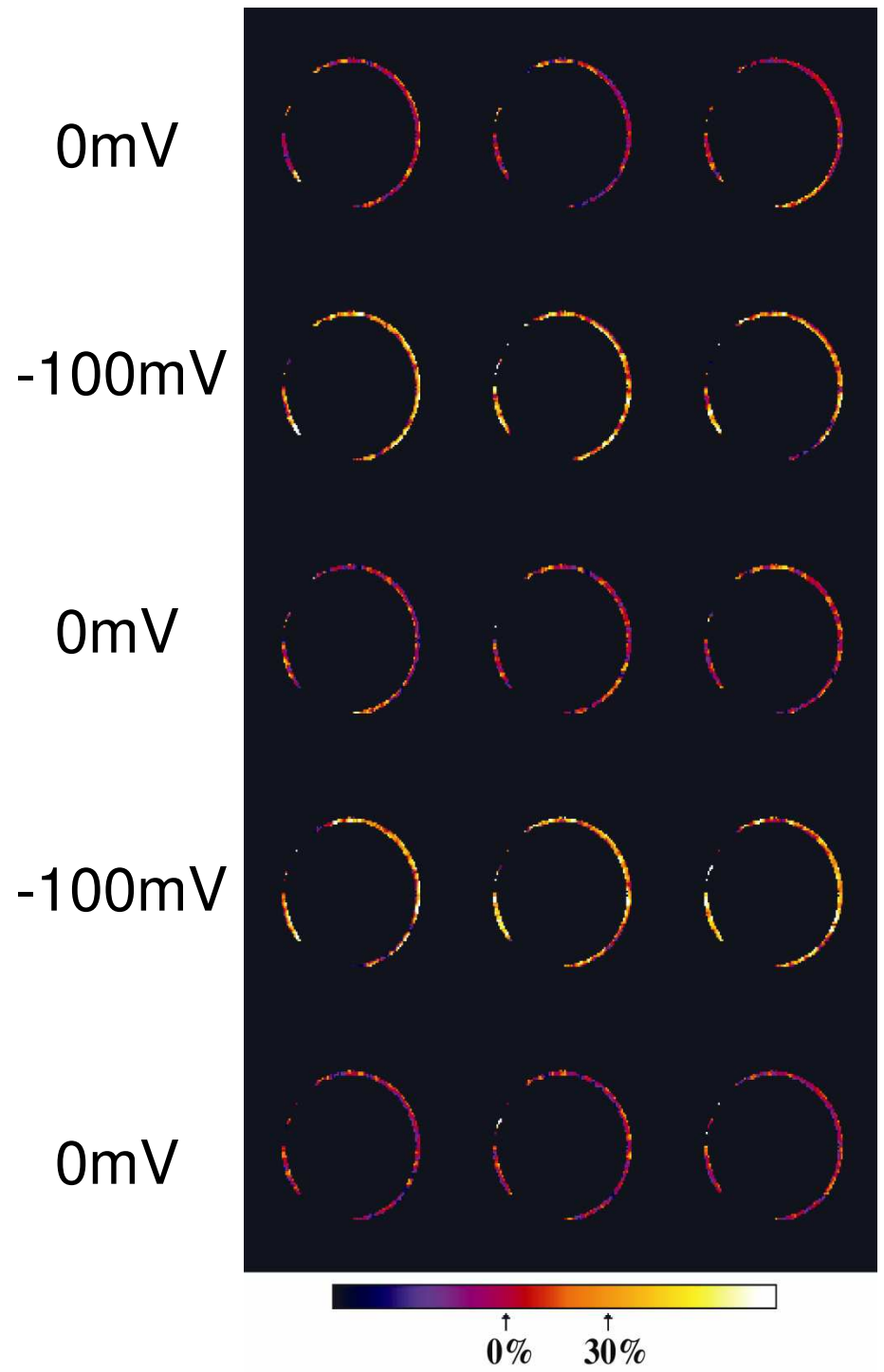
Non-Linear Imaging of Patch Clamped Cells



A. Millard, A. Lewis,
P. Campagnola
Large Sensitivity to
Membrane Potential

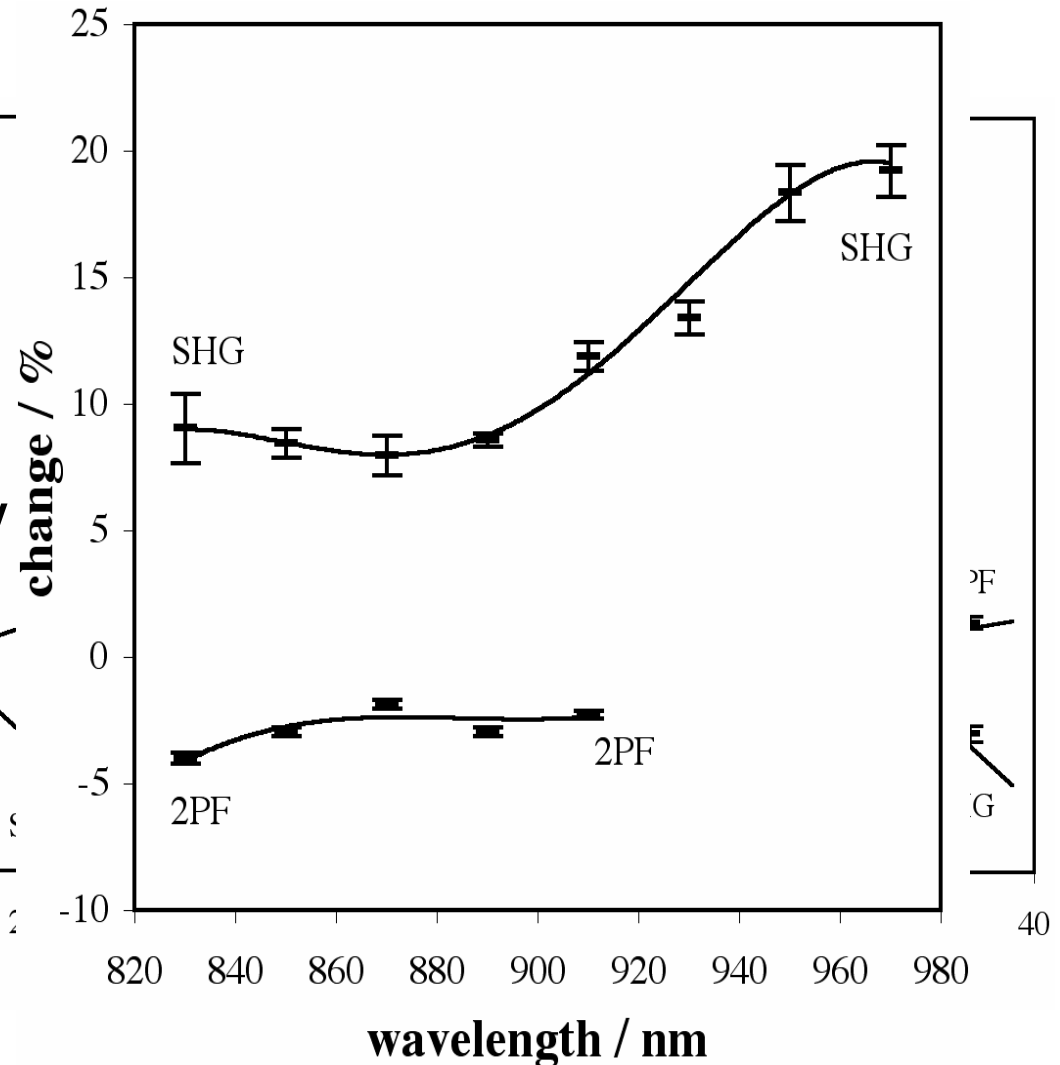
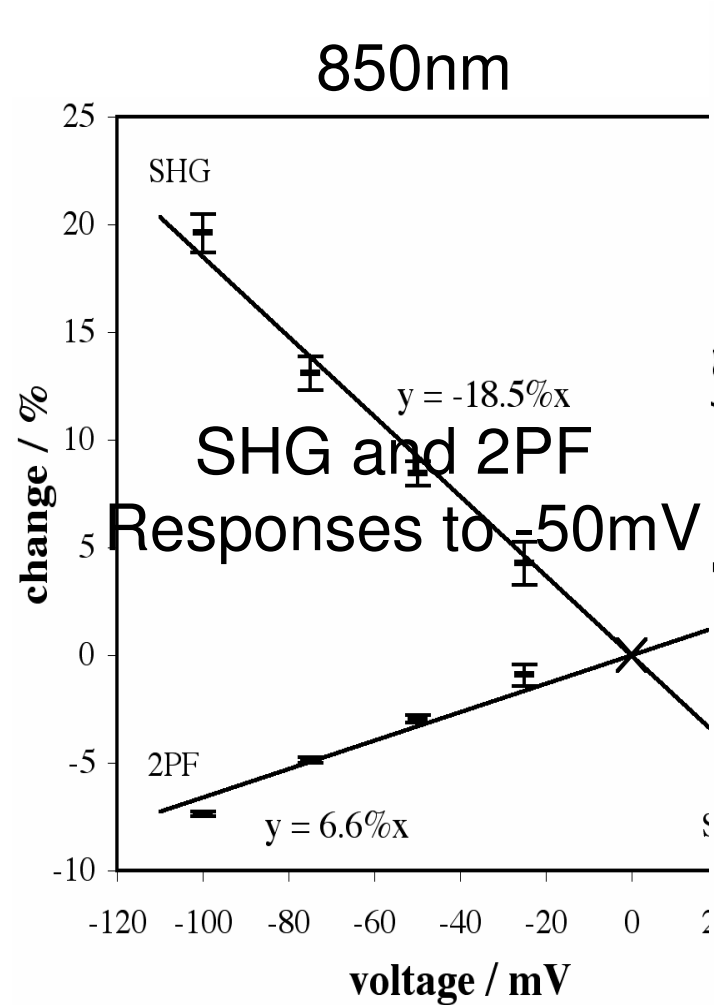


910nm, di-4-ANEPPS



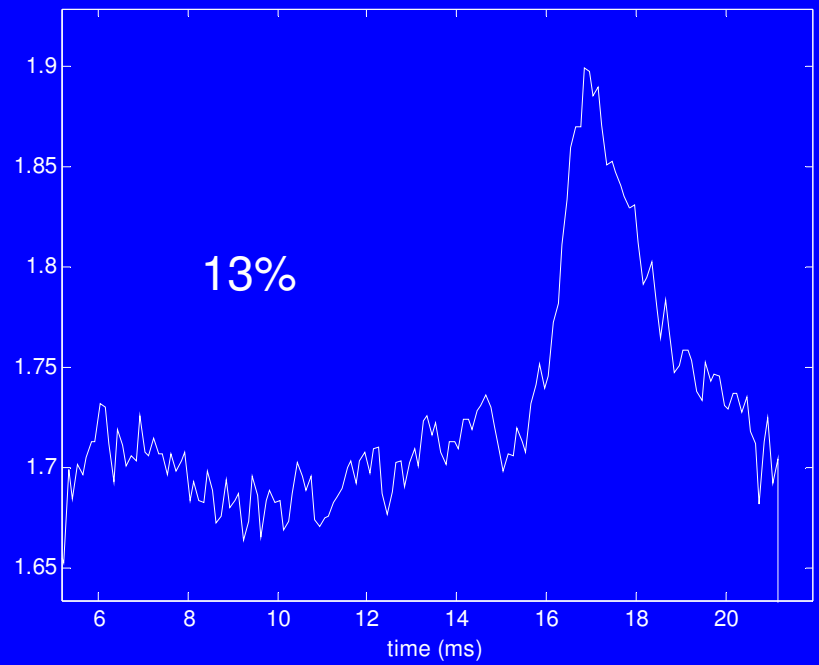
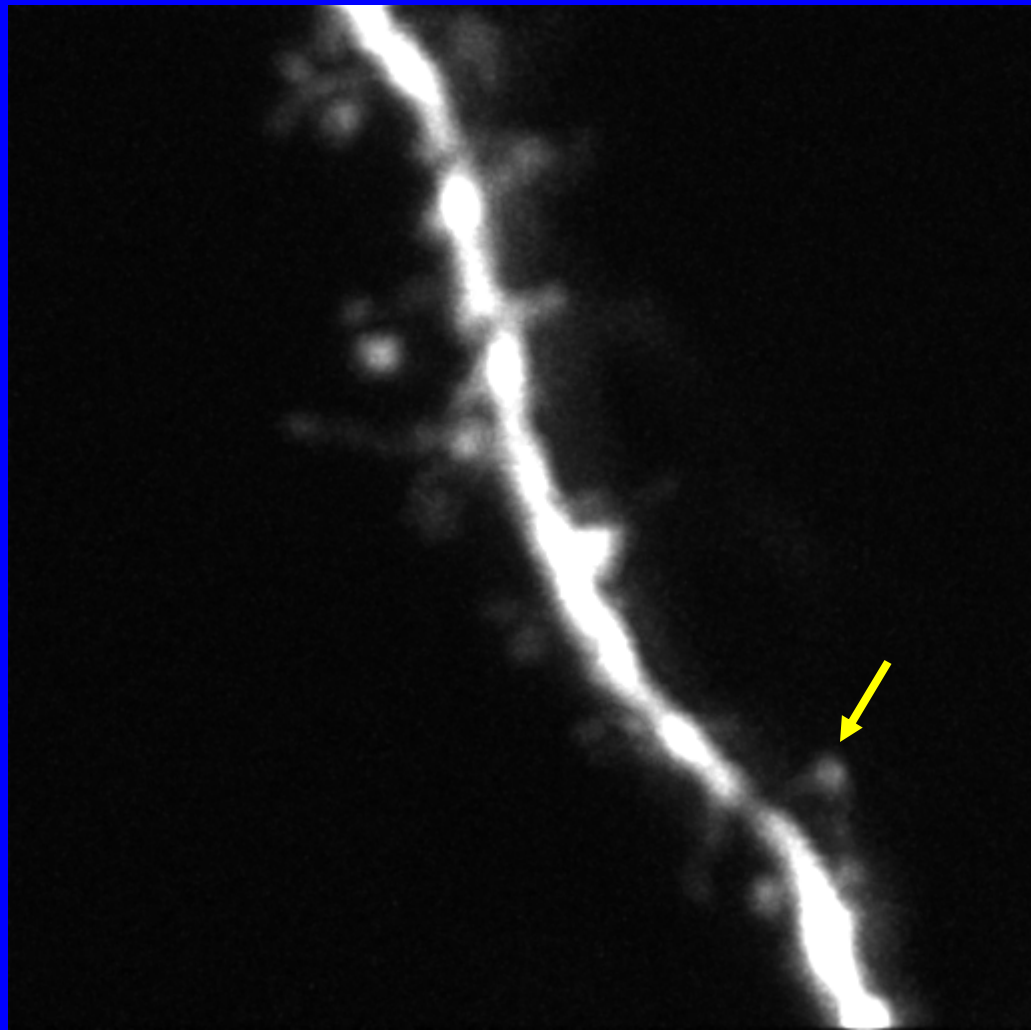
SHG is More Sensitive to Potential than 2PF

The Sensitivity Increases as Resonance is Approached

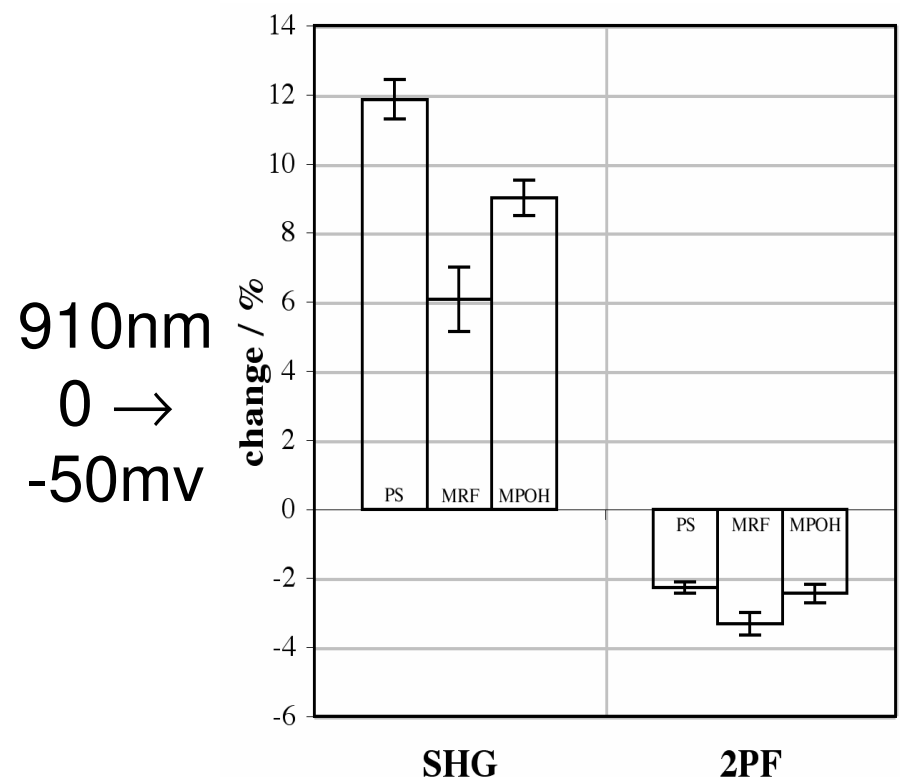
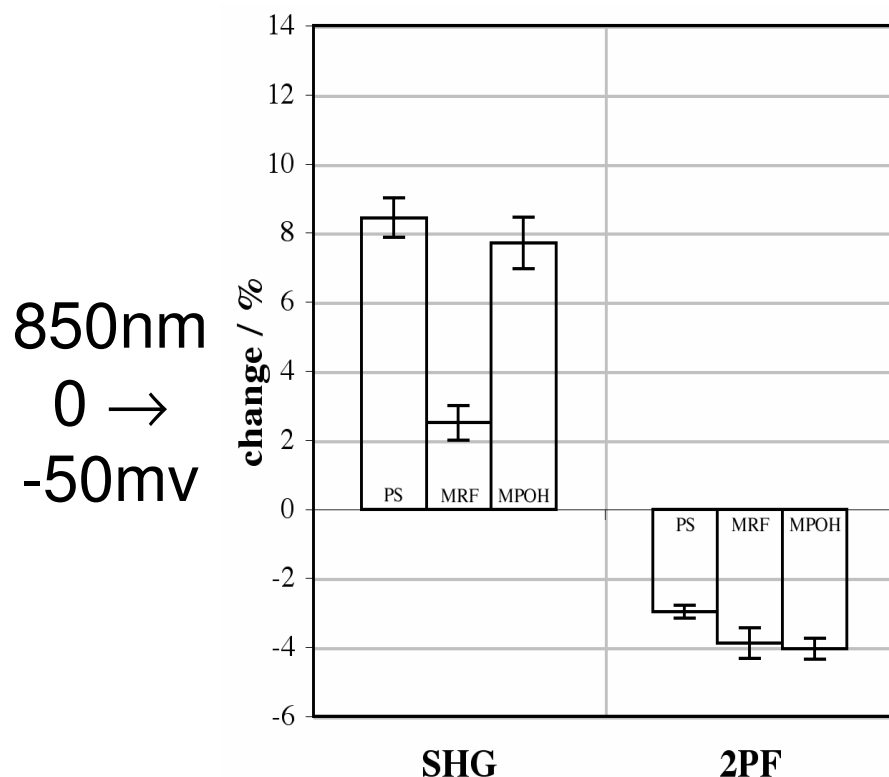
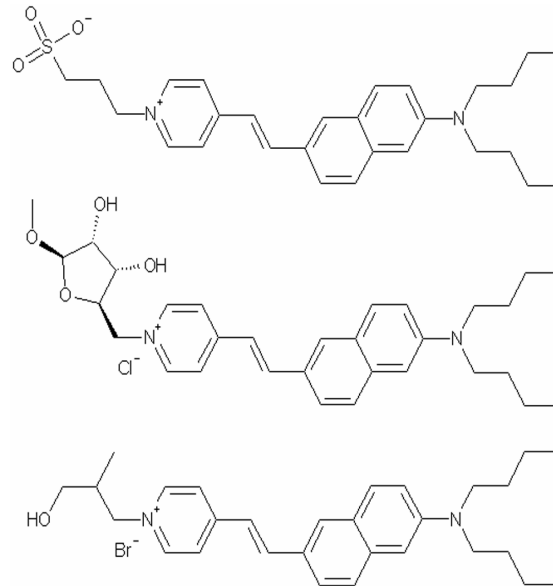


Measuring back-propagating AP in single spine

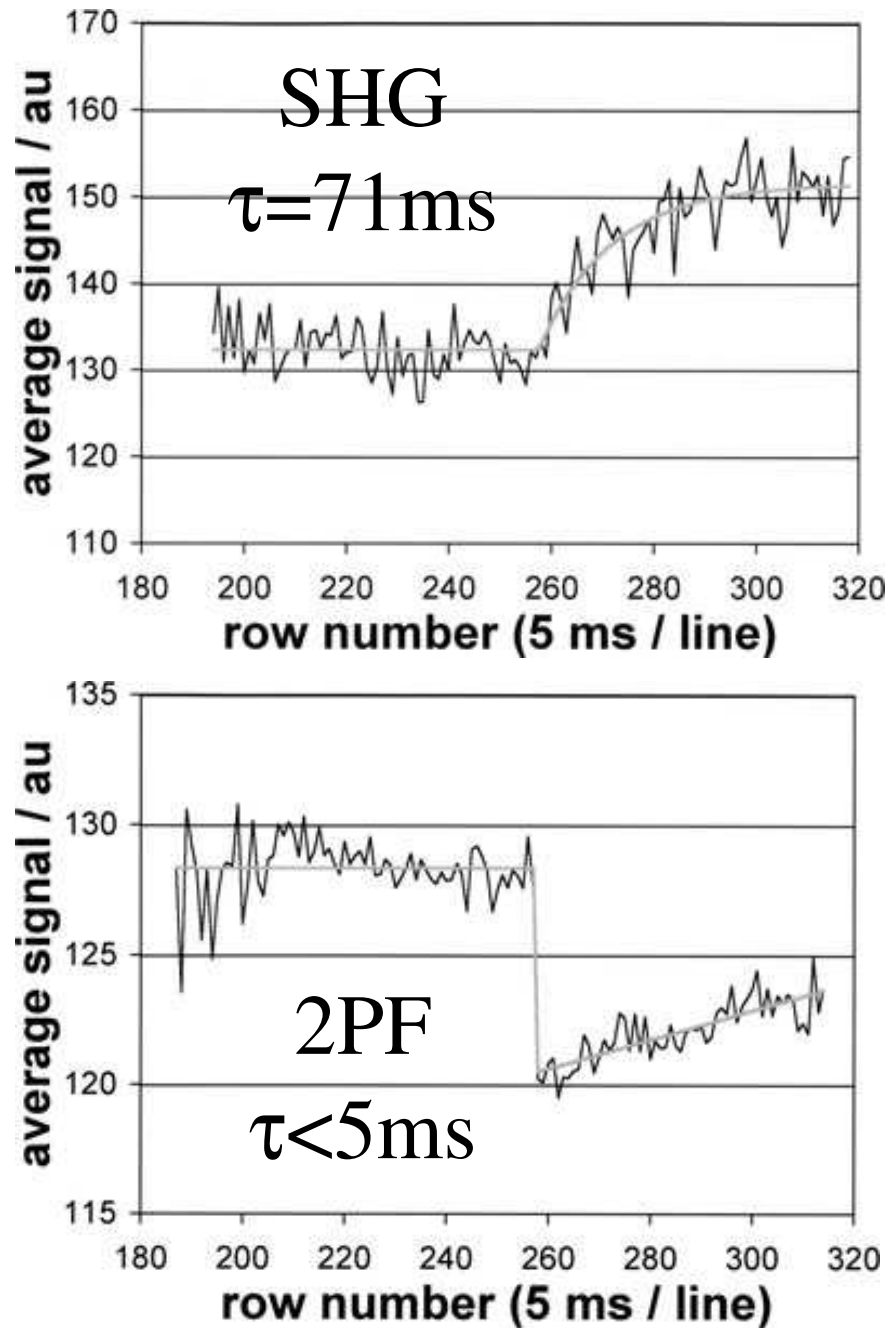
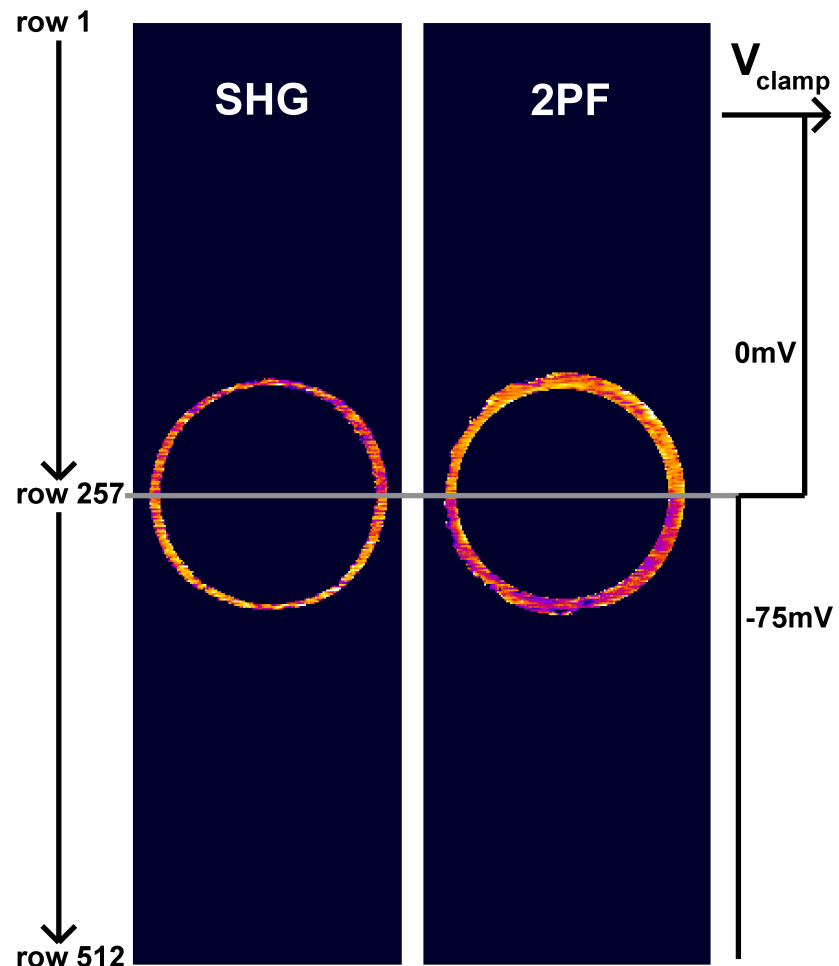
Corey Acker, 2010, unpublished



Di-4-ANEPPS is More Sensitive than Chiral Dyes

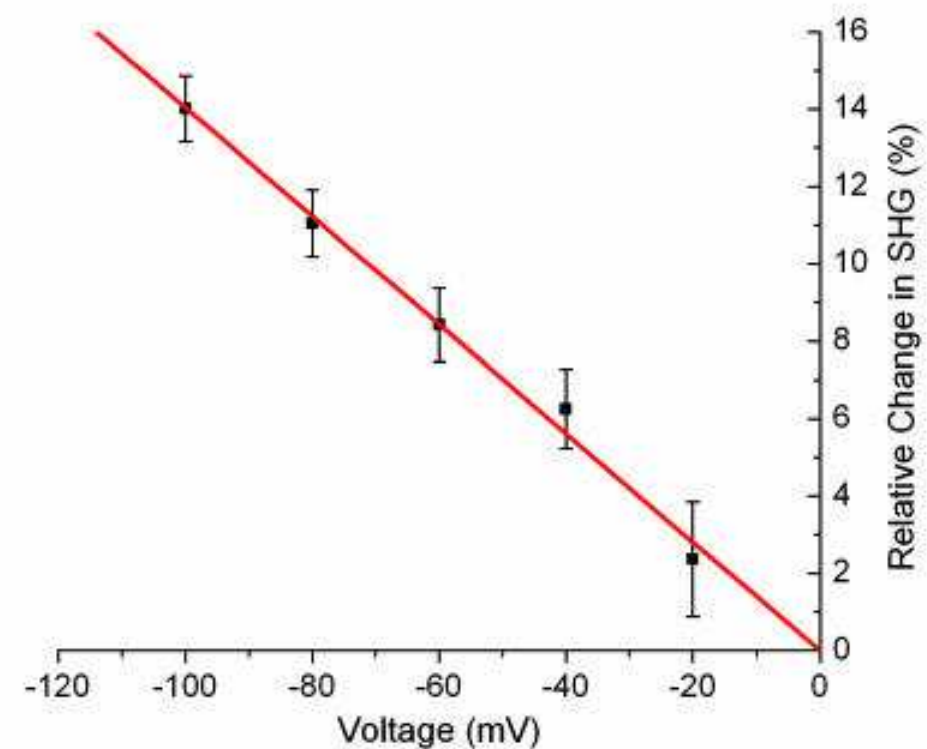
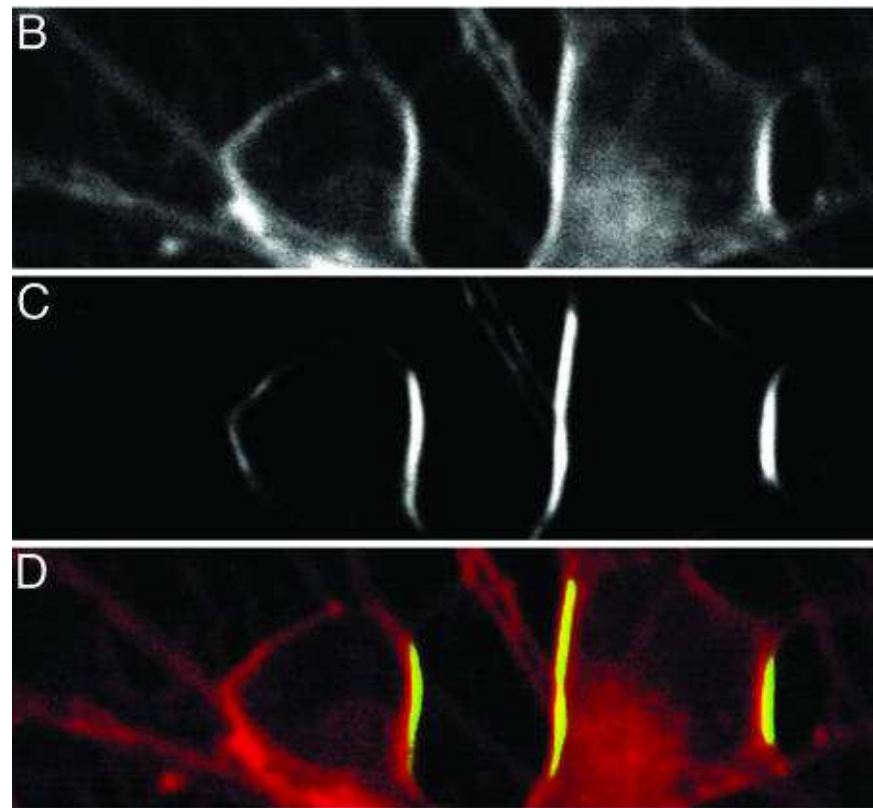
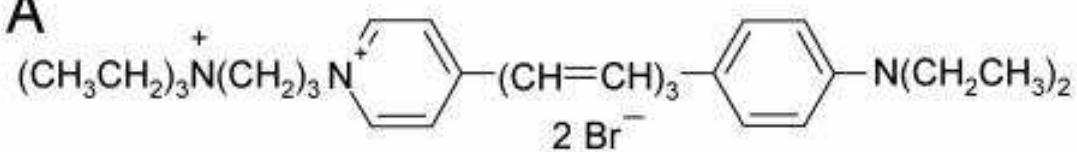


But, Di-4-ANEPPS SHG
Is Slow!
(Millard et al., 2005)



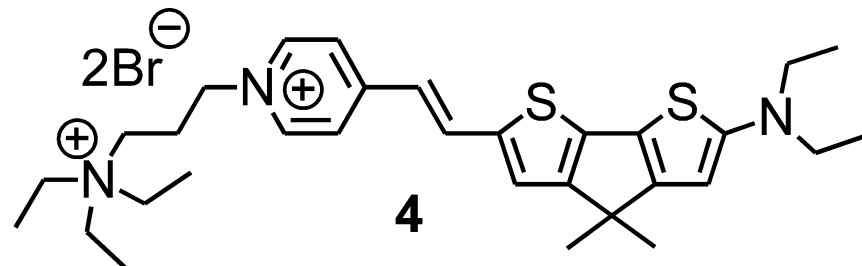
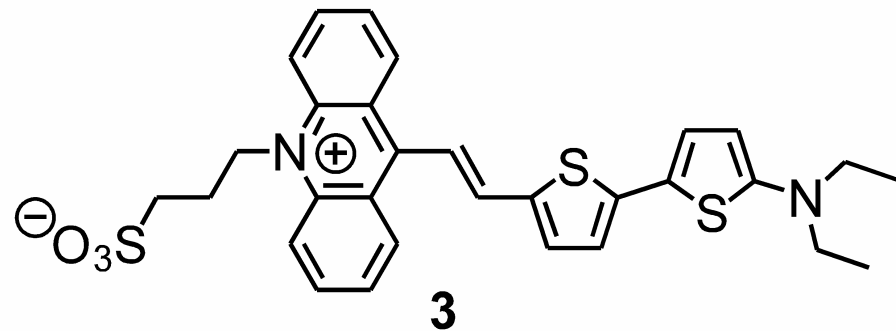
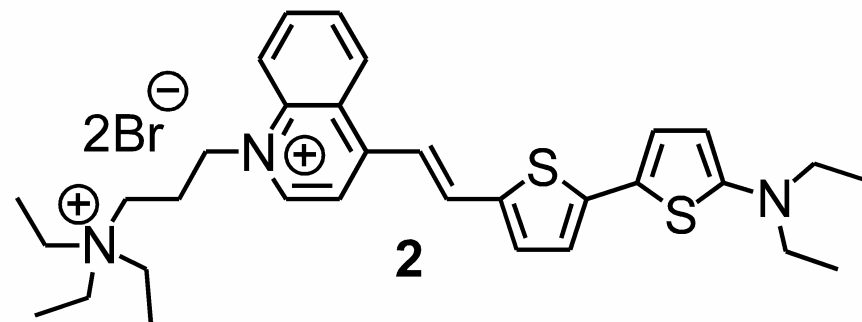
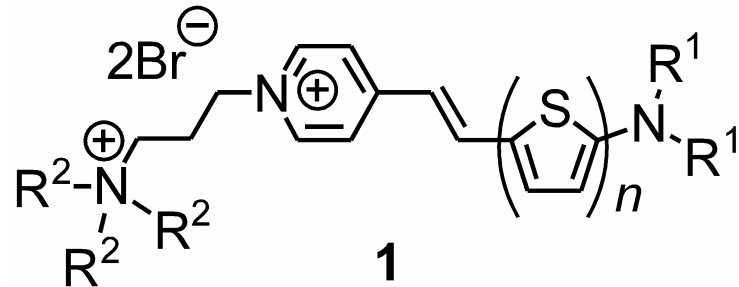
FM-4-64 Rafael Yuste et al., 2006

A



New Aminothiophene Dyes

Ping Yan, J. Org. Chem., 2008



1a: $n = 1$, $R^1 = \text{Et}$, $R^2 = \text{Et}$

1b: $n = 1$, $R^1 = n\text{-Bu}$, $R^2 = \text{Et}$

1c: $n = 2$, $R^1 = \text{Me}$, $R^2 = \text{Et}$

1d: $n = 2$, $R^1 = \text{Et}$, $R^2 = \text{Et}$

1e: $n = 2$, $R^1 = \text{Pr}$, $R^2 = \text{Et}$

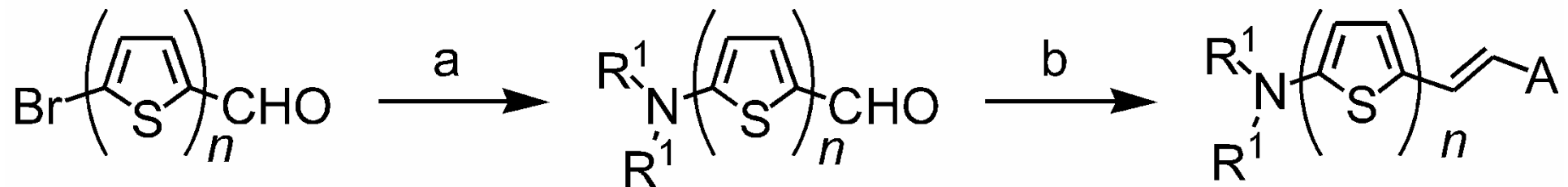
1f: $n = 2$, $R^1 = n\text{-Bu}$, $R^2 = \text{Et}$

1g: $n = 2$, $R^1 = \text{Et}$, $R^2 = \text{Me}$

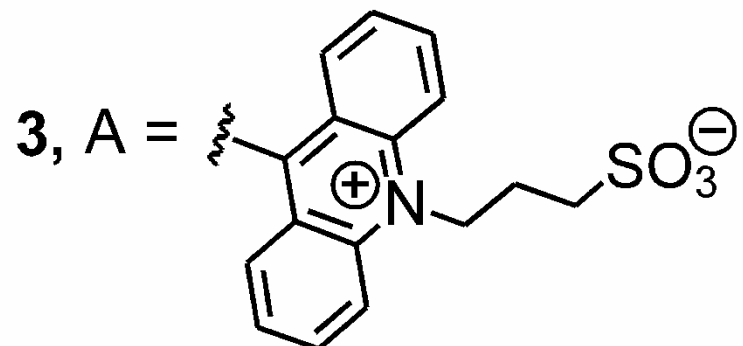
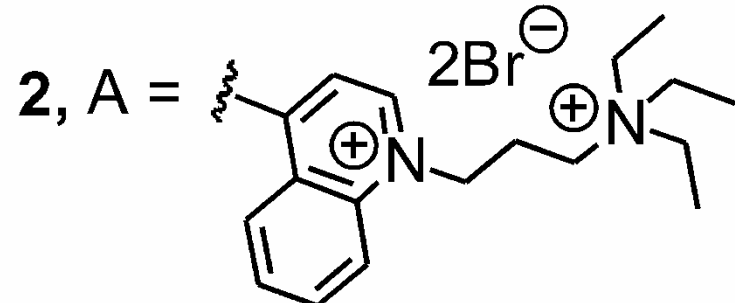
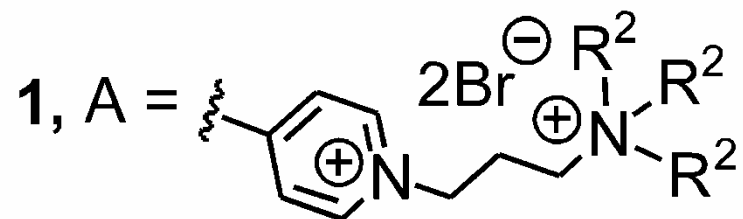
1h: $n = 2$, $R^1 = \text{Et}$, $R^2 = \text{Pr}$

1i: $n = 3$, $R^1 = \text{Et}$, $R^2 = \text{Et}$

Scheme for Synthesis of Amino-thiophene Dyes



$R^1 = \text{Me, Et, } n\text{-Pr, } n\text{-Bu.}$
 $R^2 = \text{Me, Et, } n\text{-Pr.}$



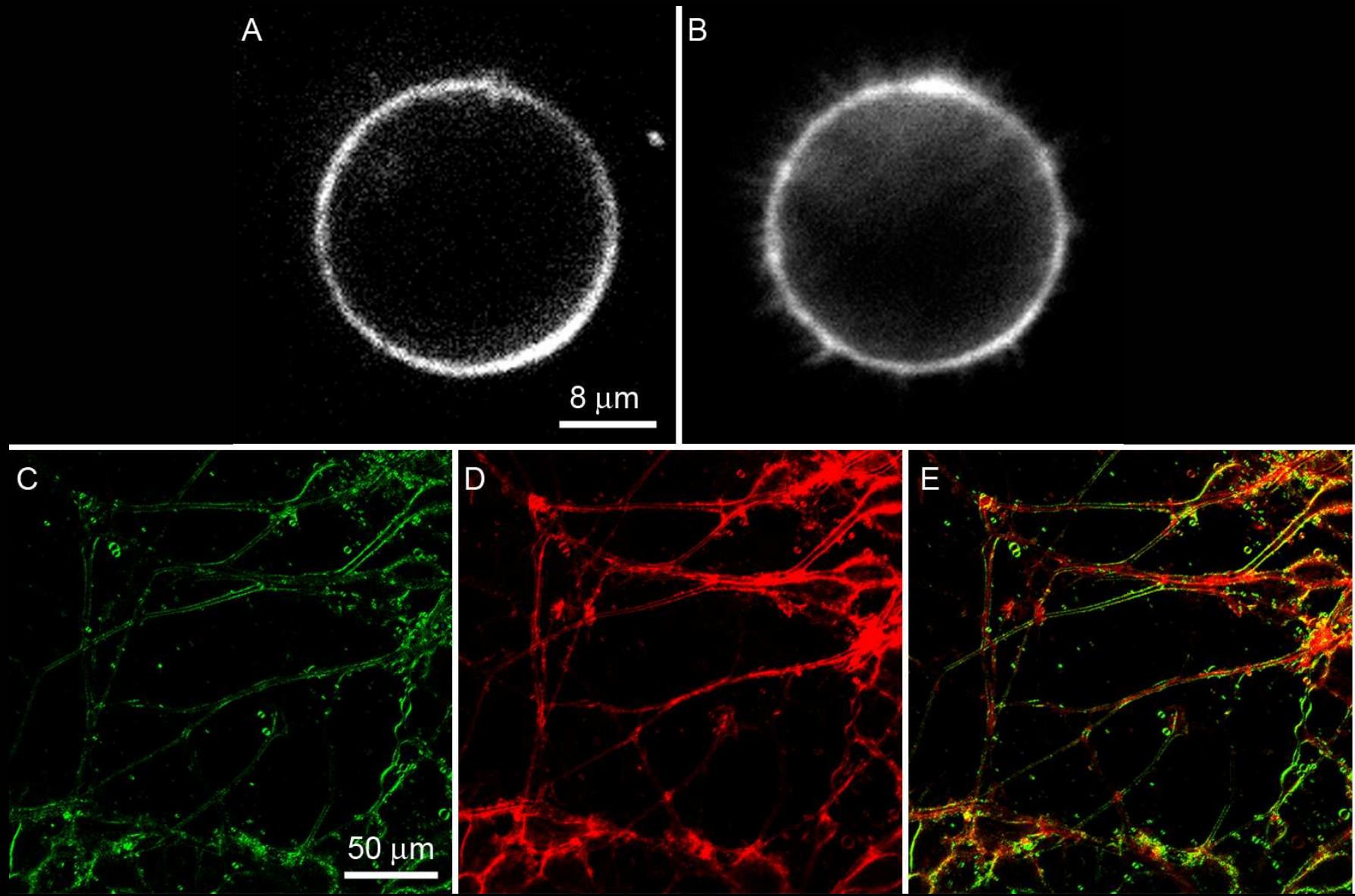
$a = \text{HNR}_2, \text{CuI}$

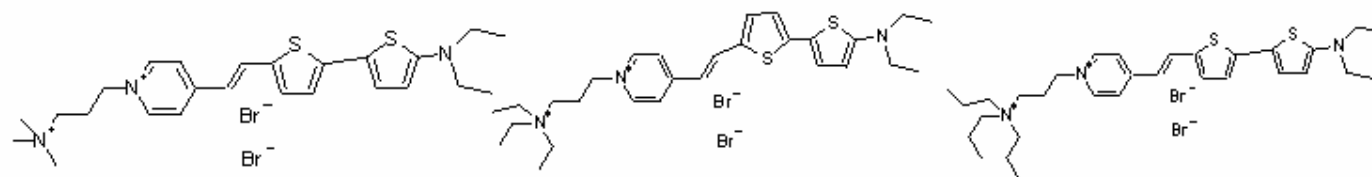
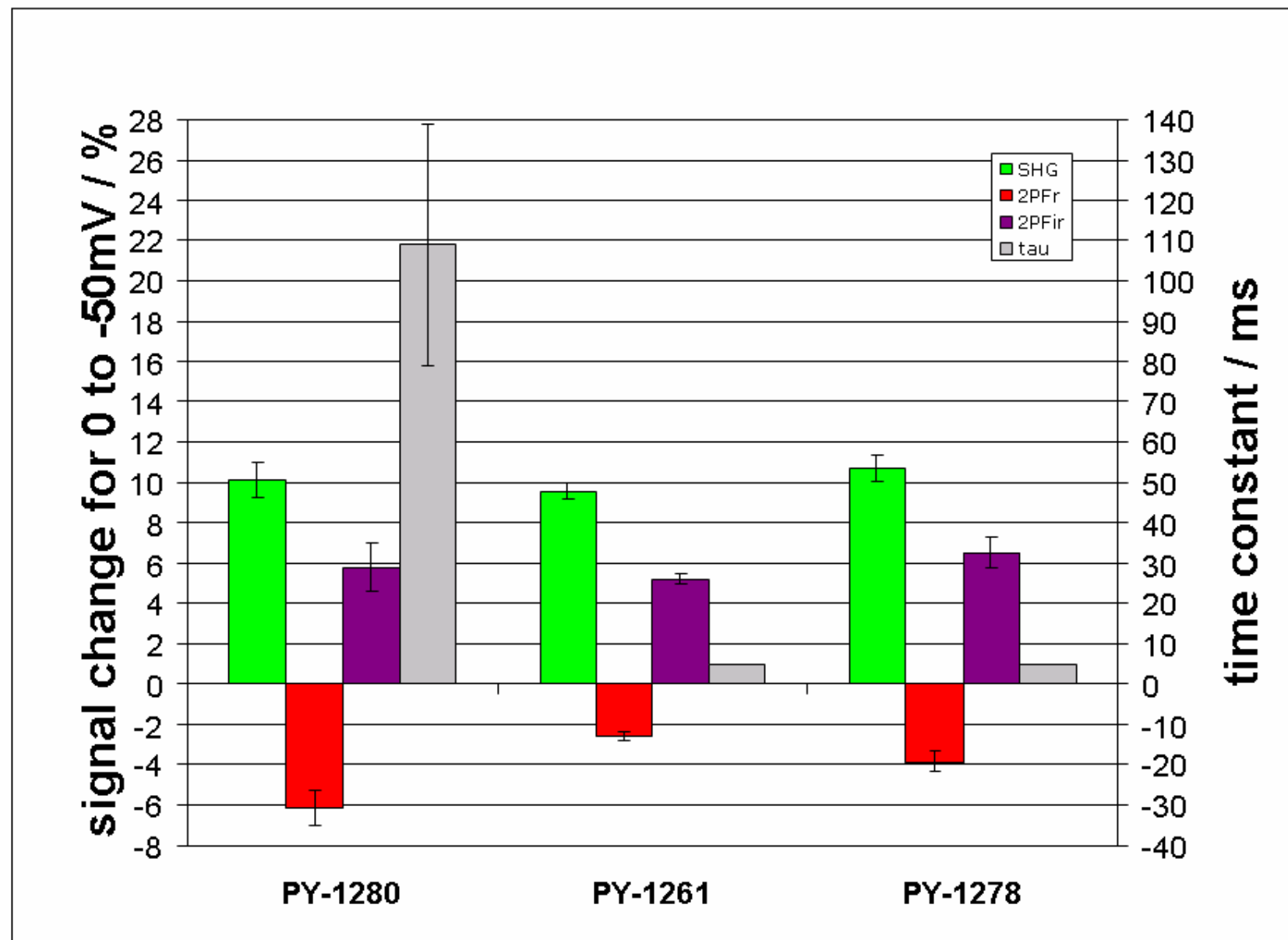
Teisseyre, et al. 2007

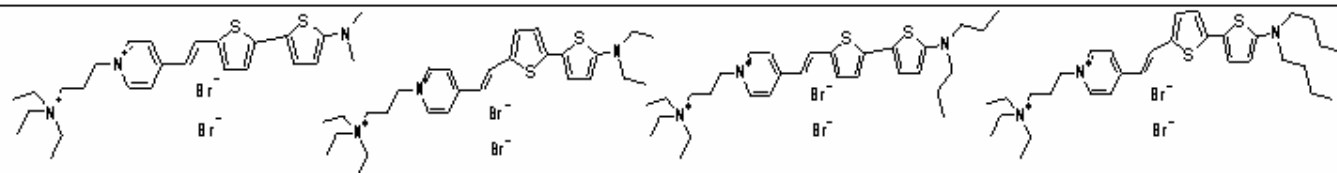
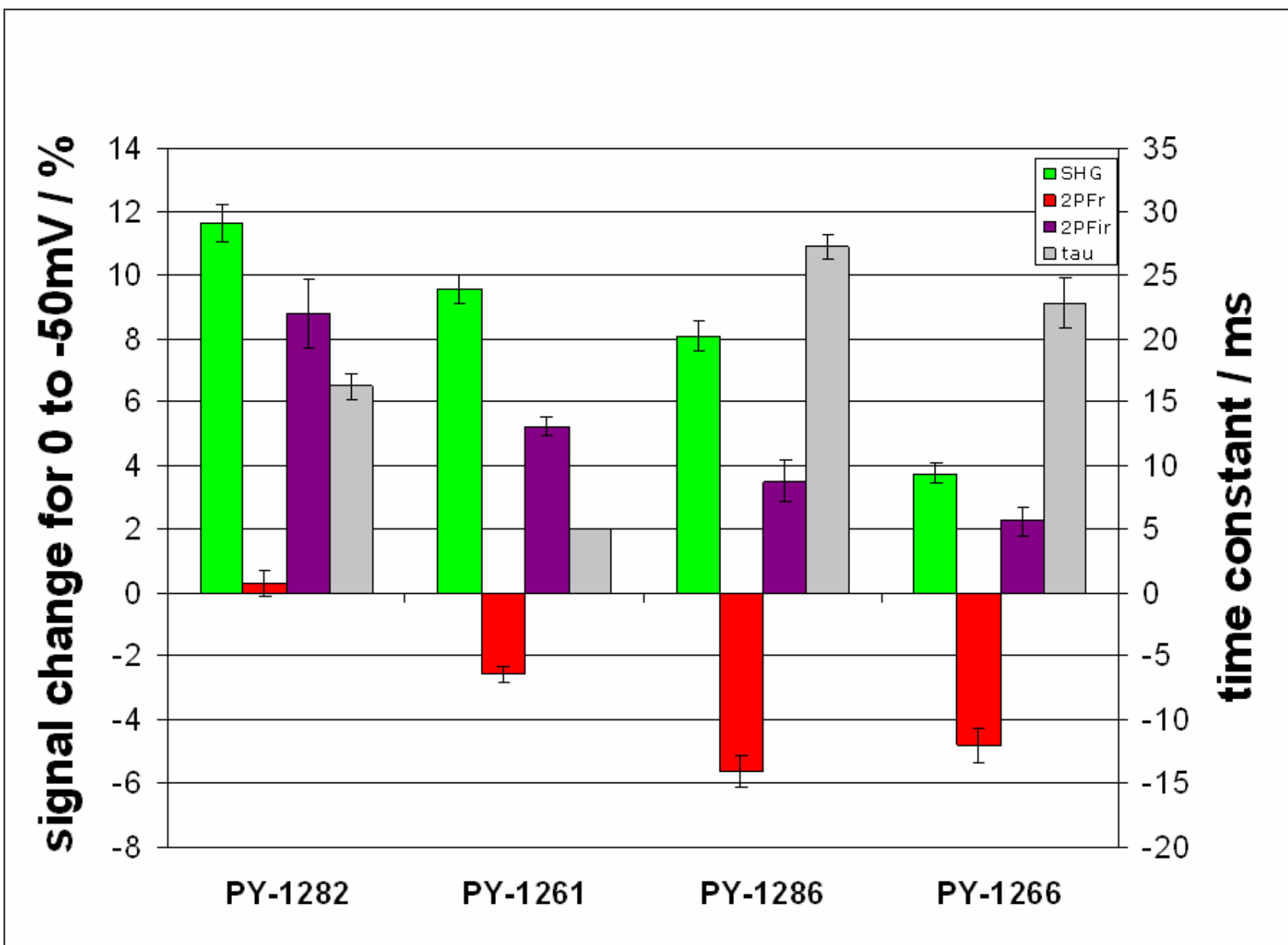
Name	Absorption/ Emission Peaks (in mlv, nm)	SHG Voltage Sensitivity (%/50 mV)	2PF Voltage Sensitivity (%/50 mV)		SHG Response Time (ms)
			615–665 nm	750–850 nm	
PY1284	536/588	6.2±0.7	6.7±0.6	N/A	(N/A)
PY1261	547/686	9.6±0.4	-2.6±0.2	5.2±0.3	< 5
PY1268	535/714	1.8±0.2	16.6±0.9	4.3±0.5	< 5
PY1282	530/676	11.6±0.6	0.3±0.4	8.8±1.1	37.0
PY1286	547/692	8.1±0.5	-5.7±0.5	3.5±0.7	27.2
PY1266	552/694	3.8±0.3	-4.8±0.5	2.3±0.5	22.8
PY1280	547/690	10.1±0.9	-6.1±0.9	5.8±1.2	109.4
PY1278	555/688	10.7±0.6	-3.9±0.5	6.5±0.8	< 5

Compound	$\lambda_{\text{max}}^{\text{abs}}$ (nm); log?	$\lambda_{\text{max}}^{\text{em}}$ (nm); FQY	Fluorescence sensitivity to membrane potential ^e $\Delta F/F$ per 100 mV Ex / Em (nm)
1a 	569; 4.8 ^a 559; 4.7 ^b 551; 4.6 ^c	606; 0.003 ^a 612; 0.001 ^b 586; 0.07 ^c	1.5% 530 / >590
1b 	571; 4.7 ^a 564; 4.6 ^b 536; 4.5 ^c	610; 0.005 ^a 614; 0.002 ^b 588; 0.10 ^c	1.5% 555 / >610
1c 	594; 4.4 ^a 529; 4.3 ^b 530; 4.3 ^c	- ^d - ^d 676; 0.10 ^c	8.0% 640 / >715
1d 	614; 4.3 ^a 539; 4.1 ^b 547; 4.2 ^c	- ^d - ^d 686; 0.10 ^c	5.0% 625 / >715
1e 	616; 4.3 ^a 567; 4.2 ^b 547; 4.2 ^c	- ^d - ^d 692; 0.10 ^c	18% 640 / >715
1f 	621; 4.4 ^a 567; 4.1 ^b 554; 4.2 ^c	- ^d - ^d 694; 0.11 ^c	10% 635 / >715
1g 	617; 4.3 ^a 544; 4.1 ^b 547; 4.2 ^c	- ^d - ^d 690; 0.12 ^c	11% 640 / >715
1h 	612; 4.4 ^a 545; 4.3 ^b 556; 4.3 ^c	- ^d - ^d 688; 0.10 ^c	7.9% 640 / >715
1i 	588; 4.3 ^a 508; 4.1 ^b 535; 4.2 ^c	- ^d - ^d 714; 0.020 ^c	4.2% 640 / >715

SHG and 2PF imaging of PY-1268



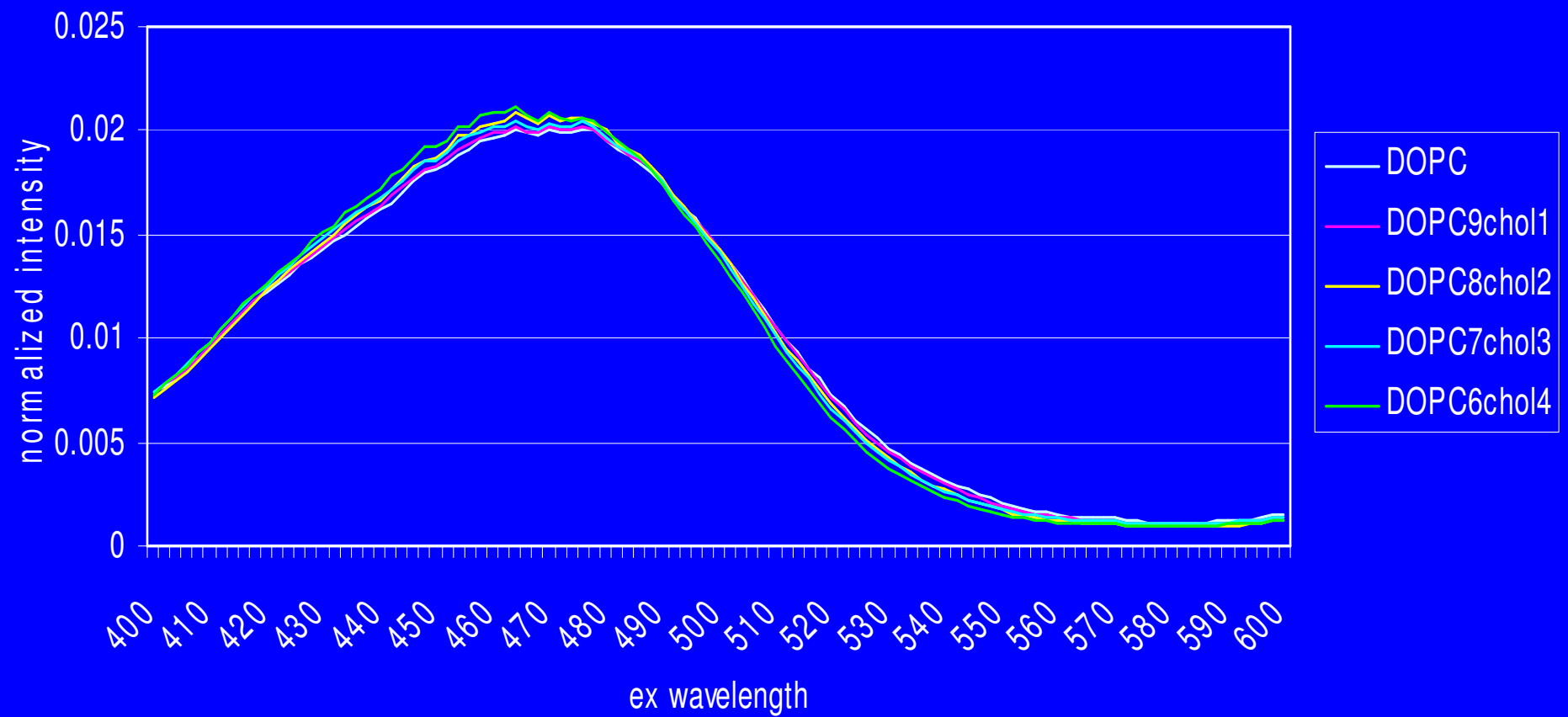




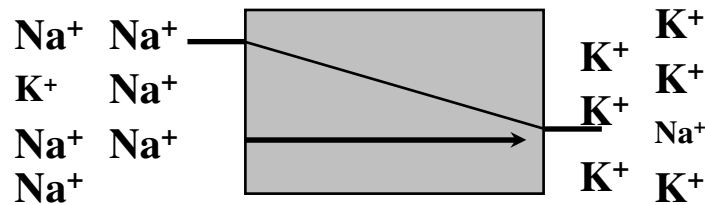
Improved Photostability with Fluorinated Dyes

Name	Structure	$\lambda_{\text{max}}^{\text{abs}}$ (nm); ϵ ($M^{-1} \text{cm}^{-1}$) ^a	$\lambda_{\text{max}}^{\text{em}}$ (nm) ^a	Brightness (relative)	$\Delta F/F;$ $\lambda_{\text{Ex/Em}}$ (nm)	Bleach $\tau_{1/2}$ (s)
PY-1261		547; 15,000	686	59±6; 14 cells (1)	5%/100mV; 625/>715	2.7±0.1; 4 cells
PY-3008		565; 25,000	706	80±6; 29 cells (1.3)	5%/100mV; 650/>715	4.1±0.1; 4 cells
PY-3009		476 22,000	616	37±2; 16 cells (1)	5%/100mV; 560/>630	8.7±0.4; 5 cells
PY-3006		488 23,000	636	51±2; 20 cells (1.4)	9%/100mV; 577/>665	12.6 ±1.3; 4 cells

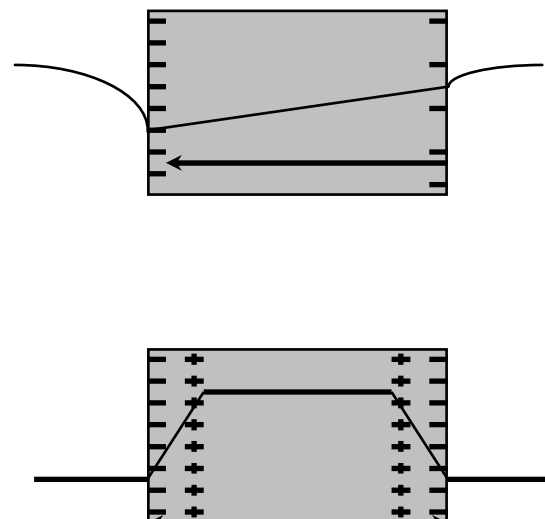
Cholesterol's Effect on the Excitation Spectrum of DOPC LUVs



Intramembrane Electric Fields

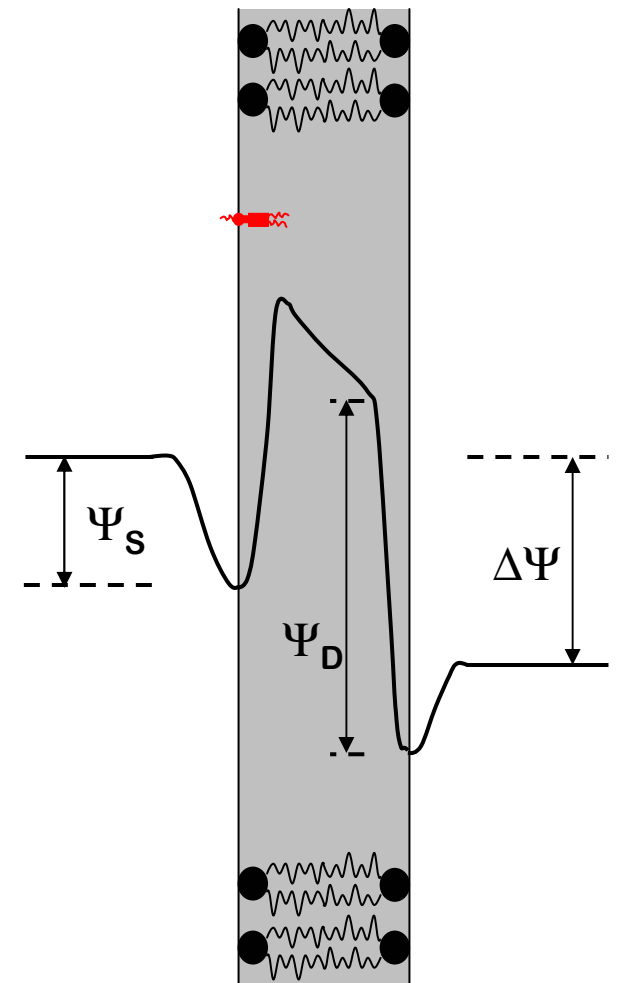


**Transmembrane
Potential**



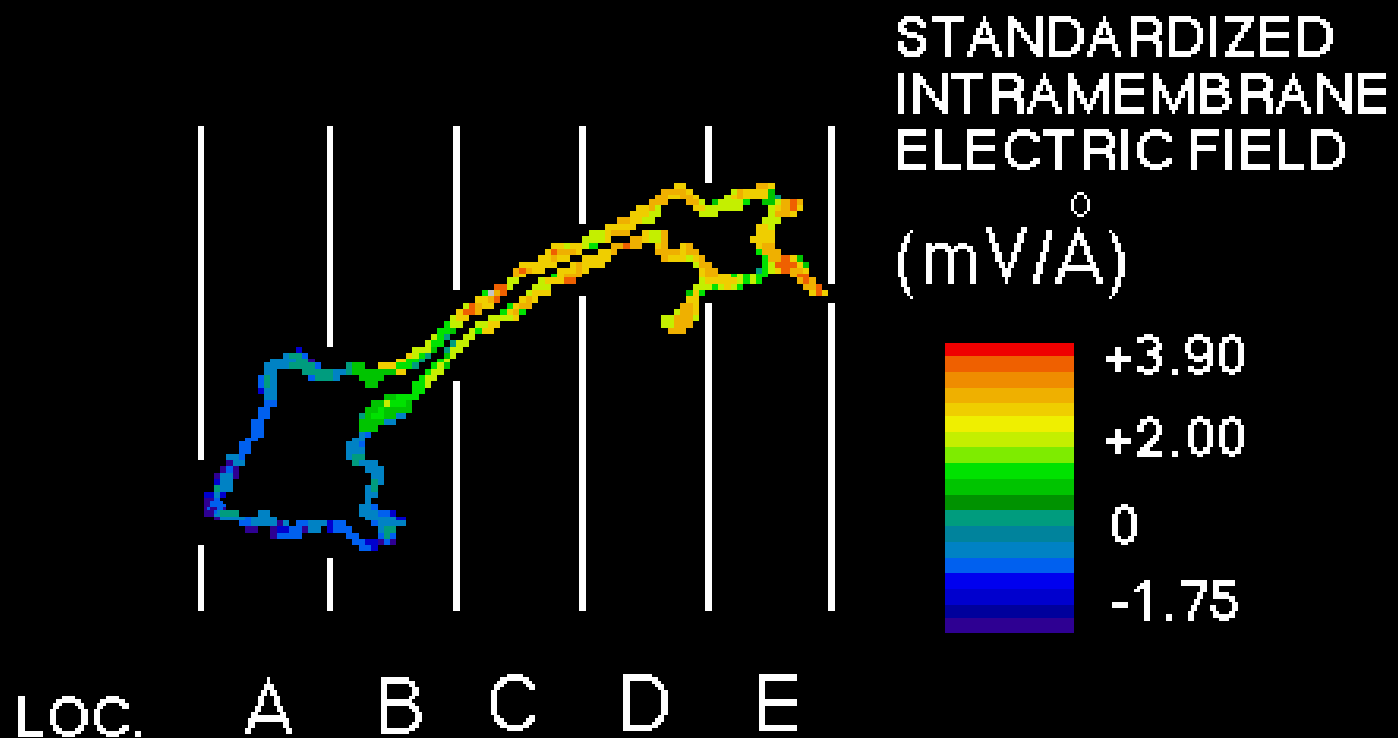
Surface Potential

Dipole Potential



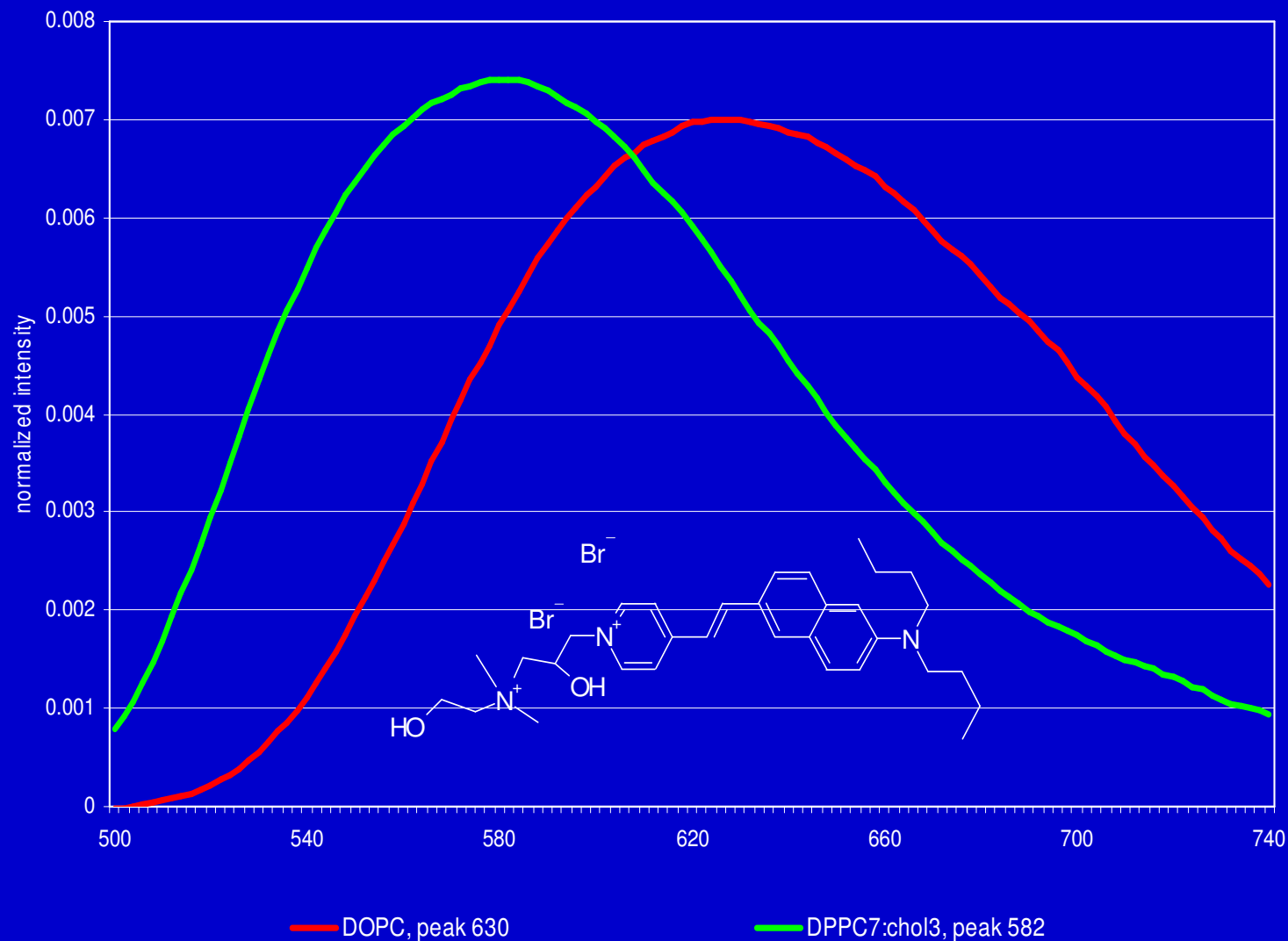
Dye Ratio Reveals Uneven Electrical Profiles Along the Surface of Single Cells

Bedlack et al., Neuron, 1994

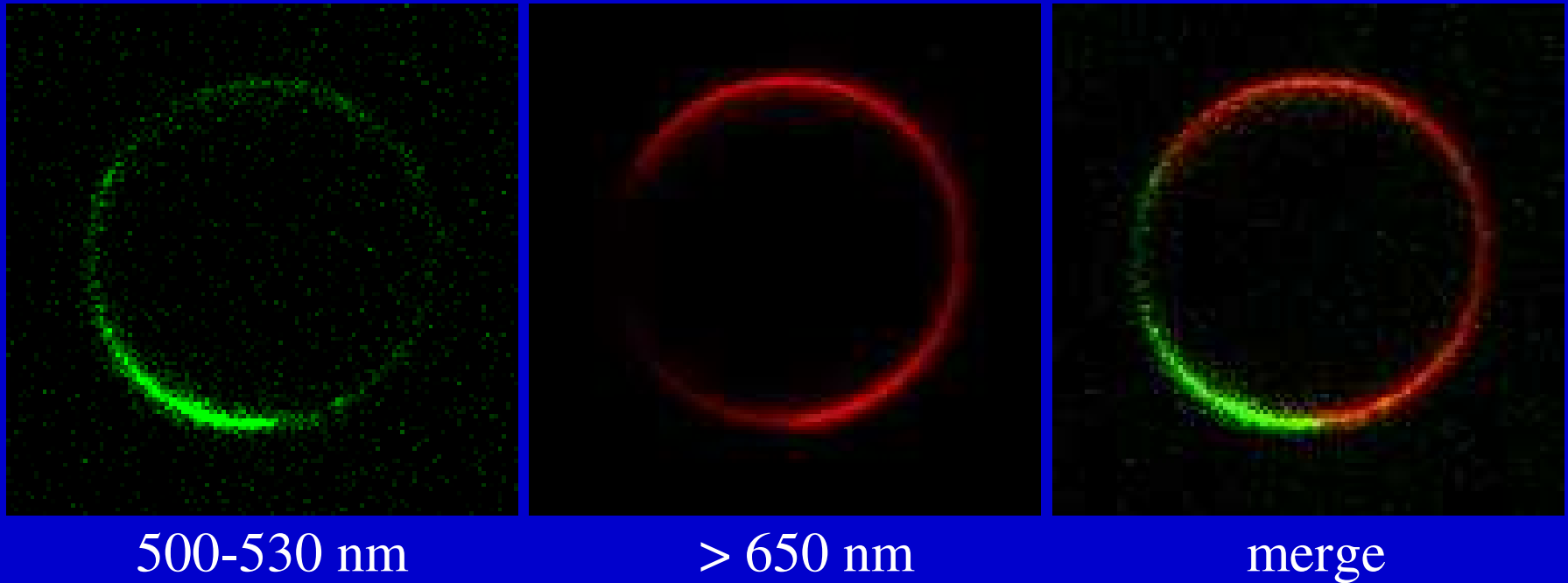


Characterization and Application of a New Optical Probe for Membrane Lipid Domains

Lei Jin et al., Biophys. J., 2006

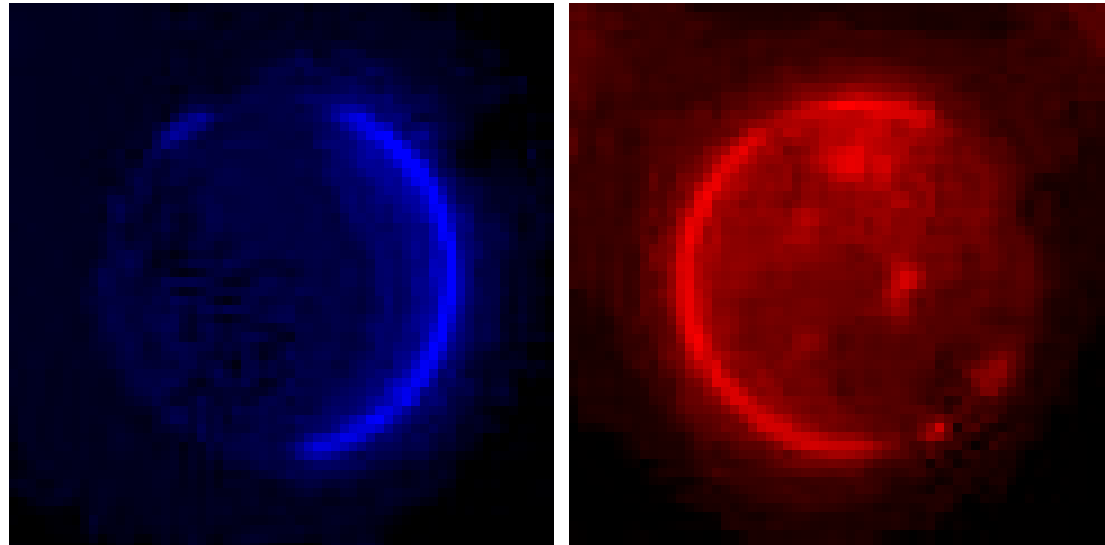


Lipid Domains in Giant Unilamellar Vesicles

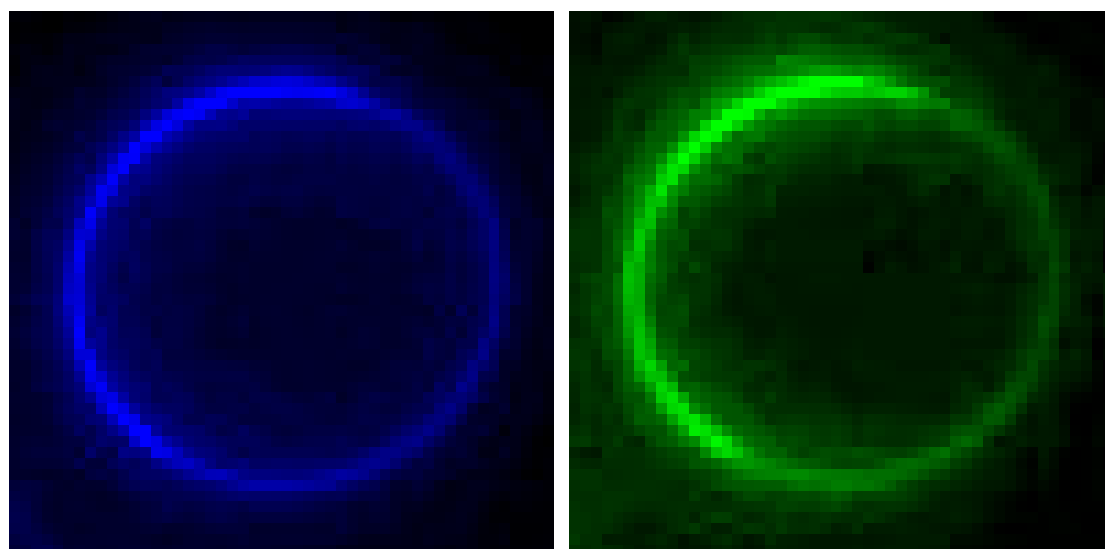


One photon fluorescent confocal images of GUV with two phases stained by di-4-ANEPPDHQ. The two phases show fluorescence of different colors.

Perylene identifies the lower wavelength emission of di-4-ANEPPDHQ as originating from the liquid ordered phase



675/50

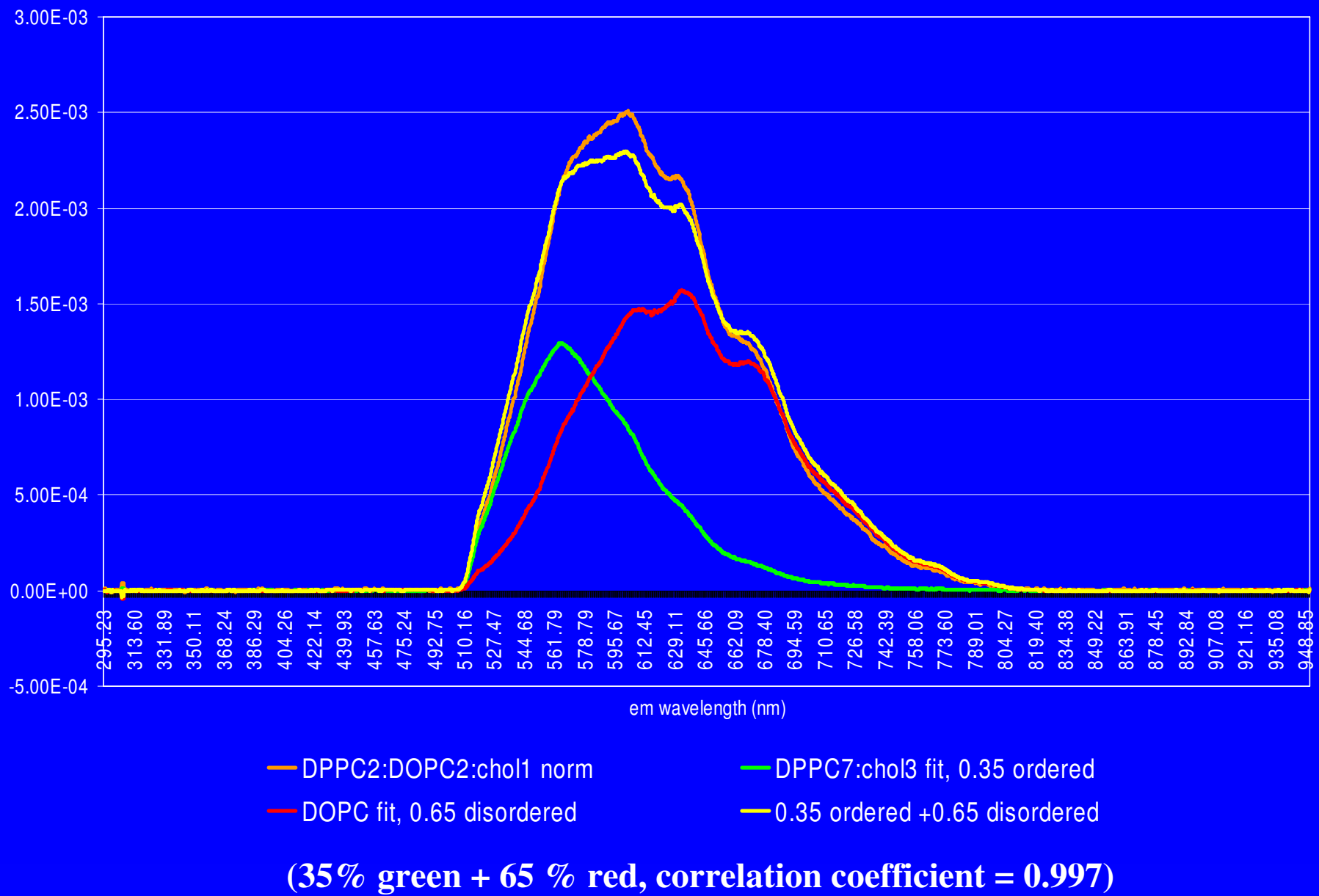


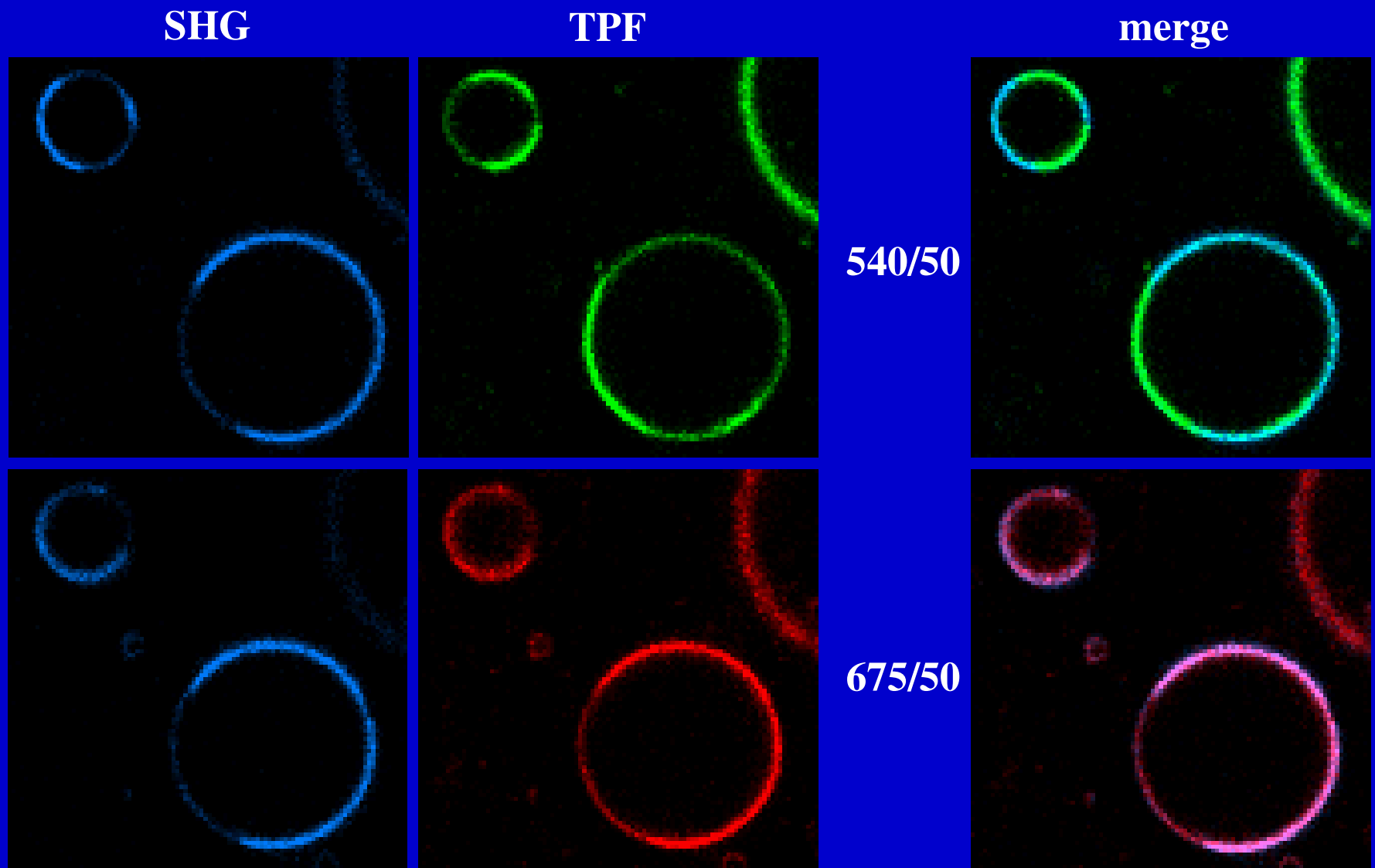
540/50

perylene

di-4-ANEPPDHQ

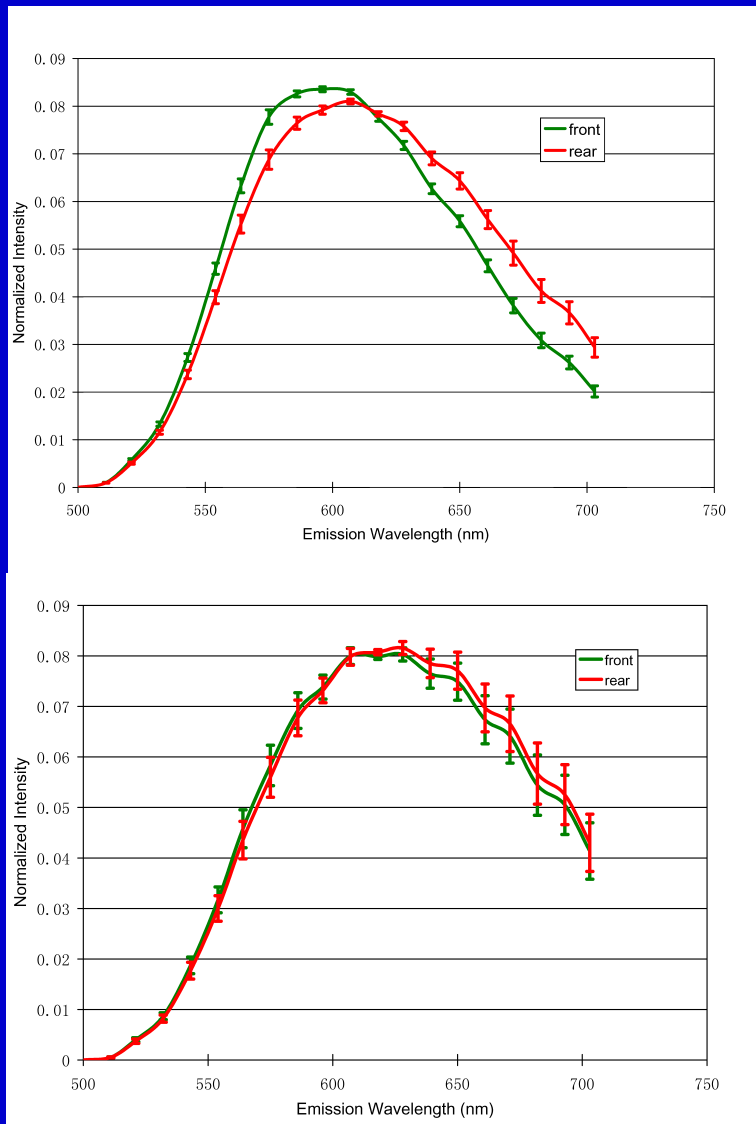
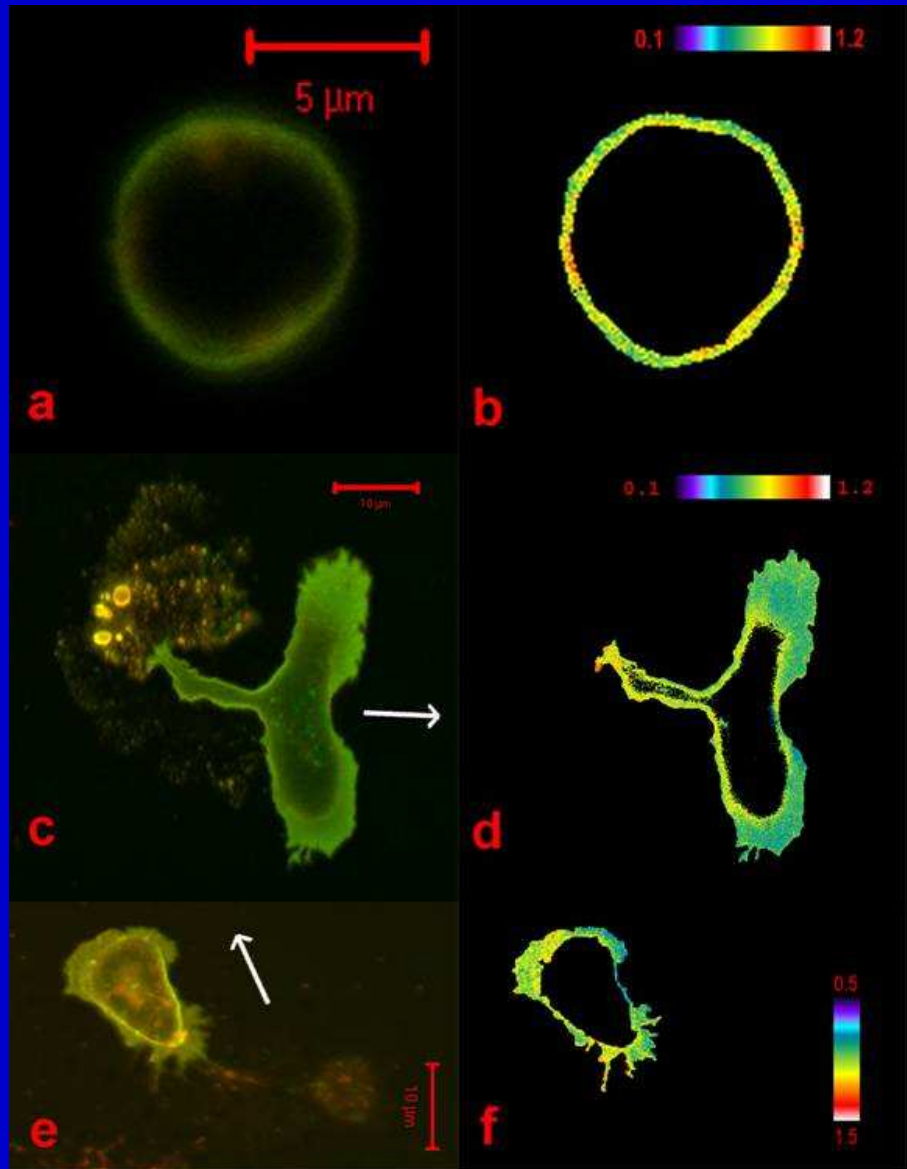
Emission Spectra of GUVs from the Microscope





**SHG and TPF images of GUVs stained by di-4-ANEPPDHQ.
The dye shows stronger SHG in the liquid disordered phase, which has the red TPF.**

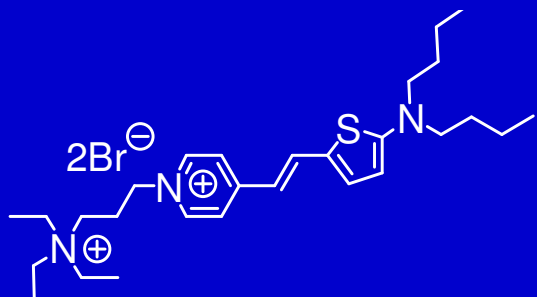
Di-4-ANEPPDHQ Reveals Lipid Polarity in Polarized Migrating Neutrophils



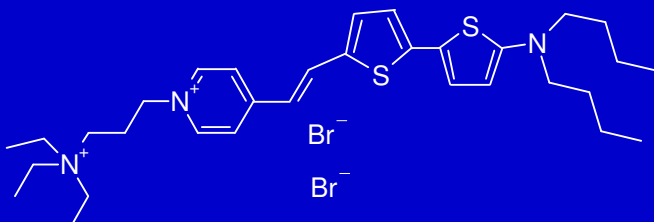
Newly synthesized dyes and their emission maxima in liquid ordered and liquid disordered lipid membranes

Ping Yan and Joe Wuskell

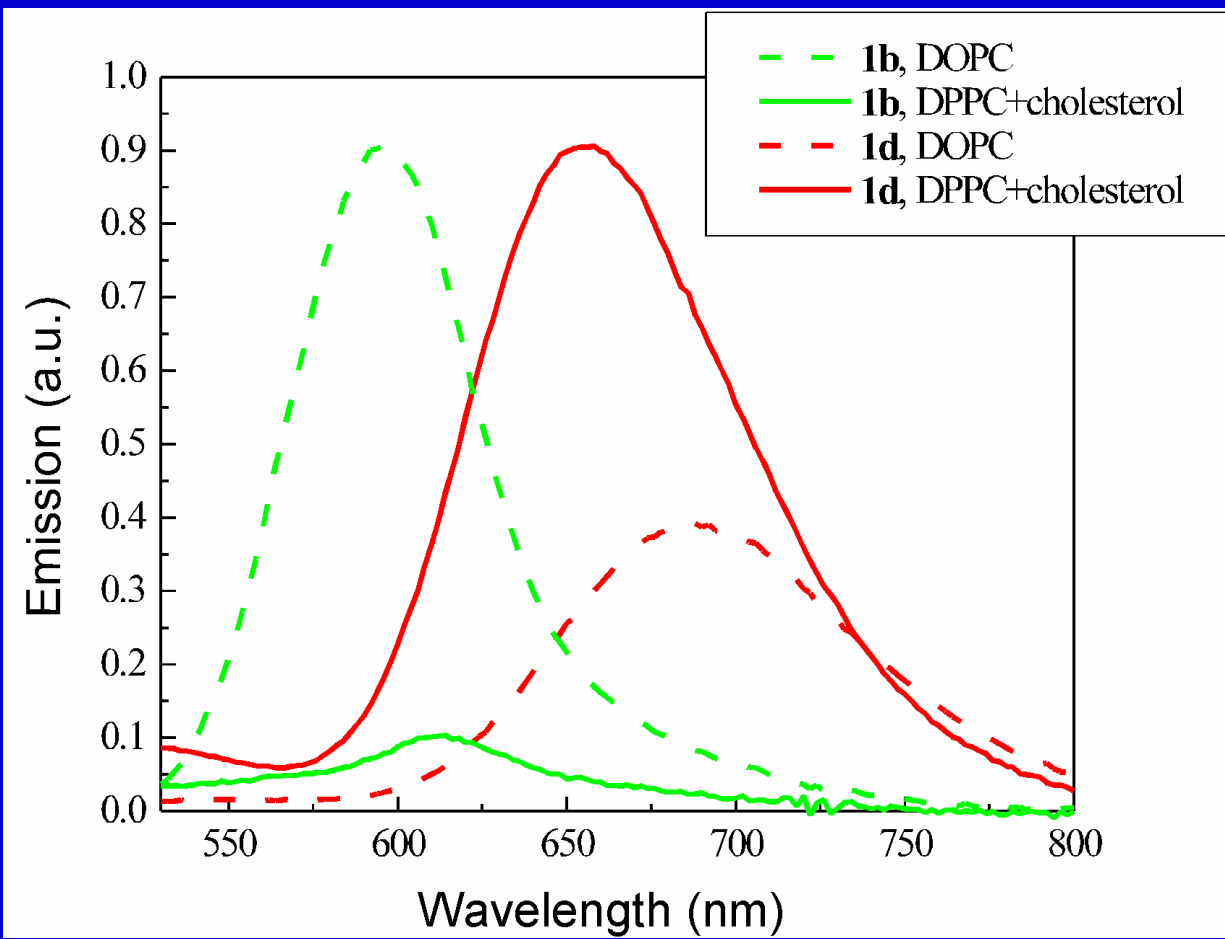
Name	Structure	λ_{Em}^{max} (nm)	
		Cholesterol/DPPC (30:70)	DOPC
JPW-6008		629	668
JPW-4090		667	708
JPW-6003		665	712
JPW-6023		630	676
PY-2045		596	639
PY-1261		654	690
PY-1266		662	696
PY-1237		606	594
PY-1284		614	596
PY-2030		NA	698



1b (1 thiophene)

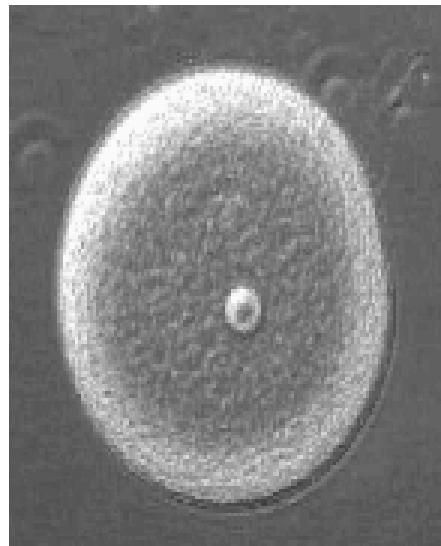


1d (2 thiophenes)

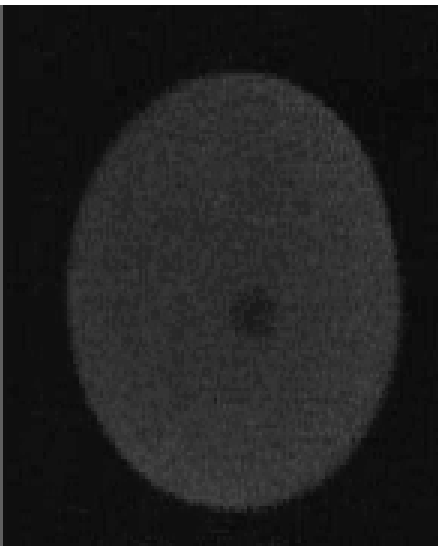


Exocytosis During Fertilization

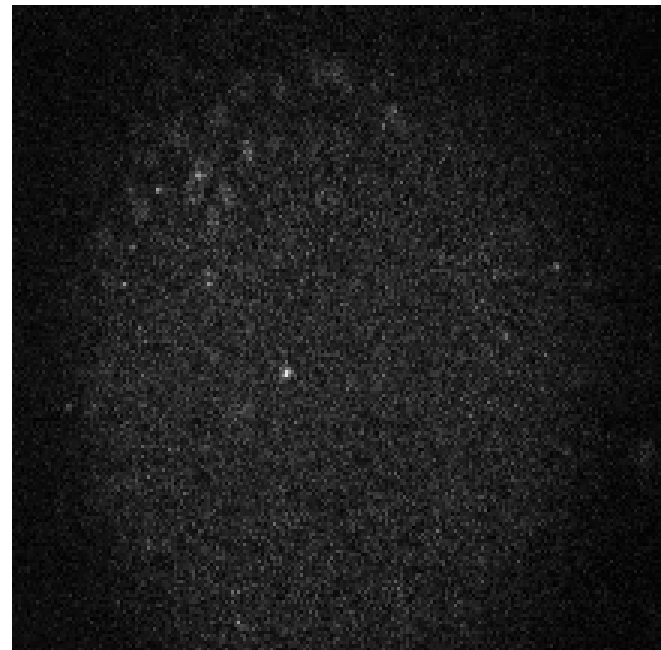
Andrew Millard and Mark Terasaki



Phase



Calcium

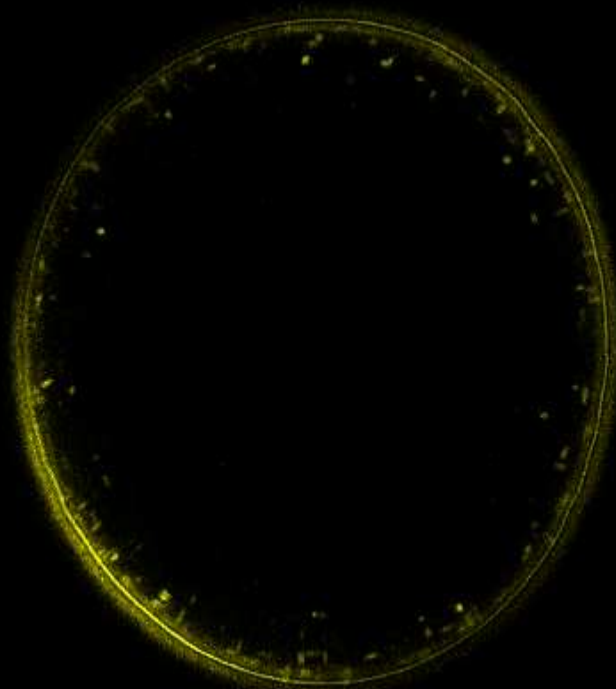


FM-143

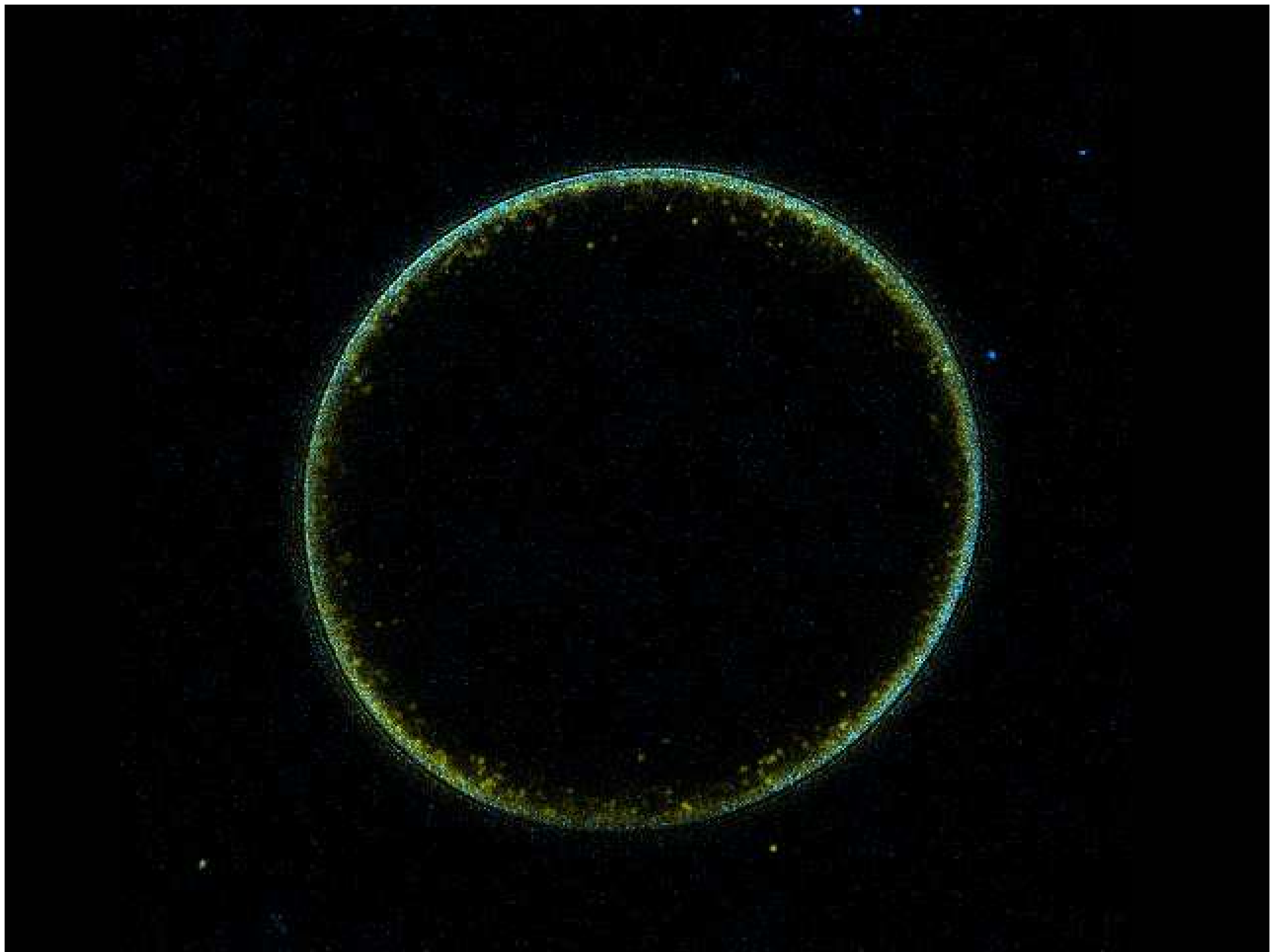
Fertilization of Di-8-ANEPPS Stained Sea Urchin Egg



SHG



TPEF



Di-4-ANEPPDHQ



Just Quadratic Dependence?

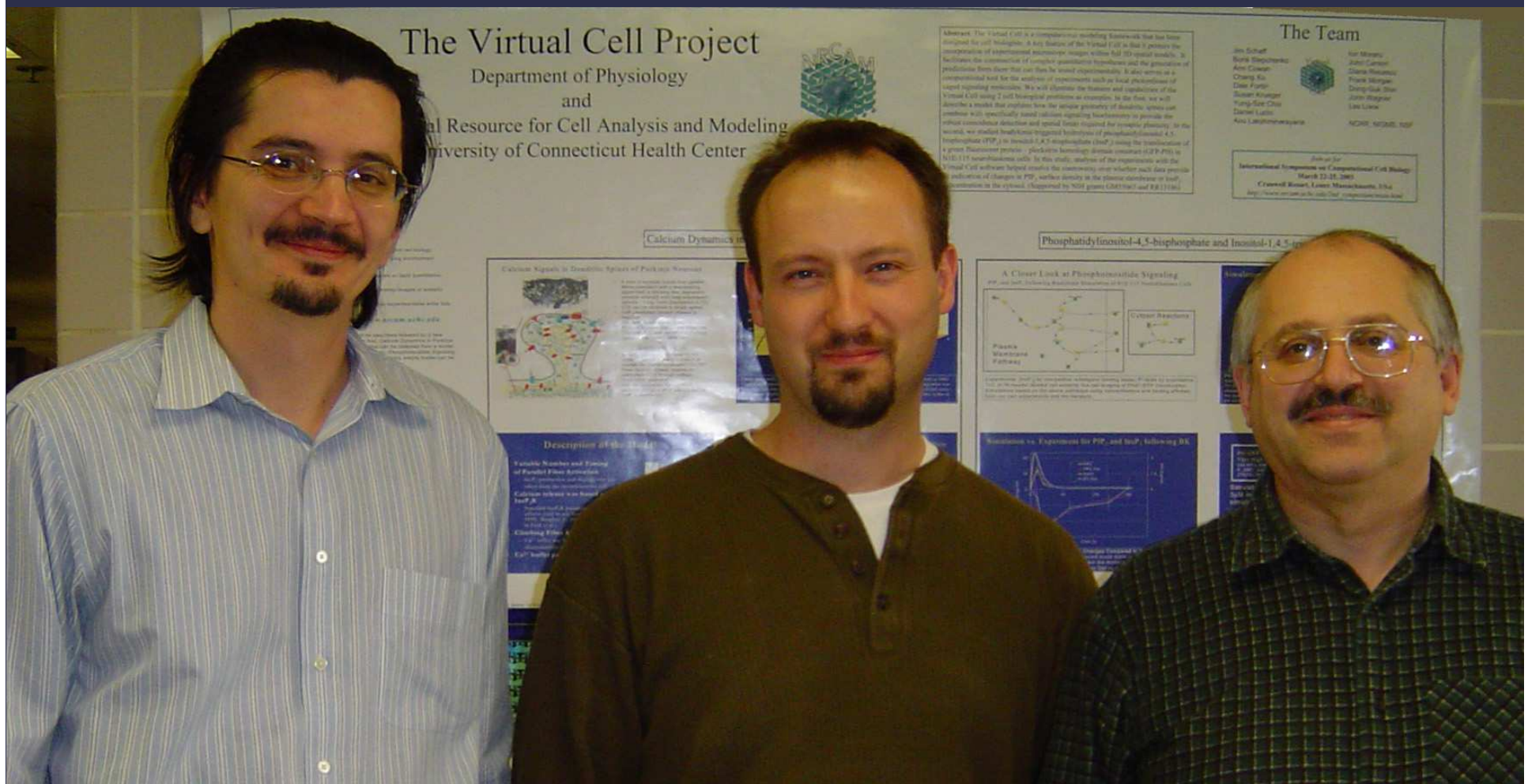
- Wimmer, Fuchs, Kryschi, Martin and Schmid (*J. Mol. Struct.* 2001)
- HBLs of oxidised cholesterol
- di-4-APEPPS (di-4-ASPPS but with a triple bond)
- seven potentials up to 140mV
- zero potential gives precisely zero SHG
- SHG intensity depends on square of potential
- signal rises and levels out over a couple of seconds
- bubbles also change size slightly (~2%)

The Virtual Cell Project

Ion Moraru

Jim Schaff

Boris Slepchenko



The Virtual Cell Project



Richard D. Berlin

Center for Cell Analysis and Modeling

National Technology Center for Networks and Pathways

John Carson

Yung-Sze Choi

Ann Cowan

Fei Gao

Susan Krueger

Anu Lakshminarayana

Frank Morgan

Igor Novak

Diana Resasco

Li Ye

Rashad Badrawi*

Nick Hernjak*

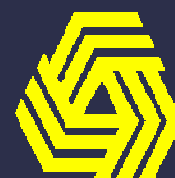
Daniel Lucio*

John Wagner*

(*alumni)



NIH Roadmap



**National Center for
Research Resources**



Cell
Migration
Consortium



National Institute of
General Medical Sciences

Virtual Cell

<http://vcell.org>

Designed to be used interactively with experiment

Enables construction and testing of complex models or rapid investigation of simple hypotheses

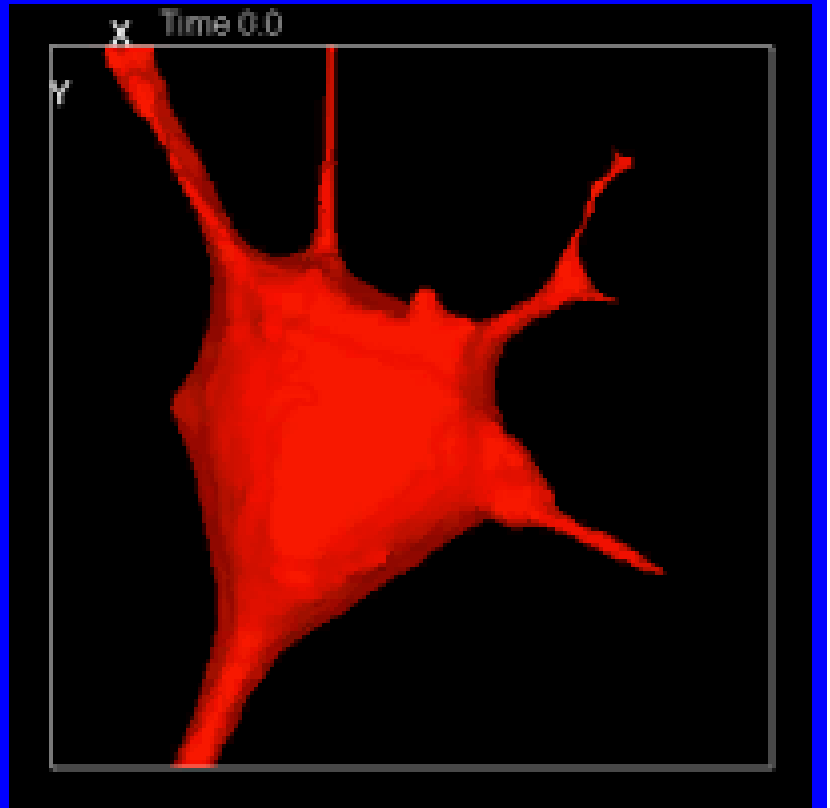
Geometry from experimental images

Math, physics, and numerics are transparent to an experimentalist while fully accessible to a theorist

Collaborative distributed database and problem solving environment

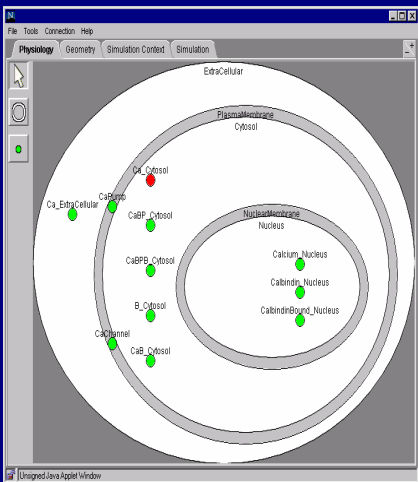
Virtual Cell Capabilities

$$\frac{\partial C_i}{\partial t} = -\operatorname{div} F_i + R_i$$

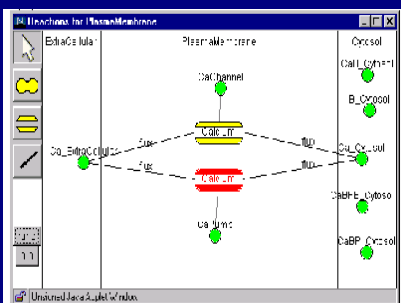


- Reaction - Diffusion - Advection - Electrophysiology
- 0, 1, 2 or 3 D including geometries from microscope images
- Stochastic simulators and Parameter Estimation for 0D
- Database of models and model components
- Biological Problems
 - Signaling and metabolic pathways
 - Intracellular trafficking
 - Ion channels
 - Fluorescent indicators and probe redistribution

Physiology

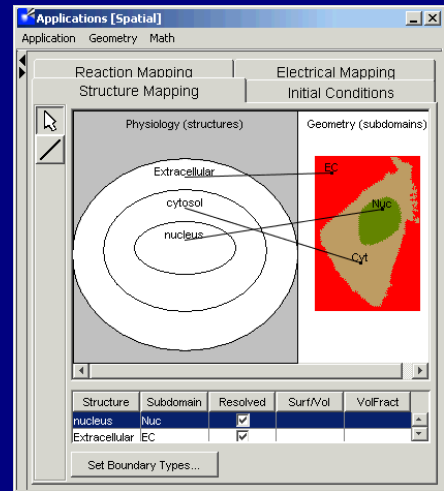


Molecular Species
Compartment Topology



Reactions and Fluxes

Applications

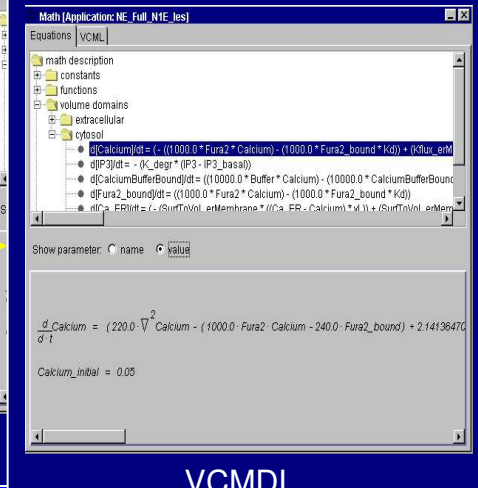


Topology → Geometry,
ODE, Stochastic, PDE

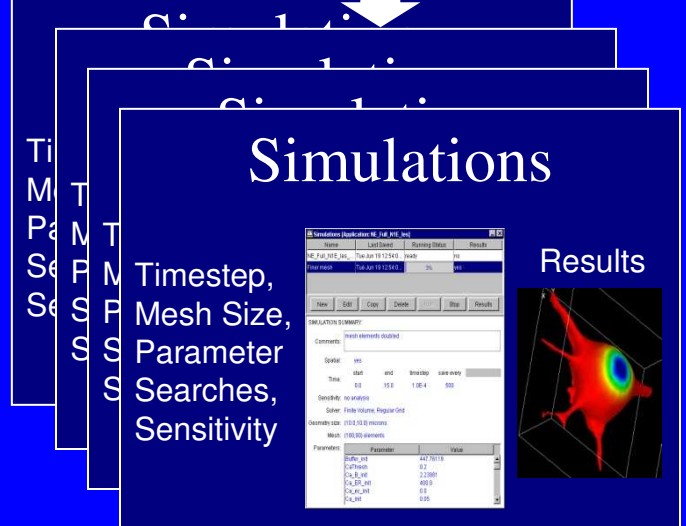
Initial Conditions, Boundary
Conditions, Disable Reactions
Electrophysiology Protocols



Math Description



VCMDL



Simulations

Results

MathModel

```
Constant Rinh_init 7.7825;
Constant RinhCa_init      3.5375;
Constant serca_init 35.38;
Constant KMOLE   (1.0 / 602.0);

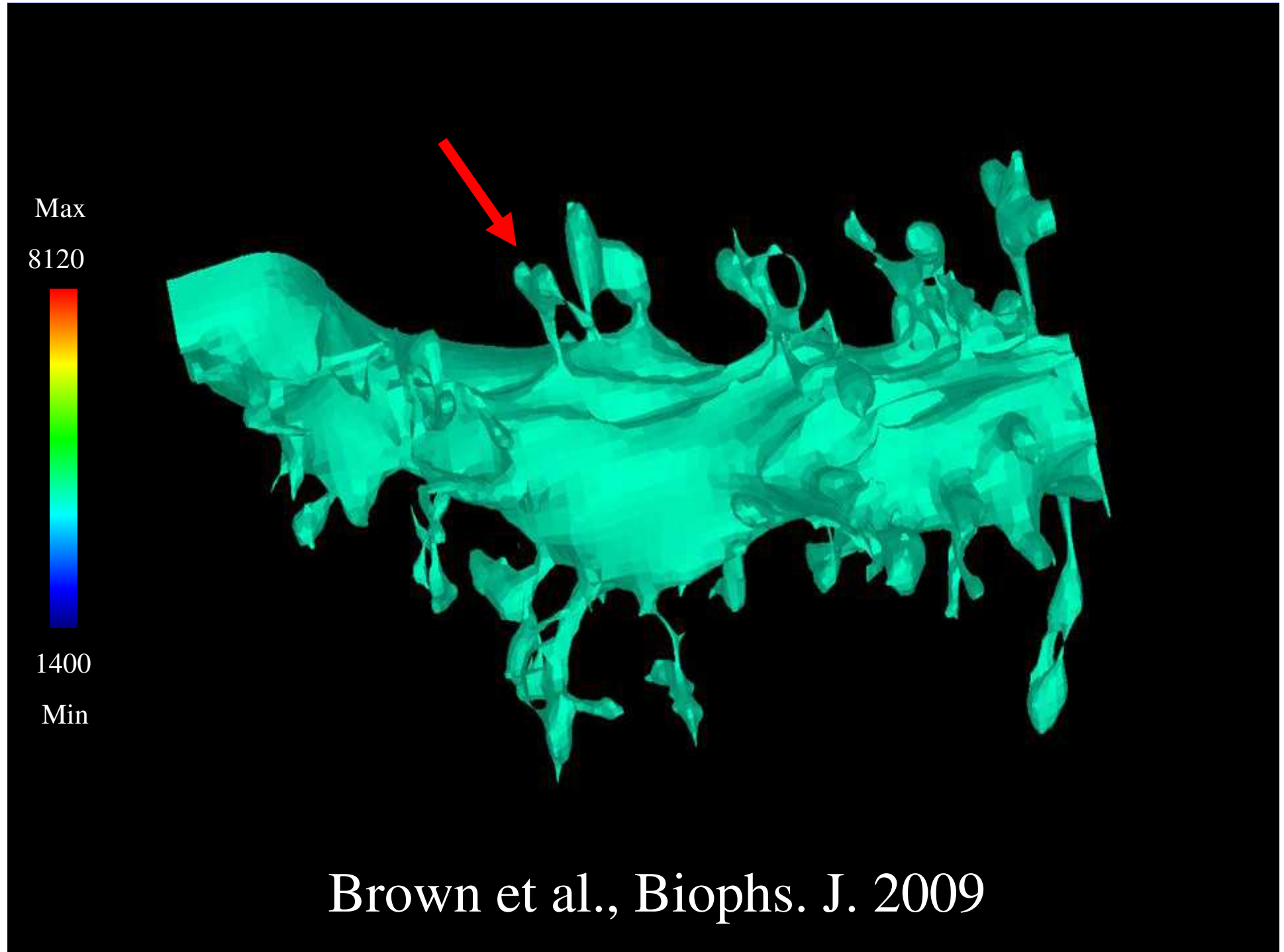
VolumeVariable Calcium
VolumeVariable IP3
VolumeVariable CalciumBufferBound
VolumeVariable Fura2_bound
VolumeVariable Ca_ER
VolumeVariable RactCa
VolumeVariable RinhCa

Function SurfToVol_erMembrane      3.84;
Function VolFract_er          0.15;
Function Kflux_erMembrane_cytosol (SurfToVol_erMembrane *VolFract_er / (1.0 - VolFract_er));
Function K_Buffer_total    (((1.0 - 0.15) * Buffer_init) + ((1.0 - 0.15) * BufferCa_init));
Function K_Fura2_total     (((1.0 - 0.15) * Fura2_init) + ((1.0 - 0.15) * Fura2Ca_init));
Function K_Ract_total      ((Ract_init * (1.0 - 0.15) * 3.84 * 0.15 * KMOLE) + (RactCa_init * (1.0 - 0.15) * 3.84 * 0.15 * KMOLE));
Function K_Rinh_total      ((Rinh_init * (1.0 - VolFract_er) * SurfToVol_erMembrane * VolFract_er * KMOLE) + (RinhCa_init * (1.0 - VolFract_er) * SurfToVol_erMembrane * VolFract_er * KMOLE));
Function K_serca_total     (serca_init * (1.0 - VolFract_er) * SurfToVol_erMembrane * VolFract_er * KMOLE);
Function Buffer        ((K_Buffer_total - ((1.0 - VolFract_er) * CalciumBufferBound)) / (1.0 - VolFract_er));
Function Fura2         ((K_Fura2_total - ((1.0 - VolFract_er) * Fura2_bound)) / (1.0 - VolFract_er));
Function Ract          ((K_Ract_total - (RactCa_init * (1.0 - VolFract_er) * SurfToVol_erMembrane * VolFract_er * KMOLE)) / ((1.0 - VolFract_er) * KMOLE));
Function Rinh          ((K_Rinh_total - (RinhCa_init * (1.0 - VolFract_er) * SurfToVol_erMembrane * VolFract_er * KMOLE)) / ((1.0 - VolFract_er) * KMOLE));
```

Apply

Cancel

View Warnings



Brown et al., Biophys. J. 2009

Virtual Cell Impact

(as of Jan. 2010)

Total Registered VCell Users	→	13,249
Users Who Ran Simulations	→	2,526
Currently Stored Models	→	34,402
Currently Stored Simulations	→	183,339
Publicly Available Models	→	720
Publicly Available Simulations	→	2,778

Conclusions

- Voltage sensitive dyes can be developed with rational chemical design principles
- Electrochromic styryl dyes produce resonance enhanced SHIM of the plasma membrane
- Non-linear optical imaging of membrane potential shows promise as a new modality for deep multi-site optical recording of electrical activity
- Fluorescence and SHIM can be used to visualize lipid phases and cholesterol distributions
- SHIM of styryl dyes detects membrane fusion during exocytosis, promising a new modality for studies of synaptic transmission

Conclusions

- Voltage sensitive dyes can be developed with rational chemical design principles
- VSD recording can reveal details of electrical activity that would be impossible to determine with electrodes
- Non-linear optical imaging of membrane potential shows promise as a new modality for deep multi-site optical recording of electrical activity
- Virtual Cell can integrate systems biology and neuronal cell physiology (but no mechanics...yet)